THE UNIVERSITY
of EDINBURGH

2018

An Investigation of Kinesin Function and Regulation for the Purpose of Proper Chromosome Segregation

Bethany Harker

Thesis presented for the degree of Doctor of Philosophy

The University of Edinburgh

2018

Declaration

I declare that this thesis was composed by myself, that the work contained herein is my own except where explicitly stated otherwise in the text, and that this work has not been submitted for any other degree or professional qualification except as specified.

Some data presented in Chapter 3 was previously published in (Talapatra *et al*, 2015), 'The far C-terminus of MCAK regulates its conformation and spindle pole focusing.' by post doctorate Sandeep Talapatra and myself, under the supervision of Julie Welburn. This study was conceived by all the authors. I carried out protein co-immunoprecipitations, cell culture work, including cell imaging both live and by immunofluorescence. Experimental contributions from Sandeep Talapatra have been clearly stated within the body of the text where appropriate.

Bethany Harker

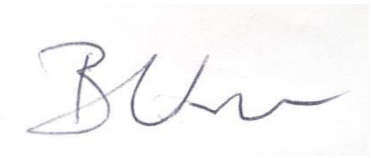

Acknowledgements

Despite turmoil throughout my PhD I have had constant support, which has helped me get through the valleys of despair and as well as the peaks of happiness. This list is by no means an exhaustive list of all the people who have given academic and emotional support between 2013 and 2018 but hopefully I have remembered those who have donated their time, expertise and enthusiasm in aid to me in my research. Without their support this research would not have been possible.

Firstly, I must thank Julie Welburn, who gave me the opportunity to peruse research in my beloved field, cell division. The first few years were full of excitement and optimism as well as the frustration, depression and anxiety. I would particularly like to thank Sandeep Talapatra for his expertise in protein purification and accepting my contributions to his work on MCAK, leading to publication (Talapatra *et al*, 2015). Members of the Welburn Lab included Sarah Young (‘ma wee pal’), Jovana Deretic, and Agata Gluszek, who grounded me and gave me motivation on grey days.

Secondly, I would like to thank Adèle Marston for welcoming me so graciously into her lab and facilitating the transition from human cell research to research using yeast. Without the continuous support, guidance and considerable patience of Adèle, I fear the thesis would have been left unfinished and my mental state in tatters. Thank you to all Marston lab members, for stimulating discussions, sharing the weekend workload and always making time for tea. Thank you to my PhD committee members, Ken

Sawin, Kevin Hardwick, and David Finnegan for their useful suggestions and invaluable comments that have helped shape my project.

Next, I would like to thank several people who have aided me with a plethora of technical support. Thank you to Christos Spanos for processing my IP samples for Mass Spec, and his excellent training in protein sample preparation. Thank you to Dave Kelly for giving me free reign of his microscopes, providing coded programs and for not mocking my image resolution too much.

Lastly, I would like to express my deepest appreciation to all the people who have kept me mostly sane during the last five years. I am forever thankful for my family, without whom I would not have aspired to apply for a PhD, let alone achieve it. My mother's daily phone calls and expert decision-making skills dragged me through the hard days, and celebrated the good days; My father's handiwork and taxi services were invaluable; my brothers gave expert IT support; and my sister was always there to snap me back into reality, give me a kick up the backside, and take me on fantastic travel adventures. I'd also like to thank to the Blenkinsop's, who have become my Edinburgh family over the past 4 years.

Abstract

Mitosis and meiosis are different forms of cell division. Mitosis is a non-reductive form of cell amplification whereby DNA chromosomes are replicated and segregated to form two progeny copies of the progenitor cell. Meiosis is a reductive form of cell division creating progeny containing half the chromosome copies of the progenitor cell. Improper chromosome segregation creates aneuploidy, which is poorly tolerated in cells. In cycling mitotic cells, aneuploidy leads to genome instability and cell death. Following meiosis, aneuploidy is associated with infertility, miscarriages, and birth defects.

To segregate chromosome copies properly, pairs are physically organized and segregated to progeny cells by a mitotic spindle, whose functionality is tightly regulated. Kinesins are a family of highly conserved dimeric ATPase proteins which; organize spindle shape and size, facilitate chromosome capture and attachment to the spindle, and generate forces which are required for segregation.

I investigated the molecular structure and function of human kinesin 13 family protein, ***M****itotic* ***C****entromere* ***A****ssociated* ***K****inesin*, MCAK. MCAK is a microtubule depolymerase whose full molecular structure and mechanism of depolymerization is not fully understood. Using *in vitro* biochemical assays and *in vivo* TIRF imaging, I found that altering MCAK molecular structure

alters MCAK sub-spindle localization and by inference, alters global microtubule dynamics. This study suggests a potential mode for regulating of MCAK activity/function requiring further testing.

Compared to over 30 kinesins in humans, showing a large amount of functional redundancy, yeast only has 6 identified kinesins whose function during meiotic cell division are still relatively unknown. I screened the importance and redundancy of yeast kinesins during meiosis. The results suggest similar roles and redundancies in meiosis to that during mitosis, despite different biochemical and biophysical spindle environments.

Together, my investigations broaden the understanding of kinesin regulation and functional redundancy during different types of cell division.

Abbreviations

aM – Astral microtubules

ATP – Adenosine triphosphate

CIN – Chromosomal Instability

CT – C terminus/C terminal

Da – Daltons

DMSO - Dimethyl sulfoxide

DNA – Deoxyribonucleic acid

EB1 – End binding protein 1

EM – Electron microscopy

ipMT – Interpolar microtubules

GFP – Green Fluorescent Protein

GST – Glutathione S-Transferase

KDa – Kilodaltons

KTs – Kinetochores

kMT – Kinetochore microtubules

CPC – Chromosomal passenger complex

SAC – Spindle assembly checkpoint

MAPS – Microtubule associated proteins

MCAK – Mitotic centrosome associated protein kinase

mCh – mCherry Fluorescent tag

MP – meiotic plaque

MT-KT – Microtubule-kinetochore attachments

MD – Motor domain / catalytic domain

MTs – Microtubules

NT – N terminus/N terminal

SDS-Page - Sodium dodecyl sulfate polyacrylamide gel electrophoresis

Table of Contents

Chapter 1:

Introduction

1.1 Cell Division

Cell division is an essential process for all living organisms, unicellular and multicellular organisms alike. During cell division, the genetic information, **D**eoxy Ribo**N**ucleic **A**cid (DNA) is duplicated and then segregated into progeny (Boyle, 2008).

For a cell to properly function it requires a complete copy of the genome. Improper segregation of DNA leads to DNA instability, aneuploidy and loss of cellular function; Aneuploidy is linked to congenital defects such as Down syndrome and Klinefelter syndrome. In each of these syndromes, cells are viable but contain an extra copy of a chromosome. Chromosome instability is linked to diseases such as cancer, where cell function is compromised, and uncontrolled cellular growth parsues (Potapova & Gorbsky, 2017).

Categorically, there are two different types of cell division; mitosis – asexual cell division, and meiosis – sexual cell division (Morgan, 2012; Marston & Amon, 2004). Where the former duplicates a parent cell, creating two cells which are genetically identical, the latter creates genetically diverse cells, with half the amount genetic material of the parent cell (Marston & Amon, 2004). In this introduction I will briefly outline key points of vertebrate mitosis and yeast meiosis, which are the focus of this thesis.

1.1.1 Eukaryotic Mitosis

Cellular cloning by mitosis generates two genetically identical daughter cells. Mitosis is a seamless orchestra of events, but for categorization, it has been defined as having distinct phases. The two main phases of the cell cycle are S-phase and M-phase, where DNA and chromosomes are replicated and segregated respectively. These two phases are separated with two gap or growth phases known as G1 and G2 (See **Figure 1.1-1**).

During S-phase, the DNA polymerisation machinery is tightly regulated to replicate the entire genome and assemble it into chromatin (Boyle, 2008). M-phase is divided further into 4 phases – Prophase, metaphase, anaphase and telophase.

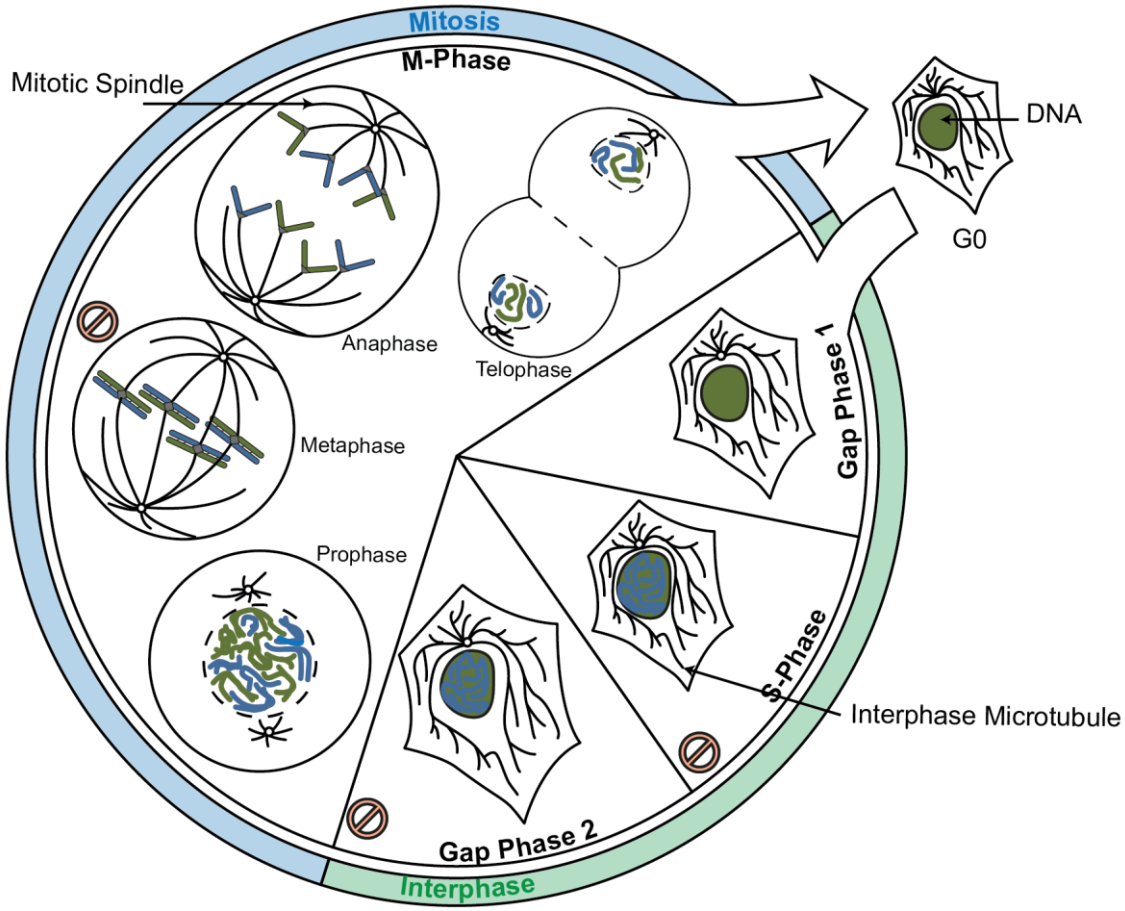

Figure 1.1-1: Diagram representation of an animal cell cycle

Diagram highlights the different stages of the cell cycle which animal cells go through – G1, S, G2, M. Emphasis has been drawn to the changes in spindle shape and movement of chromosomes. Within M-phase, the 4 stages have been depicted – Prophase, Metaphase, Anaphase and Telophase. Stop symbols represent phases of the cell cycle with described checkpoints to arrest cells in the event of a segregation error. During phase G0, cells are not dividing.

1.1.1.1 Prophase

During prophase, DNA is condensed into distinct sausage shaped chromosomes. Newly replicated chromosomes remain tethered to their sister until anaphase through cohesin protein binding (Michaelis *et al*, 1997; Koshland & Guacci, 2000). The interphase cell cytoskeleton is disassembled (Explained in more detail in (Pines & Rieder, 2001)), centrosomes are duplicated and segregated to opposite poles of the cell, and a mitotic spindle starts to assemble (see Figure 1.1-1).

Vertebrates perform 'open' mitosis, whereas fungi (such as budding yeast, *S. cerevisiae*) undergo 'closed mitosis'. During 'open' mitosis – in animal cells, the nuclear envelope breaks down at the end of prophase, exposing the condensed chromosomes to the cytoplasm, which contains the growing mitotic spindle emanating from the centrosomes.

During 'closed' mitosis the nuclear envelope remains intact. This physical barrier separates the DNA biochemically from the cytoplasm and creates two functionally distinct species of microtubules, nucleating from opposite sides of the spindle pole body (Further explained in 1.1.2) (Hildebrandt & Hoyt, 2000; Brawley & Robinson, 1985). Whilst centrosomes of animal cells and spindle pole bodies of yeast do not look similar (Animal centrosomes are free in the cytoplasm, composed of two centrioles, whereas yeast spindle pole bodies are membrane bound, composed of plates), they share function in

nucleating microtubules and related components (Brawley & Robinson, 1985).

1.1.1.2 Metaphase

Metaphase is achieved when every chromosome is aligned on the midzone of the cell, the ’metaphase plate’, bivalently attached to the mitotic spindle (see Figure 1.1-1). Each sister chromatid has its own kinetochore, which must be attached to a pole. Sister kinetochores must be attached to opposite poles if progeny cells are to get one copy of each chromosome (MAZIA, 1961). To achieve this, cells monitor progress and arrest cell division until every chromosome is attached to the mitotic spindle. One unattached kinetochore is sufficient to activate the spindle assembly checkpoint, a biochemical cascade which arrests the cell cycle at prometaphase (Rieder *et al*, 1995).

1.1.1.3 Anaphase and Telophase

Once all chromosomes are correctly aligned, the spindle assembly checkpoint is satisfied, and a biochemical cascade degrades the cohesin proteins which have been tethering sister chromatids together.
Chromosomes are segregated away from each other during anaphase A, and the mitotic spindle elongates during anaphase B, which physically pulls sister chromatids poleward (Cross & McAinsh, 2014).
After chromosome segregation, the cell body is segregated and cleaved to form two distinct, genetically identical cells. The mitotic spindle is degraded,

and tubulin is reassembled into an interphase microtubule array. At this point cells will either reenter the cell cycle or enter a stage G0, where no cell division takes place. This state of G0 can either be temporary (quiescence), or permanent (senescence) (Morgan, 2012).

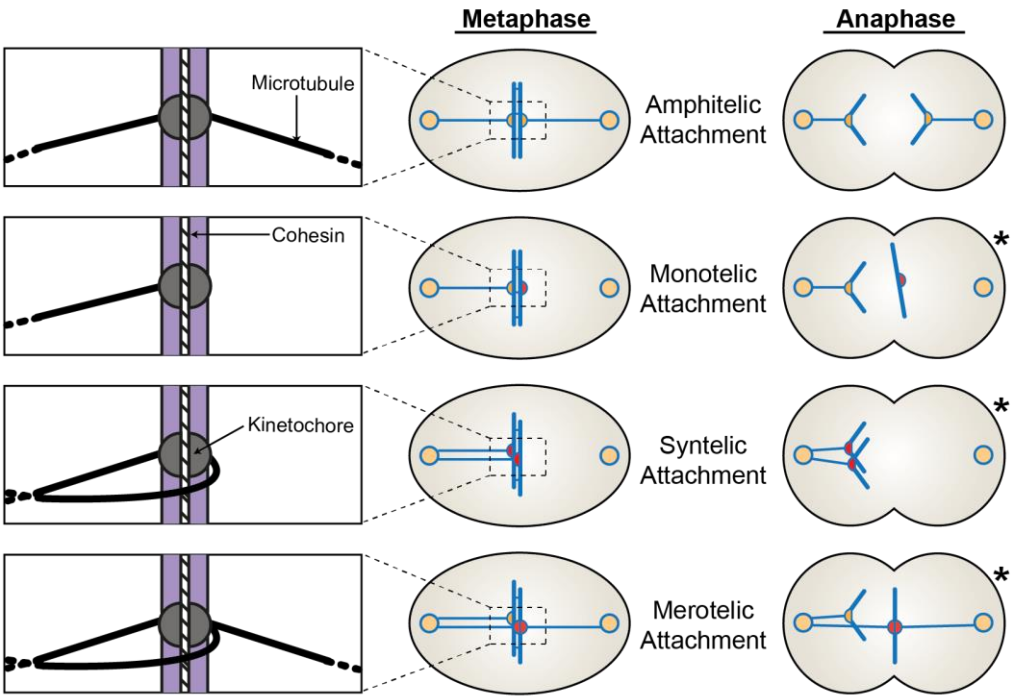

Figure 1.1-2: Misaligned chromosomes activate the spindle assembly checkpoint (SAC), arresting the cell cycle at the metaphase/anaphase transition.
Diagram shows possible kinetochore alignments on a bipolar spindle. In syntetic attachments, both poles are attached to one chromatid kinetochore of the pair. If only one pole is attached to one chromatid kinetochore the attachment is monotelic. Bivalent (amphitelic) attachments are only achieved when the two kinetochores of chromatid sisters are attached to opposite poles. This attachment generates tension across the spindle (Rieder *et al*, 1995). * indicates improper chromosome segregation, which is avoided by activating the spindle assembly checkpoint.

1.1.1.4 Mitotic Checkpoints

As described above, incorrect DNA duplication or segregation leads to aneuploidy and chromosome instability (Potapova & Gorbsky, 2017). As a result, the cell cycle is unidirectional and carefully monitored for errors. Biochemical checkpoints throughout mitosis prevent the cell from progressing through the cycle until it has not fulfilled specific criteria. If the cell is unable to progress, cell death (apoptosis) is triggered (Morgan, 2012).

1.1.2 Eukaryotic Meiosis

Meiosis is a specialized form of cell division which generates cells with nuclei containing half of the normal compliment of chromosomes (See **Figure 1.1-3**). This is essential for sexual reproduction in eukaryotes and diploid organisms to produce gametes – such as the human egg and sperm. Many mechanisms employed during meiosis are the same as mitosis, but meiosis also includes several specific features; namely, generating genetic variance between resultant nuclei and undergoing two rounds of chromosome division without an intervening S-phase (Page & Hawley, 2003; Ohkura, 2015). Below, I will outline the current understanding of meiosis in budding yeast *S.cerevisiae*.

During S phase, chromosomes are replicated and tightly tethered by the protein complex called cohesin, as in mitosis. However, during prophase I

homologue chromosomes are paired in zygotene phase, and recombination occurs (pachytene) (Morgan, 2012). Recombination involves the exchange of DNA between homologues through tightly regulated DNA crossover (See review (Baudat *et al*, 2013)). Genetic diversity within a species is considered important for long term survival (Ohkura, 2015). Newly formed crossovers, chiasmata, act as a physical link between homologue pairs, allowing for bivalent homologue alignment on the meiotic I spindle during metaphase I. A single chiasmata is sufficient for proper tension support in metaphase I (Marston, 2014; Ohkura, 2015; Morgan, 2012; Hillers & Villeneuve, 2003).

Within homologue chromosomes, sister chromatids are tethered together by cohesin protein. Cohesin secures sister chromatids along the entire length of the DNA, and is enriched around the centromere (at the pericentromere) to support chromosome structure when tension is applied (Duro & Marston, 2015). Unique to meiosis; chromosome cohesion must be lost in a step wise manner during meiosis rather than uniformly at anaphase onset.

To resolve chiasmata, and segregate homologous chromosomes, the cohesin on the arms must be resolved, however to maintain cohesion between sister chromatids the pericentromeric cohesin is protected (Morgan, 2012; Paliulis & Nicklas, 2000).

Following homologue segregation, the first meiotic spindle is disassembled and two spindles form for a second round of DNA division, and sister

chromatids are segregated by cleaving the remaining pericentromeric cohesin (Morgan, 2012; Paliulis & Nicklas, 2000). Compared to meiosis I, meiosis II is considered mechanistically like mitosis. The resulting progeny each receive just one copy of chromosome, half the amount compared to mitosis and, are therefore haploid (Roeder, 1997; Marston, 2014).

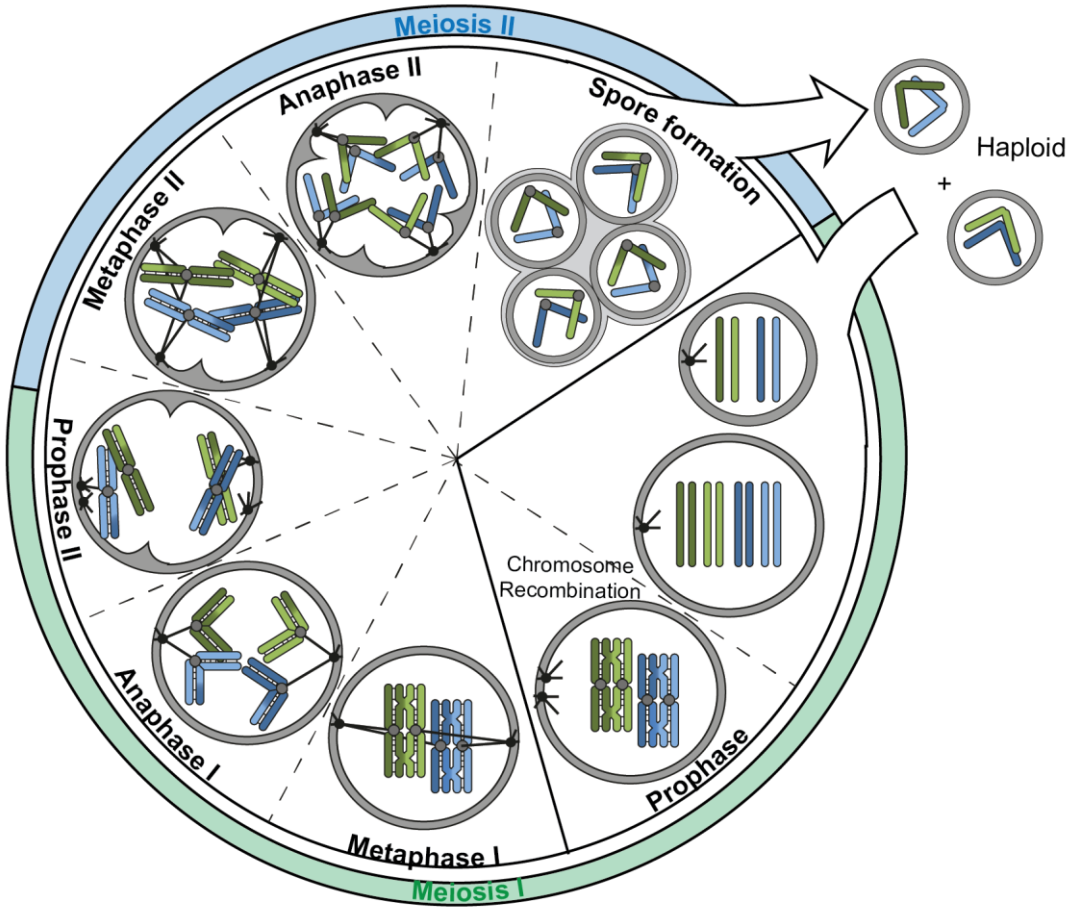

Figure 1.1-3: Diagram showing chromosome segregation during *S. cerevisiae* meiosis. Haploid cells of opposite mating type form a diploid cell which goes through meiosis to form four haploid spores. Two rounds of chromosome division are uninterrupted by growth or DNA replication.

1.2 Microtubule Dynamics and Regulation

Microtubules are dynamic polymers of tubulin proteins, tubulin α and β. Essential roles include; capturing chromosomes at the kinetochore, bivalently aligning chromosomes on the mitotic spindle, separating sister chromatids to opposite poles, forming the cytokinesis midbody scaffold, and acting as a transport pathway. The function of the spindle is dictated by microtubule dynamics, which are tightly regulated by protein interactions and upstream kinase phosphorylation (Morgan, 2012).

Tubulin heterodimers polymerize to form long, strong, tube like structures. Electron microscopy studies have shown that the asymmetrical structure of α and β tubulin affords microtubules intrinsic molecular polarity; one end is different to the other no matter how long the microtubule or whether it is broken (Amos & Klug, 1974). Microtubules preferentially grow from the '+ end' and shrink at the '- end' (Borisy *et al*, 1974).

Microtubules undergo phases of polymerisation and depolymerisation. Due to intrinsic GTP hydrolase activity, tubulin has two forms, GTP associated, which has a preferred straight protofilament confirmation, and GDP bound, which has a preferred curved ring like confirmation (Nogales, 2003). GTP bound tubulin dimers assemble end on to form polar protofilaments. 13 filaments associate laterally to create ridged hollow cylinders in a degenerate helix with an outside diameter ~25-nm (Li *et al*, 2002; Chretien, 1995; Wang & Nogales, 2005; Desai & Mitchison, 1997). Microtubules display high

dynamic instability, stochastically switching between states of growth and shrinkage via catastrophe and rescue (Mayr *et al*, 2011; Desai & Mitchison, 1997).

As '-ends' are often anchored in mammalian cells, the majority of MT dynamics take place at the '+end' of microtubules where GTP bound tubulin forms a 'cap'. During polymerisation the cap is constantly renewed with GTP-tubulin association, while downstream intrinsic tubulin GTP hydrolysis creates a GDP bound lattice. GTP bound tubulin filaments have a straight conformation, compared to curved GDP bound tubulin protofilaments (Grishchuk *et al*, 2005). Conformational constraints of the lattice held by the GTP bound tubulin or an artificial protein 'cap' locks GDP-tubulin in a high energy 'GTP-like' straight confirmation, storing energy from GTP hydrolysis within the microtubule body (Nogales & Wang, 2006; Grishchuk *et al*, 2005).

Stored energy is released during depolymerisation of microtubules as protofilaments adopt their preferred conformation, often as kinetic energy to physically move objects relative to each other in the cell. A 13 protofilament microtubules can produce an estimated 65 pN of force during depolymerisation, much higher than the 0.1pN required for chromosome segregation (Grishchuk *et al*, 2005; Nicklas, 1983).

The rate of GTP-bound tubulin addition to the '+ end' determines the rate of growth and state of the GTP cap. If the cap is lost, i.e. by a lack of free GTP bound tubulin; GDP bound protofilaments take on their low energy

confirmation, actively pealing from the tip, releasing stored energy by rapid depolymerisation or ‘catastrophe’ (Nogales, 2003; Nogales & Wang, 2006). Compared to nucleation at the centrosome during mammalian cells, budding yeast microtubules emanate from either side of a spindle pole body (SPB) (Brawley & Robinson, 1985).

Microtubules play important roles during chromosome segregation, acting as tracks on which motors can physically carry chromosomes, and exerting forces to move statically attached components around the cell. The former is essential during the ‘search and capture’ of chromosomes in prometaphase, whilst the prior is used during anaphases, to push poles, and pull chromosomes apart to opposite poles of the cell. Microtubules, together with associated proteins assemble to form a spindle during cell division.

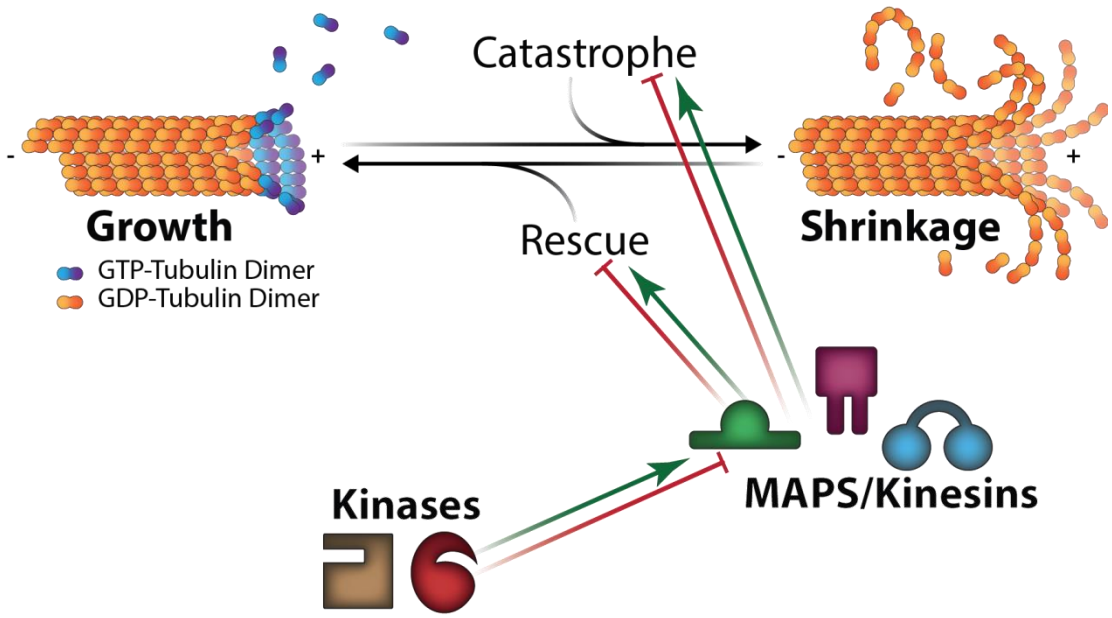

Figure 1.2-1: Diagram showing microtubule dynamics.

Microtubules are dynamic polymers which switch from phases of growth to shrinkage after catastrophe events but can be rescued into growth phase again. Microtubules grow by the addition of GTP-Tubulin dimers. Once attaches, internal GTP hydrolysis converts GTP-Tubulin dimers to GDP-Tubulin dimers, which possess a different confirmation. The rate of catastrophe and rescue is influenced by microtubule attached proteins and kinesins as well as direct kinase action.

1.3 The Mitotic and Meiotic Spindle

The proper distribution of replicated chromosomes is essential for organism vitality. This function is carried out by the mitotic spindle, composed of microtubules. Despite proper DNA Duplication, aneuploidy and chromosome instability can arise from microtubule and spindle defects. During chromosome segregation the spindle undergoes a series of well-defined motility events, generating forces within the cell (Hoyt *et al*, 1993; Cross & McAinsh, 2014).

During prophase, the centrosomes/spindle pole bodies are duplicated and segregated to opposite poles of the cell. The force generated to push these bodies apart is created through sliding antiparallel microtubules (Morgan, 2012; Hoyt *et al*, 1993; Hoyt & Geiser, 1996). Similar mechanisms are used to drive the spindle poles apart further by elongating the spindle during anaphase stages I and II (Cross & McAinsh, 2014).

Spindle positioning in cells is controlled by forces generated both at metaphase kinetochores and at the connecting points between the cell membrane and microtubule spindle (Kiyomitsu & Cheeseman, 2012; Shrestha & Draviam, 2013). To achieve bivalent microtubule-kinetochore attachments, microtubules ‘search and capture’ kinetochores. Rapid microtubule dynamics and directed growth promotes rapid chromosome attachment, and reinforces proper kinetochore attachments, severing the incorrect (Wilde & Zheng, 1999).

Whilst microtubules do spontaneously polymerase in high enough concentration, dynamics and organization is achieved through carefully regulated mechanisms. Microtubule associated proteins (MAPs) bind to microtubules and can affect polymerisation and depolymerisation rates, rates of catastrophe and rates of rescue (Cassimeris & Spittle, 2001; Maiato *et al*, 2004; Heald *et al*, 1996). Upstream, MAP function is regulated by phosphorylation of kinesin motor proteins which affects kinesin localisation and activity.

1.4 Microtubule interacting proteins (MAPS) and Kinesin proteins

Microtubule dynamics are coordinated by Microtubule associated proteins (MAPs) and motor proteins. This regulation converts polymerisation/depolymerisation into pushing and pulling forces which align chromosomes amphitelically in metaphase and pulls them to opposite poles during anaphase (Wu *et al*, 2006; Melbinger *et al*, 2012). MAPs are fundamentally different to motor proteins in that they have no catalytic domain (Wu *et al*, 2006).

Motor proteins use energy liberated from phosphonucleotide hydrolysis to do mechanical work. A change in nucleotide state causes conformational changes within the protein, often coordinated to direct movement along a

microtubule lattice or exert forces upon them (Moore & Wordeman, 2004a). Major motor proteins include kinesins and dyneins. Dyneins are '- end' directed motors which specify function using differential binding partners, while there are 45 different kinesins, grouped into 14 different families (Cross & McAinsh, 2014).

Motor proteins are generally categorized as N- or C-terminal, depending on where the motor/catalytic domain is on the protein sequence. N-terminal kinesins have catalytic domains at their N-terminus and vice versa with C-terminal kinesins (Cross & McAinsh, 2014; Moore & Wordeman, 2004a). Likewise, C-terminal kinesins are '-end' directed and N-terminal kinesins are '+ end' directed, with some exceptions which are bidirectional, non-motile, or have their catalytic domain in the center of the peptide sequence (Cross & McAinsh, 2014; Moore & Wordeman, 2004a).

The general components of kinesins are a motor domain, a coiled coil region, and a globular domain - usually at the opposite end of the motor domain. The catalytic domains of Kinesins are highly conserved between families and across species (Kull *et al*, 1996). Despite similarities, kinesin subfamilies have evolved to perform differentiated tasks within the cell to organize the microtubule spindle, – a review by Cross & McAinsh (2014) clearly summarizes nomenclature and understanding as of 2014. (see Figure Figure **1.4-1**)

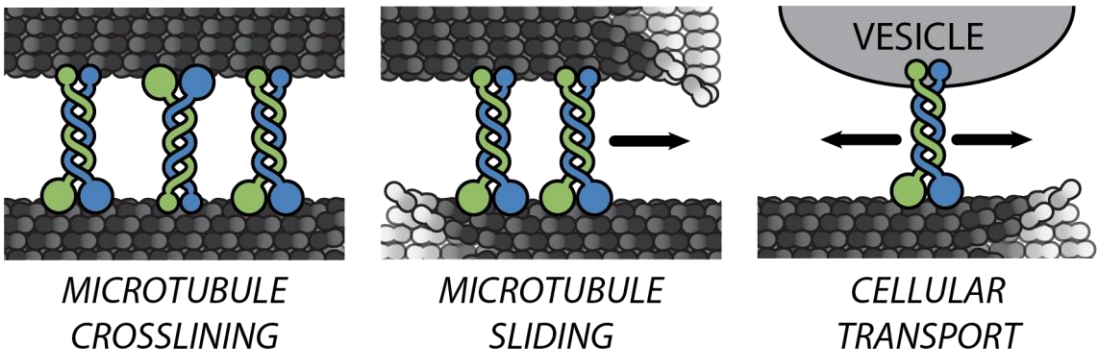

Figure 1.4-1: Diagram demonstrating the principal known functions of kinesin proteins Kinesins generally act in three distinct ways. Firstly, they can crosslink antiparallel microtubules by binding to microtubules both at N and C termini. Progressive movement of one kinesin is cancelled out by movement of a kinesin on the cargo microtubule, leading to 0 net movement. Alternatively, if kinesins are all bound to the same microtubule, progressive movement along it with a microtubule 'cargo' leads to microtubule sliding respective of each other. Finally, the canonical use of kinesins; as cargo delivery systems, walking progressively along microtubules with a cargo. Cargos include other proteins, membrane vesicles, DNA, and kinetochores (Cross & McAinsh, 2014).

1.4.1 Kinesin 13 family

Kinesin 13 family members were originally called M-kinesin kinesins (Middle-types) or part of the KinI family (Kinesin internal), owing to the central position of the catalytic motor domain within the protein sequence (Lawrence *et al*, 2004). The kinesin 13 family is composed of two subfamilies, Kif24 and Kif2. The former family has the motor domain closer to the amino terminus, where the latter is mammalian specific and has a motor domain localisation more central in the amino acid sequence. The Kif2 family is composed of just 3 kinesins – Kif2a, Kif2b and Kif2c (MCAK), each uniquely coded (Noda *et al*, 1995; Wordeman & Mitchison, 1995; Ogawa *et al*, 2004) .

1.4.1.1 H.Sapiens MCAK

MCAK is a kinesin 13 family member and unlike canonical kinesins, its structure looks closed, compact and globular by EM studies (Noda *et al*, 1995). Consequently, the domain organisation of MCAK is unlike that of other kinesin families; the MCAK Motor Domain does not reside at the N- or C-terminus, and instead is in the interior of the protein sequence (Cross & McAinsh, 2014; Vale & Fletterick, 2003). MCAK exists as a homodimer in vitro and in vivo, though the monomer is capable of depolymerising microtubules (Maney *et al*, 2001).

MCAK is used to regulate microtubule dynamics. MCAK is known to associate with the '+end' growing tip of microtubules, and uses energy derived from ATP hydrolysis to trigger lattice catastrophe via a

conformational change in tubulin dimers (Moore *et al*, 2005; Rankin & Wordeman, 2010). At the kinetochore, MCAK is believed to be involved in a plethora of events during mitosis.

Firstly, MCAK suppresses chromatid oscillations after metaphase alignment, to promote chromosome congression at the metaphase plate, equidistant to the poles, and avoid lagging chromosomes during anaphase (Maney *et al*, 2001; Walczak *et al*, 1996; Garcia *et al*, 2002).

Secondly, MCAK at the kinetochore is proposed to ensure faithful chromosome segregation by destabilizing erroneous KT-MT attachments (for example merotelic attachments - see Figure 1.1-2) which could lead to missegregation and aneuploidy (Gadde & Heald, 2004; Kline-Smith *et al*, 2004). Lateral kinetochore attachments created by CENP-E are detached by MCAK, at the lateral-end on conversion, to facilitate full end-on conversation.

Additionally, MCAK, with binding partner Kif18A, regulates the length of astral microtubules which generates an inward force on the spindle, inward force is balanced with Eg5 activity, generating outwards force. This fine balance is important for proper spindle orientation and maintenance of spindle position within the cell (van Heesbeen *et al*, 2016).

MCAK has also been implicated in proper end-on conversion on lateral kinetochore-microtubule attachments. MCAK disconnects the lateral

connections made by CENP-E once a partial end-on connection is made, to facilitate full connection (Shrestha & Draviam, 2013).

Finally, MCAK is implicated in the depolymerisation of attached kinetochore fibers during mitosis, to force poleward movement of sister chromatids to the poles during anaphase, though this work was carried out in Drosophila, studying MCAK homologue, Klp56C (Rogers *et al*, 2004).

Many kinases have been implicated to regulate MCAK activity (Plk1, CDK1, Aurora B) and/or its localisation (EB1, Kif18a) (Tanenbaum & Medema, 2011; Domnitz *et al*, 2012; Hood *et al*, 2012; Tanenbaum *et al*, 2011b)

1.4.1.1.1 MCAK Localisation during mitosis

MCAK is strongly enriched on microtubule +ends, and kinetochores during mitosis, weakly at centrosomes, and at spindle midzone during anaphase (Wordeman & Mitchison, 1995; Walczak *et al*, 1996; Maney *et al*, 1998). Depletion of MCAK activity during cell division leads to improper spindle maintenance, misaligned chromosomes, often lagging during anaphase, and consequently aneuploidy in progeny (Walczak *et al*, 1996; Maney *et al*, 1998; Walczak *et al*, 2002). These results support suggestions that MCAK is essential for proper chromosome segregation by mitosis.

MCAK binds with strong affinity to microtubule ends compared to along the microtubule lattice (Hunter *et al*, 2003) . This could be caused by a higher

affinity to the curved conformation of microtubule protofilaments at the growing end of microtubules (Desai *et al*, 1999; Brouhard & Rice, 2014).

MCAK is believed to diffuse through the cytoplasm to microtubules, and rapidly move towards high binding affinity end through electrostatic interactions between MCAK and microtubule lattices (Hunter *et al*, 2003). In vivo, MCAK is more concentrated on growing microtubule tips compared to - end tips (Moore & Wordeman, 2004b). This is due to recruitment by partner proteins. MCAK is recruited by EB1 and Kif18b to growing, GTP bound Microtubule + ends, (Maney *et al*, 2001; Lee *et al*, 2008; Honnappa *et al*, 2009; Hunter *et al*, 2003; Desai *et al*, 1999).

The core catalytic domain of MCAK binds to microtubules in cell culture, but sequences in both the N- and C-terminus of MCAK are required for proper kinetochore and microtubule tip targeting during mitosis (Welburn & Cheeseman, 2012). Lack of C terminus in vitro caused a marked increase of microtubule lattice binding, decrease in microtubule end binding and a decrease in kinetochore targeting (Ems-McClung *et al*, 2007).

Other members of the kinesin 13 family member include Kif2a and Kif2b. Whilst Kis2a/2b motor domains are highly conserved with Kif2c/MCAK (92% and 85% sequence identity respectively), the N terminus and C terminus are much more divergent (~38% and ~45% sequence identity on average respectively). Kif2A is strongly localized at the centrosome during mitosis

whilst MCAK is primarily localized to kinetochores and microtubules + ends during mitosis.

The N-terminus of MCAK, upstream of the motor domain, is sufficient for kinetochore localisation as a peptide alone (*ΔMC* – truncated at the neck), and can even fused to the motor and C terminus if Kif2a, which is normally centrosomal (Welburn & Cheeseman, 2012). Despite weaker kinetochore localisation of MCAK N terminus peptide alone, this data suggests that sequences in the N terminus of MCAK are primarily responsible for kinetochore localisation (Welburn & Cheeseman, 2012).

In vitro, studies support the above findings, where removal of N terminus compromised kinetochore targeting in cell extracts (Ems-McClung *et al*, 2007). In Xenopus extracts, MCAK phosphorylation by Aurora B at serine 196 is responsible for proper centrosome/kinetochore localisation, and proper kinetochore bipolar spindle attachment and chromosome segregation (Lan *et al*, 2004)

Fluorescently labelled MCAK is visualized at the poles of the cell, though weaker than at the kinetochores (Welburn & Cheeseman, 2012; Zhang *et al*, 2008). In *in vitro* experiments using Xenopus cell extracts, pole localisation is achieved through phosphorylation at the C terminus on serine 719 by Aurora A, whilst further phosphorylation at serine 196 contributes to MCAK

functionality, focusing poles to ensure proper transition from monopolar microtubule asters to bipolar mitotic spindles (Zhang *et al*, 2008).

1.4.1.1.2 Regulation of MCAK Depolymerase Activity

MCAK is specifically localized to subdomains of the spindle and is distinctly different from other family 13 proteins such as Kif2a, which is primarily polar rather than centrosomal. It is increasingly the case that MCAK activity is orchestrated spatially and temporally rather than intrinsically, depending on the function it is performing, namely, moving MCAK closer or further away from subsections of the spindle machinery throughout mitosis (Moore & Wordeman, 2004a; Wordeman *et al*, 1999).

Investigation into capture and bi-orientation of chromosomes during prometaphase indicate that heavy Aurora B phosphorylation on the N terminus inhibits MCAK depolymerase activity, hindering chromosome capture. Aurora B phosphorylation of MCAK at serine 196 is highly conserved between human and Xenopus, some of which are on the neck region of the N-terminus (Lan *et al*, 2004). Phosphorylation of MCAK on S196 induces a phosphoconformational switch in the structure of MCAK, which reduced MCAK association with microtubules, and this rates of depolymerisation (Ems-McClung *et al*, 2013).

In the case of MCAK, a reduced affinity for the spindle upon S169 phosphorylation in cells leads to sequestered MCAK elsewhere on the

spindle and segregation infidelities (Andrews *et al*, 2004; Ohi *et al*, 2004; Lan *et al*, 2004). In addition to causing conformational changes to proteins, phosphorylation can also be used to alter the charge of a protein region, and thus the affinity for the charged proteins surrounding it.

In addition to regulating MCAK localisation availability of its substrate, the intrinsic activity of MCAK is also tightly regulated. Whilst the catalytic domain of MCAK is not sufficient for proper MCAK localisation to kinetochores, the catalytic domain of MCAK alone is also not sufficient for depolymerase activity, however the 50 amino acids N-terminal of the catalytic domain, the Neck domain, are sufficient to restore full depolymerase activity (Maney *et al*, 2001; Ems-McClung *et al*, 2007). This indicates that the N-terminus has a regulatory effect on MCAK activity as well as localisation.

The C terminus us MCAK has also been shown to provide important regulatory function. Studies on murine MCAK showed the last 8 amino acids are important for reducing MCAK activity in cells. When MCAK ATP hydrolysis activity is increased, so too is the amount of global microtubule depolymerisation, supporting the theory that ATP hydrolysis is required for continues MCAK depolymerase activity (Moore & Wordeman, 2004b). The C-terminus of MCAK has been reported as a phosphorylation site for both Polo Like Kinase 1 (Plk1) and Aurora A (Santamaria *et al*, 2011; Shao *et al*, 2015; Zhang *et al*, 2011).

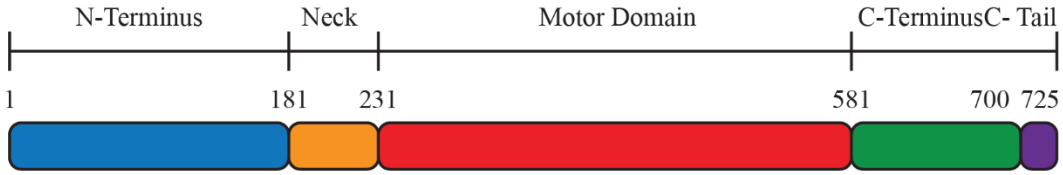

MCAK Domain	Abbreviation	Amino Acids
N-Terminus	N	1-181
N-Terminus and Motor Domain	NM	1-581
Motor Domain	MD	232-581
C-Tail	CT	700-725

Figure 1.4-2: Diagram to show MCAK domains

Amino acids 1-180 denote the N-Terminus, amino acids 181-231 denote a flexible neck region. The motor domain/ATPase domain is composed of amino acids 232-581 and the remainder is the C-terminus. Within the C-terminus the far 25 amino acids have since been named the C-tail, as regulation of that region has been shown to alter the functionality of MCAK (Moore & Wordeman, 2004b)

1.4.1.1.2.1Aurora B kinase:

Aurora B is a member of the Ipl1 kinase family originally identified in Drosophila with well-defined functions during mitosis (Bischoff *et al*, 1998). Aurora B localisation to the inner centromere creates a phosphorylation gradient around the site of spindle attachment (Wang *et al*, 2011).

During mitosis Aurora B at the centromere forms the chromosome passenger complex (CPC) with INCENP, Survivin and Borealin, an essential compound of the spindle assembly checkpoint (SAC) (Vader *et al*, 2006; Gassmann *et al*, 2004). Principally, the CPC converts syntelic microtubule attachments at the kinetochore to merotelic, allowing proper conversion to amphitelically attachments (Cimini *et al*, 2006; Welburn *et al*, 2010; Chan *et al*, 2012).

Previously, studies have described downstream targets of Aurora B how they influence microtubule dynamics, e.g. MCAK (Zhang *et al*, 2007; Tanenbaum & Medema, 2011)

1.4.1.1.3 Mechanism for MCAK depolymerisation

It is proposed that the motor domain of MCAK complements the curved GDP-bound confirmation of tubulin in a ‘lock and key’ mechanism. A current understanding is that MCAK depolymerises microtubule by binding to tubulin in its straight, GDP bound ‘in lattice’ and triggering a curvature in the tubulin conformation, leading to dissociation from the microtubule and its subsequent unraveling (Moore & Wordeman, 2004b).

It is not surprising then that MCAK has a higher affinity for microtubule ends compared to the lattice face, is recruited to growing microtubule ends particularly, and that this is consequently where microtubule dynamics are generally higher (Moore & Wordeman, 2004a).

MCAK can depolymerase tubulin in the absence of ATP, in a 1:1 stoichiometries of MCAK to tubulin, otherwise ATP hydrolysis is required for complete microtubule depolymerisation (Desai *et al*, 1999; Hunter *et al*, 2003; Newton *et al*, 2004). One proposed use for ATP hydrolysis is that it is required to allow MCAK uncoupling from tubulin after dissociation from the tubulin lattice, to recycle MCAK back into the free MCAK population (Newton *et al*, 2004; Desai *et al*, 1999).

A more recently proposed theory is that ATP hydrolysis in MCAK bound to a tubulin dimer triggers a conformational change in MCAK, creating a more ‘closed’ conformation, This change in conformation induces longitudinal and lateral stress on the microtubule end, preventing polymerisation and supporting depolymerisation (Burns *et al*, 2014).

In vitro studies surrounding MCAK ATP hydrolysis and its role in microtubule depolymerisation often show discrepancies in their data and conclusions. Studies using GMP-CPP, a non-hydrolysable form of ATP (Which

strengthens longitudinal interactions on microtubule lattices (Orr *et al*, 2016) show greater activity than studies using paclitaxel (Which stabilizes lateral interactions in microtubule lattices (Nogales, 2000; Hyman *et al*, 1992).

These differences could owe to the confirmation shape of tubulin bound to GMP-CPPP, which is straighter and not a good candidate for MCAK binding (Hyman *et al*, 1995, 1992). Depolymerisation rates without free tubulin sequestering MCAK away from growing microtubule tips is likely to be higher. Consequently, studies using physiological environments, measuring rates of depolymerisation within cells must be preferred over in intro studies using artificially stabilized microtubules (Newton *et al*, 2004).

1.4.1.1.4 MCAK and Cancer

MCAK and its regulating kinases are expressed at increasing protein levels as cells progress towards and enter mitosis (Whitfield *et al*, 2002). Over expression of these proteins could be sufficient for cells to bypass checkpoint signals, and progress through mitosis with chromosomal abnormalities (Moore & Wordeman, 2004a).

Both overexpression of MCAK and its regulatory Aurora Kinases (and Plk1 kinase) and chromosomal instability (CIN) which results from erroneous MCAK and Kinase regulation are linked to tumorigenesis (Sircar *et al*, 2012; Fu *et al*, 2007; Katayama & Sen, 2010; Kumar *et al*, 2013; Sanhaji *et al*,

2011). In cell culture, overexpression of Aurora kinases is sufficient for transformation (Perou *et al*, 1999).

Taxol is a commonly used cytotoxic drug used as part of chemotherapy treatment. It aims to arrest cell division by triggering mitotic checkpoints and stimulate downstream cell death (Sudakin & Yen, 2007; Schmidt & Bastians, 2007; Vader & Lens, 2008).

MCAK can depolymerase taxol stabilized microtubules. Some Taxol resistance cancer cell lines show elevated MCAK expression levels, which affords them microtubule dynamic instability despite the presence of Taxol (Ganguly *et al*, 2011a, 2011b).

With increasing use of chemotherapy drugs which interfere with microtubule dynamics in cell, and the emergence of cancers resistance to these drugs, depolymerizing kinesins are providing promising targets for future combined cancer therapies.

1.4.2 Kinesin 8 family

Like kinesin 13 family members, Kinesin 8 proteins promote disassembly of microtubules by removing subunits from the ends. Kinesin 8 proteins also localize to the plus ends of microtubules, like kinesin 13 proteins. Unlike Kinesin 13 proteins, kinesin 8 proteins are able to slowly, progressively ‘walk’

along microtubules to microtubule ends, a property which promotes length-dependent regulation of spindle length (Helmke *et al*, 2013; Varga *et al*, 2006).

1.4.2.1 H. Sapien Kif18A

Loss of human kinesin protein, Kif18a, activity creates hyper stable microtubules, elongated spindles, incorrect tension across sister kinetochores and aberrant congression (Mayr *et al*, 2007; Stumpff *et al*, 2008, 2012). Kif18a consists of an N-terminal motor domain, a coiled coil region and a small globular region followed by a relatively unstructured C-terminal tail domain.

The motor domain confers the ability to suppress microtubule growth (creating tension across sister kinetochores) and migrate along microtubule tracts, while the C- terminal contains an ATP-independent microtubule binding domain to tether the motor to the spindle, and enhances motor function to accumulate Kif18a at the k-fibre '+end' (Mayr *et al*, 2011; Stumpff *et al*, 2011; Weaver *et al*, 2011).

1.4.2.2 S. cerevisiae Kip3

Kip3 is an N-terminal kinesin 8 Klp6/Klp67A/Kif18A homologue, directed to the plus ends of microtubules in vivo. During mitosis it localizes to cytoplasmic and spindle microtubules, followed by the midzone during anaphase (Miller *et al*, 1998; DeZwaan *et al*, 1997).

Kip3, like MCAK in human cells, is important for proper spindle positioning within the cell and assembly of a proper spindle and maintenance during mitosis (Cottingham & Hoyt, 1997; Hildebrandt & Hoyt, 2000; Endow *et al*, 1994). Deletion of Kip3 causes a delay in anaphase exit and longer spindle lengths (Straight *et al*, 1998).

Mechanistically, Kip3 serves its function by acting as a microtubule depolymerase, similar to MCAK. However, dissimilar to MCAK, Kip3 only depolymerises microtubules from the positive growing end, and not on the lattice or minus end (Rizk *et al*, 2014). Controlled depolymerization of microtubules at the positive growing end is required to maintain the spindle scaled to the length of the cell (Rizk *et al*, 2014).

Spindle elongation is achieved through altering the ratio of microtubule polymerisation at the midzone of interdigitated antiparallel Interpolar microtubules (ipMT), and the rate of antiparallel ipMT sliding. The latter is achieved through Cin8-Kip1 crosslinking and sliding at the midzone (Cottingham & Hoyt, 1997). The former is apparently suppressed by Kip3 when the spindle reaches the appropriate length for the cell. How the cell senses this achievement is a remaining question (Rizk *et al*, 2014).

Kip3 has shown an unusually long progressive walking length on microtubules of up to 10µm, which would favour enrichment on long

microtubules, to shorten them in a length-dependent manner (Varga *et al*, 2006).

Double knockout of Kip3 and Kar3 is lethal, and deletion of Kip3 results in long pre- and post- anaphase spindles, known as a ‘lasso’ phenotype (Rizk *et al*, 2014).

1.4.3 Kinesin 14 family

Kinesin 14 family members are C-terminal minus end directed kinesins. In plant cells, which do not have dynein minus end directed motors, kinesin 14 proteins are proposed to act as an alternative (Yamada *et al*, 2017; Cross & McAinsh, 2014)

Kinesin 14 family members regulate spindle organization and assembly by crosslinking parallel microtubules and sliding antiparallel microtubules (She & Yang, 2017). Of the Kinesin 14 family there are two subfamilies, Kinesin 14A and Kinesin 14B. Kinesin 14A proteins include *H.sapiens* HSET, Drosophila ncd, *M.musculus* KIFC1 and *S.Pombe* Pkl1 and Klp2 (She & Yang, 2017).

1.4.3.1 S. cerevisiae Kar3

The mitotic spindle is comprised of different types of microtubules; kinetochore microtubules (kM), Interpolar microtubules (ipMT) and astral microtubules (aM). In budding yeast, there are 32 kMTs and ipMTs (Hepperla

et al, 2014). To segregate chromsomes during anaphase, kMTs shorten, to move attached chromosomes poleward, whilst ipMTs elongate, to enhance spatial segregation. Studies suggest that Kar3 could function in both mechanisms (Hepperla *et al*, 2014).

Kar3 was first identified in a screen for integral karyogamy proteins Kar3 is essential for haploid nuclear fusion in diploid formation (Meluh & Rose, 1990). Since then it has been identified in roles pertaining to mitotic spindle formation and meiotic progression (Bascom-Slack & Dawson, 1997). Kar3's motor domain is located on the C-terminus, and has most common homology to human HSET, drosophila ncd protein and it has a crosslinking domain outside of the motor domain (Endow *et al*, 1994; McDonald *et al*, 1990). In mitotic cells *kar3-Δ* mutants displayed delayed/arrested mitosis (Polaina & Conde, 1982).

Early studies on Kar3 function during mitosis showed that Kar3 localizes to microtubules and pole bodies – in a microtubule dependent manner. Like ncd, Kar3 can progressively translocate along microtubules at a rate of 1-2 μm/min, however unlike positive end directed ncd, Kar3 is minus end directed and, during *in vitro* motility assays, is able to depolymerise microtubules preferentially at the minus ends (Endow *et al*, 1994; Meluh & Rose, 1990).

Like Kinesin 13 member MCAK, Kar3 is also able to destabilize taxol stabilized microtubules (Endow *et al*, 1994). Later studies found that though Kar3 can perform mitotic and meiotic function of its own, it can also form heterodimers with two kinesin like proteins, Cik1 and Vik1, both of which are non-catalytic peptides (Barrett *et al*, 2000; Gardner *et al*, 2008; Manning *et al*, 1999).

During meiosis; Kar3-Cik1 is localized at puncta at the spindle midbody and spindle pole bodies, and is essential for karyogamy; whereas Kar3-Vik1 is localized primarily at the spindle poles and is non-essential for karyogamy (Gardner *et al*, 2008; Hepperla *et al*, 2014; Manning *et al*, 1999; Shanks *et al*, 2001).

1.4.3.1.1 Functions of Kar3-Cik1

Kar3 forms a stable heterodimer with Cik1 (Sproul *et al*, 2005). Most studies of Kar3-Cik1 have been carried out in mitotic cultures or during karyogamy. In mitosis, at the spindle midzone, Kar3-Cik1 heterodimer is a minus ended microtubule crosslinker and important for ipMTs organization and alignment, facilitating Cin8 antiparallel sliding action and thus spindle elongation (Probably in conjunction with other crosslinking proteins such as ase1p) (Hepperla *et al*, 2014).

Deletion of either Cik1 or Kar3 show reduced spindle length and metaphase arrest, which is lethal when combined with a spindle checkpoint protein

mutation indicating that resultant spindle disorganization is responsible for triggering the spindle checkpoint (Hepperla *et al*, 2014; Endow *et al*, 1994; Saunders *et al*, 1997; Hoyt *et al*, 1993).

During karyogamy, studies of Kar3-Cik3 heterodimer function during karyogamy showed that whilst Kar3 is most similar to a HSET in sequence, Kar3-Cik1 shares function with MCAK - with its ability to promote plus-to-minus end microtubule shortening. MCAK ATPase activity is stimulated by free tubulin heterodimers *in vitro*, or by addition of stable tubulin microtubules. This finding has led to the theory that ATP turnover is required in MCAK to dissociate from tubulin dimers, after microtubule destabilization (Hunter *et al*, 2003).

Whilst Kar3-Cik1 does not hydrolyze ATP at a higher rate in the presence of soluble free tubulin dimers, it is increased in the presence of taxol stabilized microtubules (Though ~20 times slower than MCAK). Depolymerisation was observed primarily from the positive end of the microtubules, and was dependent on either the motor, or hydrolysable ATP being present in the in vitro reaction (Sproul *et al*, 2005)

Meiotic studies of Kar3-Cik1 show depletion of either causes a meiotic arrest at prophase 1, with Cik1 deletion the less severe of the two consistent with the idea that Kar3 has additional unique roles during meiosis to Kar3-Cik1 (Shanks *et al*, 2001, 2004). Kar3 null cells were unable to achieve proper

synaptonemal complexes, to perform proper recombination, indicating that spindle regulation could play an important role in meiosis long before the bipolar spindle is formed (Bascom-Slack & Dawson, 1997).

1.4.3.1.2 Functions of Kar3-Vik1

During mitosis, In vitro studies suggest at Kar3-Vik1 at the pole bodies could promote kinetochore microtubule depolymerisation, triggering poleward tubulin flux (Endow *et al*, 1994; Hepperla *et al*, 2014). Studies assaying Vik1 importance during meiosis indicate that Kar3-Vik1 play relatively smaller, redundant roles during meiosis, and that abnormalities are likely owing to chromosome instability present in diploid cells as a result of mitotic defects and chromosome segregation abnormalities (Manning *et al*, 1999; Shanks *et al*, 2001).

1.4.4 Kinesin 5 family

Kinesin 5 proteins are classified by their localisation to spindle microtubules and essential role in spindle formation by pole segregation. Human kinesin 5 protein Eg5, is homologous to drosophila KLP61F, Budding yeast Cin8/Kip1 and Fission yeast Cut7 (Sawin *et al*, 1992; Roof *et al*, 1992; Lawrence *et al*, 2004).

Compared to the many kinesins in human cells, *S.cerevisiae* contains only 6 known kinesins, as such they provide a useful model for studying microtubule

based motor proteins. Of the 6 motor proteins, Kip1p, Kip3, Kar3 and Cin8 operate within the nucleus, whilst Dynein, Kip2, kip3 and Kar3 operate within the cytoplasm of the cell (Hildebrandt & Hoyt, 2000; Tytell & Sorger, 2006).

Each protein has a unique amino acid code and overlapping functions, meaning the absence of one protein does not fully compromise cell function (Hoyt *et al*, 1993; Saunders & Hoyt, 1992). Despite large genetic differences, many budding yeast processes and mechanisms are conserved in higher eukaryotes, providing an opportunity to study a stripped-down version of complex mechanisms during cell division.

1.4.4.1 S.cerevisiae Cin8 and Kip1

Cin8p and Kip1 are *Saccharomyces cerevisiae* protein members of the kinesin-5 family plus-ended directed motors (BimC motors), localized at kinetochores (Tytell & Sorger, 2006). They act redundantly during mitosis to generate outward force on the spindle poles in an assembling, bipolar, mitotic spindle (Hoyt *et al*, 1993). In Xenopus and human, homologue Eg5 is essential for bipolar spindle assembly, absence of which results in monopolar asters (Sawin *et al*, 1992). In addition to establishing a bipolar spindle, Cin8 and Kip1 are redundantly essential for maintenance of a bipolar spindle. *cin8-Δ* results in frequent spindle collapse and as a result, delayed mitotic progression (Saunders & Hoyt, 1992).

Stabilization of pre-anaphase spindles is achieved by counteracting forces. Outward forces are provided by Cin8 and Kip1 antiparallel microtubule sliding, whilst the inward force is provided by Kar3 depolymerase action at spindle poles (Saunders *et al*, 1997). *kar3-Δ* is able to partially counteract *cin8-Δ kip1-Δ*, indicating an antagonistic action of microtubules, whilst specific mutations in Kar3 force generating motor domains are able to completely nullify the unviability caused by *cin8-Δ kip1-Δ*.

Together this indicates that Kar3 has antagonistic functions to Cin8 and Kip1 with regards to bipolar spindle assembly, but also may share some functions which allow proper chromosome segregation for future viability (Hoyt *et al*, 1993; Saunders & Hoyt, 1992).

This thesis aims to establish an in cell model to illustrate current thinking on MCAK action on microtubules. Mainly, it aims to Investigate in cell relationship between MCAK 3D conformation and activity. In detail, it tries to look in finer resolution, at MCAK distribution on different microtubule populations within a cell and whether changes in conformation alter localisation on the microtubule, and whether this translates to a change in activity.

The second half of the thesis aims to assay the individual contributions of kinesins to proper meiosis, with a long term vision to compare kinesin function in mitosis and meiosis, using budding yeast as a model.

Chapter 2:

Experimental Procedures

2.1 General Information

2.1.1 Supplier information

Reagents and consumables were provided by G.E. Healthcare, Life Technologies, Roche, Sigma, Starlab, Thermo Fisher Scientific, Qiagen and VWR International, Biolabs unless stated otherwise. *S.cerevisiae* growth component were supplied by Formedium, Difco and Sigma. Human cell growth components were provided by Lonza

2.1.2 Sterilization

Most solutions used were sterilized by filtration using a 0.22 μm bottle top (Nalgene) or 0.22 μm syringe (Millipore) filters. Growth media was autoclaved at 120°C and 15 pounds/inch^2 for 15 min. Glassware was sterilized by baking at 250°C for 16 h.

2.2 Microbiology

2.2.1 Bacterial Methods

2.2.1.1 Bacterial Strains

DH5α [Invitrogen] or TOP10 [Invitrogen] E. coli strains were used for cloning and amplification of plasmids. BL21- CodonPlus[DE3]-RIL E. coli strain [Stratagene] were used for protein expression.

Strain genotypes:

TOP10 Chemically competent E. coli [Invitrogen]

F- mcrA Δ(mrr-hsdRMS-mrcBC) φ80lacZΔM15 ΔlacX74 nupG recA1 araD139 Δ(araleu)7697 galE15 galK16 rpsL(StrR) endA1 λ-

DH5α Chemically competent E. coli [Invitrogen]

F- endA1 glnV44 thi-1 recA1 relA1 gyrA96 deoR nupG Φ80dlacZΔM15 Δ(lacZYAargF)U169, hsdR17(rK - mK +), λ–

BL21-CodonPlus[DE3]-RIL E. coli [Stratagene]

F– ompT hsdS(rB - mB +), dcm+ Tetr gal endA Hte (argU ileY leuW Camr)

2.2.1.2 Bacterial Growth Media

Media	**Composition**	**Concentration**
Luria Bertani (LB)	Difco Bacto-tryptone	1% (w/v)
	Difco Bacto-yeast extract	0.5% (w/v)
	NaCl	0.5% (w/v)
	Difco Bacto Agar (solid media only)	2% (w/v)
	(pH adjusted to 7.2 with NaOH)	
SOC	Bacto-tryptone	2% (w/v)
	Bacto-yeast extract	0.5% (w/v)
	NaCl	20mM
	Glucose	20mM
	$MgCl_2$	10mM
	$MgSO_4$	10mM
	KCl	10mM

Table 2.2-1 Bacterial Growth Conditions

2.2.1.3 Bacterial Growth Conditions

All *Escherichia coli (E. coli)* strains were grown at 37ºC in liquid LB media or on solid LB-agar plates. DH5α [Invitrogen] or TOP10 [Invitrogen] E. coli

strains were used for cloning and amplification of plasmids. BL21-CodonPlus[DE3]-RIL *E. coli* strain [Stratagene] was used for protein expression. Antibiotics were added to media and Agar (Ampicillin/Kanamycin) at 100 mg/mL/ 50 mg/mL respectively. Cultures were typically incubated at 37°C with shaking at 200prm and kept on LB plates at 4°C for 1-2 weeks with the appropriate resistance drug. For long-term storage, bacterial strains were re-suspended in 20-25% glycerol in cyrotubes and frozen at -80°C.

2.2.1.4 Transformation of E.coli strains by *Heat Shock*

50-100 μl chemically competent DH5α *E.coli* cells were thawed slowly on ice in 1.5 ml eppendorf tubes. An appropriate amount of DNA, 0.5-5 μl of DNA dissolved in TE buffer (0.01M Tris-HCl pH7.5, 0.001M EDTA) to a total amount of ~500ng, was added to cells and mixed by tapping. Cells were incubated for >10' on ice then at 42 °C on a heat block for 60", then returned to the ice for several minutes to cool samples to 4°C. For recovery, Cells reaction mixes were incubated at 37 °C for >30' with 300 μl of SOC. Cultures were centrifuged at 3000 rpm for 3' to loosely pellet the cells. The majority of the supernatant was aspirated leaving ~150 μl with which to re-suspend the cells and spread onto pre-warmed LB solid media plates containing the appropriate resistance drug. Glass beads or a sterile glass rod were used to spread cells on Agar plates.

2.2.2 S.cerevisiae Methods

2.2.2.1 S.cerevisiae strains

All *S. cerevisiae* strains used in this study are derivatives of SK1. All strains are diploids. Strains in this study are listed in the appendix. The origins of alleles used in this study are as follows:

Allele	**Source**
Previously publishes alleles	
ndt80Δ::LEU2	(Xu *et al*, 1995)
SPC42-tdTomato::NatMX6	(Fernius & Hardwick, 2007)
CNM67-3mCherry::NatMX4	(Matos *et al*, 2008)
leu2::pURA3-TetR-GFP::LEU2	(Michaelis *et al*, 1997)
leu2::pURA3-TetR-tdTomato::LEU2	(Katis *et al*, 2010)
CEN5::tetOx224::HIS3	(Nasmyth *et al*, 2000)
pGAL1-NDT80::TRP1 ura3::pGPD1-GAL4(848).ER::URA3	(Schindler *et al*, 2003)
his3::HIS3p-GFP-TUB1-HIS3	(Matos *et al*, 2008)
Gene Deletions	
kip1Δ::NatMX6	PCR-based deletion (Longtine *et al*, 1998) using AMp683 Creator: Colette Fox
kip2Δ::NatMX6	
kip3Δ::NatMX6	
cin8Δ::NatMX6	

Promoter Replacements	
kar3::KANMX6::pCLB2-3HA-KAR3	PCR based Replacement (Longtine *et al*, 1998) using AMp348, Modified pFA6a-kanMX6-PGAL1-3HA plasmid, replacing PGAL with -1000 to +6 of CLB2 gene) Creator: Brian Lee
cin8::pCLB2-3HA-CIN8::KanMX6	
Gene Tagging	
cin8-GFP::KanMX6	PCR based tagging (Longtine *et al*, 1998) using AMp296 Creator: Frank Stegmeier
KIP1-3HA::KANMX6	PCR based tagging (Longtine *et al*, 1998) using AMp270 Creator: Brian Lee
CIN8-3HA::KanMX6	PCR based tagging (Longtine *et al*, 1998) using AMp270 Creator: Brian Lee
CIN8-SZZ(TAP)::KanMX6	PCR based tagging (Longtine *et al*, 1998) using AMp636 Creator: Jin Shin

Table 2.2-2 S. cerevisiae strains used in this study.

2.2.2.2 S.cerevisiae media

Solution	**Reagents**
YPDA	2% (w/v) Bacto-peptone 1% (w/v) Bacto-yeast extract 2% (w/v) Glucose 0.3 mM Adenine
YPG	2% (w/v) Bacto-peptone 1% (w/v) Bacto-yeast extract 2.5% (w/v) Glycerol
4%-YPDA	2% (w/v) Bacto-peptone 1% (w/v) Bacto-yeast extract 4% (w/v) Glucose
BYTA	2% (w/v) Bacto-peptone 1% (w/v) Bacto-yeast extract 1% (w/v) Potassium Acetat 50 mM Potassium Phthalate
Sporulation media	0.3% (w/v) Potassium acetate (pH 7)
For making solid media plates, 2% (w/v) agarose was added to liquid solutions prior to autoclaving.	

Table 2.2-3 *S.cerevisiae* Media used throughout this study

2.2.2.3 G418 treatment:

Used for KanMX6 selection in solid media. G418 powder was dissolved in sterile water, filter sterilized and added to cooled melted agar-media at a final concentration of 300 µg/ml.

2.2.2.4 Hygromycin treatment:

Used for HPHMX6 selection in solid media. Hygromycin solution (50 mg/ml) was added to cooled melted agar-media at a final concentration of 300 µg/ml.

2.2.2.5 Clonat treatment:

Used for NatMX4 selection in solid media. Clonat stock solution (200 mg/ml) was added to cooled melted agar-media at a final concentration of 100 µg/ml.

2.2.2.6 Induction of S.cerevisiae Sporulation

For meiotic experiments, diploid strains were removed from -80°C storage and grown on YPG solid media plates ~16 h. Next, cells were patched to 4% YPDA plates ~24h. YPDA liquid cultures were inoculated with *S.cerevisiae* strains and grown ~24h before dilution to OD_{600} =0.2 in BTYA liquid media until OD_{600} = 6-10 (~24h). Cells were washed twice, centrifuged at 3000rpm for 3' between washes, in sterile water and resuspended in SPO liquid media at OD_{600} = 1.8. Meiosis was performed asynchronously at 30°C and 250rpm shaking.

2.2.2.7 GAL-NDT80 block and release method for synchronous meiosis

To create a more synchronous cell cycle entry in cultures I used the GALNDT80 block and release mechanism, explain in Picard, D (1999). The Gal1,10 UAS is placed upstream of NDT80 and controlled by Gal4-ER transcription factor in the presence of estradiol. Diploid strains homozygous

for *GAL-NDT80* and *GAL4(848)-ER* arrest in pachytene in the absence of NDT80, and commence the cell cycle upon β-estradiol addition and consequential NDT80 transcription. (Carlile & Amon, 2008).

Before block-release, strains were prepared for sporulation as described in (Carlile & Amon, 2008) and remained in SPO media for 6h. 1 μM of β-estradiol is added to strain cultures to induce transcription of *NDT80* and thus progression through meiosis. Samples were taken at 15' intervals for 3 h, then at 30' intervals for a total meiotic progression time of 6h (Picard, 1999).

2.2.2.8 Depletion of proteins specifically in meiosis

To specifically deplete proteins during meiosis, the native promoter of the relevant gene was replaced with *pCLB2*, a mitosis-specific promoter (Lee and Amon 2003).

2.2.2.9 S.cerevisiae storage

For long-term storage of strains, *S.cerevisiae* were resuspended in 20% glycerol in cryotubes and stored at -80°C.

2.2.2.10 Lithium Acetate transformation

S.cerevisiae strains were grown to OD_{600}=>6 before dilution in YPDA to OD_{600}=0.2. Cells were grown until OD_{600}=0.8-0.9 at which point they were centrifuged at 3000rpm for 3', resuspended twice in sterile water and transferred into a 1.5ml Eppendorf tube. Cells were washed in 1ml LiTE and resuspended in 250 μl LiTE. 50μl of cells were added to precipitated PCR

product from a 400 µl PCR reaction and 10 µl sonicated, single-stranded salmon sperm DNA. 300 µl of LiTE in 40% PEG was added to the cell mixture, which was then shook at 250rpm for 1h at 37°C, then at 42°C for 15 minutes without shaking. Cells were gently pelleted by centrifugation 3000rpm for 3' and resuspended in 200 µl of sterile water to spread on YPDA agar plates. For drug selection YPDA were replica plated onto appropriate drug-selection plates one day after transformation.

Solution	**Reagents**
LiTE	0.1 M LiAc
	10 mM Tris.HCl (pH 7.5)
	1 mM EDTA
40% PEG	0.1 M LiAc
	40% PEG 4000
	10 mM Tris.HCl (pH 7.5)
	1 mM EDTA

Table 2.2-4 Reagents required for Lithium Acetate Transformation

2.2.2.11 Gene crossing between S.cerevisiae strains.

Diploids of strains cumulatively containing the required gene modification were formed by mixing opposite mating types a and α on 4% sucrose YPDA agar plated. To select for diploid colonies later, fewer cells of the strain containing a unique marker, or the α strain were added to the cross. Cell mixtures were left >6h at 37°C or more than 12h at room temperature to

allow for mating and diploid formation. Diploids were selected by streaking diploid mixtures to single colonies on the plates containing selective pressures of the limiting strain of the cross. Alpha factor – WHWLQLKPGQPMY, synthesized by Peptide Protein research, was used if fewer α mating type cells were used). Diploid colonies were patched on 4% YPDA agar plates to increase biomass before transfer onto SPO agar plates. After48h on SPO agar media tetrad asci were digested in 20µl 0.1mg/ml zymolyase (AMS Biotechnology), diluted in 1M sorbitol. Cells were digested for 15-60'. Digestion was halted using 1ml of sterile distilled water. 20µl of *S.cerevisiae* tetrad solution were transferred to a YPDA plate and dissected using a Singer MSM 400 micromanipulator. Dissected spores were incubated at 30˚C for 2-3 days and replica plated onto selective plates to test the genotype of each spore. Colony PCR was carried out to identify constructs, if required.

2.3 Human Cell Manipulation

2.3.1 Cell Lines

Polyclonal U2OS GFP-EB3, mCherry-CENPA were designed and created by Julie Welburn, using viral integration of the pBABE vector into the genome, selected using Blastocidin 2mg/ml. (Cheeseman & Desai, 2005).

2.3.2 Cell Culture

Cell cultures were maintained at 37 °C in a humid atmosphere with 5% CO2 in DMEM (Lonza) supplemented with 10% FBS (Invitrogen), 100 U/ml penicillin and 100 μg/ml of Streptomycin (Gibco).

2.3.3 Cell Passage

Cell cultures were passaged when a confluency of 70-80% was reached, and never seeded into new dishes at a confluency <10%. Old media was aspirated and washed off with 10ml DPBS (SH30028.02 - Thermo Scientific HyClone). Cells were incubated ~1' in 1ml TripleE media (12563029 - Gibco) to detach them from the dish, re-suspended and diluted in modified DMEM before seeding onto fresh 10cm dishes (430167 - Corning B.V Life Science).

2.3.4 Cell Seeding for immunofluorescent or live cell imagining

For live imaging, cells were seeded and cultured on sterile 35-mm glass bottom micro-well dishes (MatTek). Dishes were washed with sterile DPBS before cell cultures were added to the wells. Cells were incubated 24h to allow reattachment to the new surface before further manipulation. For immunofluorescence, cells were seeded on 18-mm glass coverslips coated with poly-L-lysine (Sigma–Aldrich).

2.3.4.1 Preparing Poly-Lysine Coated Coverslips

To prepare 18mm glass coverslips for poly-L-lysine coating they were incubated in 1M HCl at 50-60°C for 4-16h; cooled; washed extensively - first

with sterile water, then ethanol; and dried. Coverslips (Marienfield) were coating using 10-15ml 1mg/ml poly-L-lysine (Sigma–Aldrich) for 30’ with agitation, before a repeat of water, ethanol and drying steps described above.

2.3.5 Transient plasmid transfection and RNAi

Plasmid transfection was performed on cell cultures at 70-80% confluency while siRNA was performed at a cell confluency of 40-50%, both using Lipofectamine 2000 (Invitrogen) kit. Cells were incubated with OPTI-MEM (ThermoFisher) 1h prior to transfection.

400ng-1µg of plasmid was incubated with OPTI-MEM to a total volume of 250µl and 5µl of Lipofectamine was incubated with OPTI-MEM to a total volume of 250µl separately. After 5’ incubation the Lipofectamine mix was added to the plasmid mix dropwise and incubated together for 30’ at room temperature. Cells were washed with OPTI-MEM and left with 1.5ml fresh modified DMEM before adding the Lipofectamine/Plasmid mix to the cells dropwise.

RNAi oligos previously described in (Welburn & Cheeseman, 2012) (Pharmacon SMART-pool siRNA, CGAAAUGGGUUGCGAUGAU, GCUCAGAAACUCCACAUAU, GCACAUGAUCGAAGAGUAU, and CAAGGUGUAUGAUUUGUUG) were used and obtained full depletion of GFP-Kif2b. Full depletions was confirmed by Western blot using a polyclonal anti-MCAK antibody (GL Biochem) recognizing the C-terminus peptide -

$_{709}$QLEEQASRQISS$_{720}$.

2.4 Genetic Engineering

2.4.1 Plasmids

Plasmid number	Name	Description	Origin
AMp195	*pFA6a-kanMX6*	Described in (Longtine, McKenzie et al. 1998)	Mark Longtine
AMp199	*pFA6a-GFP(S65T)-His3MX6*	Described in (Longtine, McKenzie et al. 1998)	Mark Longtine
AMp348	*pFA6a-pCLB2-3HA-kanMX6*	Described in (Lee and Amon 2003)	Brian Lee
AMp495	*pFA6a-6HA-kanMX6*	6HA cloned into AMp195	Brian Lee
AMp636	*pFA6a-SZZ(TAP)-kanMX6*	SZZ(TAP) cloned into AMp195	
AMp683	*pFA6a-NAT*	Described in (Hentges, Van Driessche et al. 2005)	Kevin Hardwick

Table 2.4-1 Plasmids used in this study

2.4.2 Extraction of Genomic DNA from E.coli by Phenol:chloroform

Solution	Reagents
DNA breakage buffer:	2% (w/v) Triton X-100
	1% (w/v) SDS

	100 mM NaCl
	10 mM Tris.HCl (pH 8.0)
	1 mM EDTA

Table 2.4-2 Buffers required for Phenol:chloroform extraction of genomic DNA from *E.coli*

A small amount of *S.cerevisiae* was resuspended in 200µl DNA breakage buffer (2% Triton X-100, 1% SDS, 100mM NaCl, 10mM Tris-Cl pH8.0, 1mM EDTA). Approximately 100µl of silica beads (Biospec) and 200µl phenol:chloroform were added and the mixture and vortexed for 4 minutes. Samples were centrifuged at 13000rpm for 5' before adding the upper aqueous layer of the supernatant to 900 µl of cold ethanol. Samples were spun at 13000rpm and the pellet washed with 70% ethanol. Pellets were left to air-dry and subsequently resuspended in 50µl TE buffer (0.01M Tris-HCl pH7.5, 0.001M EDTA). DNA concentration was measured by NanoDrop [Thermo Scientific] and the sample was stored at -20°C.

2.4.3 Extraction of plasmid DNA from *E. coli by* mini-prep (Non-Qiagen)

Solution	**Reagents**
GTE buffer:	50 mM glucose
	10 mM EDTA
	25 mM Tris (pH 7.5)
Alkaline SDS:	200 mM NaOH
	1 % (w/v) SDS
High salt buffer:	2.5 M potassium acetate (pH 4.8)
TE buffer:	0.01M Tris-HCl pH7.5,
	0.001M EDTA

Table 2.4-3 Buffers required for *E.coli* plasmid miniprep (Non-Qiagen)

2 ml of LB-Amp, with appropriate selection drug, was inoculated with *E. coli* and incubated at 37°C overnight. Cells were centrifuged at 3000 rpm for 3' and resuspended in 100 µl of GTE by vortexing. 150 µl of alkaline SDS was added and mixed via inversion, then 150 µl of cold high salt buffer before incubation on ice for 15 mins. The reaction centrifuged at 14000 rpm for 5'. DNA was precipitates from the supernatant by the addition of 900 µl of cold ethanol and 10' incubation at -20 °C. After centrifugation at 14000 rpm for 5', the DNA pellet was washed with 200 µl of 70% ethanol, air dried, and resuspended in 50 µl of TE.

2.4.4 Extraction of plasmid DNA from *E.coli* by mini-prep (Qiagen)

2 ml of LB-Amp, with appropriate selection drug, was inoculated with *E. coli* and incubated at 37°C overnight. Cells were centrifuged at 3000 rpm for 3' and resuspended in 250 µl of P1 buffer. 250 µl of P2 was added and the mixture was inverted. 250 µl N3 was added and the mixture further inverted before centrifugation for 10' at 13000rpm. Plasmid containing supernatant was added to an equilibrated QIAprep column on a QIAvac vacuum manifold. Columns were washed with 1ml PB. Remaining buffer was removed by centrifugation at 13000 rpm. Plasmids were eluted with 30 µl elution buffer by centrifugation at 13000rpm after 2min incubation to increase yield.

2.4.5 Agarose gel electrophoresis

Solution	Reagents
TAE buffer:	40 mM Tris
	1 mM EDTA
	0.11% (v/v) acetic acid

Table 2.4-4 Reagents required for agarose gel electrophoresis

Agarose was dissolved in TAE buffer using heat applied by electrophoresis. Ethidium bromide was added to the gel at a final concentration 0.5 µg/ml. DNA samples were mixed with 1 x Orange G DNA loading buffer (NEB) and electrophoresed at 90-140 V, alongside a 1kb DNA ladder (NEB). DNA was visualized using a UV trans-illuminator system.

2.4.6 Polymerase Chain Reactions

PCR was performed using a Bio-Rad DNAEngine Thermal Cycler.

2.4.6.1 General PCR Reactions

For most PCR reactions pertaining to yeast genetics applications, Taq polymerase purified in the lab was used.

Solution	Reagents
10x PCR buffer:	100 mM Tris-HCl (pH 8.3)
	500 mM KCl
	20 mM $MgCl_2$
	0.1% (w/v) gelatin
PCR reaction:	10-500 ng template DNA
	1 µM of each oligonucleotide primer
	0.2 mM dNTPs
	1x PCR buffer
	DNA polymerase
	Sterile distilled water

Table 2.4-5 Solutions required for PCR

Programme Phase	Cycles	Temperature (°C)	Time
Pre-incubation	1	95	5’
Amplification	24	95	30”
		55	30”
		72	1’/kb
Final Extension	1	72	5’

Table 2.4-6 General PCR Program

For reactions where sequence fidelity was essential, ExTaq DNA polymerase (TaKaRa) was used with 10x PCR buffer and dNTPs provided by the manufacturer.

PCR reaction pertaining to Human cell transformation or protein expression in *E.coli* was performed using Phusion (Fisher Scientific) was used.
PCR programmes varied depending on the size of the expected product and the annealing temperature of primers used.
Where possible plasmid mutagenesis was performed using standard PCR protocol described here, integrating the mutagenesis into the primers used in the reaction.

2.4.6.2 S.cerevisiae colony PCR

A fraction of *S.cerevisiae* colony DNA was added to 0.2 ml PCR tubes (Axygen) containing 20 µl of PCR reaction. PCR programmes varied depending on the annealing temperature of primers used.

Programme Phase	**Cycles**	**Temperature (°C)**	**Time**
Pre-incubation	1	95	10’
Amplifiction	30	95	30”
		55	30”
		72	1’

Final Extension	1	72	5’

Table 2.4-7 *S.cerevisiae* colony PCR programme

2.4.6.3 Sequencing of S.cerevisiae genome

To confirm point mutations in *S.cerevisiae* strains, the desired section of DNA was amplified from purified genomic DNA by PCR using ExTaq polymerase (TaKaRa). 3µl of PCR products were treated with 0.5µl ExoI (Biolabs) and 0.5µl thermo-sensitive alkaline phosphatase (Biolabs). Reactions were incubated at 37˚C for 15 minutes and then at 80˚C for 15 minutes to deactivate enzymes. 4µl of 1X BigDye Terminator v3.1 (Applied Biosystems) and 2µl 8µM primer were added to digested PCR reactions. PCR was then carried out with the following conditions:

Programme Phase	**Cycles**	**Temperature (°C)**
Pre-incubation	96˚C	30 seconds
Amplification (25 cycles)	96˚C	30 seconds
	55˚C	15 seconds
	60˚C	4 minutes
Final extension	72˚C	5 minutes

Table 2.4-8 Sequencing PCR Program

Samples were sequenced on an ABI 3730 DNA analyzer (Applied Biosystems) by the School of Biological Sciences sequencing service, University of Edinburgh.

2.4.6.4 Restriction digest and ligation

Restriction digests and ligations were performed using New England Biolab (NEB) restriction enzymes and buffers according to manufacturer's instructions. Digests were subject to agarose gel electrophoresis (section 2.4.5) to quickly confirm the identity of plasmids fragment. Ligations were performed to a total volume of 10 µl and the whole amount transformed into *E.coli.*

2.5 Immunostaining and Immunofluorescence

2.5.1 Immunofluorescent Staining of Human cell cultures

To stain cells immunofluorescently, cells seeded on 18mm coverslips in 35-mm glass bottom micro-well dishes (MatTek) were first fixed using methanol of formaldehyde. Cells were washed with DPBS at 37 °C to remove excess modified DMEM. 2ml methanol stored at -20 °C or 3.4% formaldehyde at room temperature was added to cells, and incubated at the same temperature for 10'. Cells were washed three times with Tris-buffered Saline solution with 0.1% Tx100 detergent (TBST)

Solution	**Reagent**
TBST	50mM Tris-HCl
	150mM NaCl
AbDil	2% BSA
	0.5% Sodium Azide

Table 2.5-1 Solutions required for immunofluorescence of human cell cultures.

After fixation, cell adhered coverslips were moved to a humid, light free chamber and incubated with 500μL AbDil blocking solution at room temperature for 30' before primary antibody was added, diluted in AbDil for ~1h at RT. Coverslips were washed three times with 3ml TBST, always adding buffer at one edge and removing at the other to create a clean wash flow. Secondary antibody was diluted in TBST and incubated with coverslips for ~1h at RT. After three 1ml TBST washes cells were incubated with 1mg/ml of Hoechst diluted to 1 μg/ml in TBST for 3' at RT. Cells were washed a final three times with 1ml TBST and mounted on Starfrost glass slides (Fisher Scientific) using prolong mounting solution (Molecular Probes). After ≥12h coverslips were sealed with nail varnish and stored at -20°C until imaging.

Antigen	**Species**	**Concentration**	**Supplier**
NDC-80	Rabbit	1:1000	Cheeseman Lab
Tubulin	Mouse	1:500	Sigma
Centrin	Rabbit	1:1000	Cheeseman Lab
EB1	Mouse	1:1000	BD biosciences

Table 2.5-2 Catalogue of antibodies used on human cell cultures

Cy2, Cy3, and Cy5-conjugated secondary antibodies (Jackson Laboratories and Life Technologies) were used at 1:200, 1:300 and 1:300 respectively.

Hoechst was used at 1μg/ml

2.5.2 Sample preparation and imaging or live Human cells

Before live cell imaging media in human cell cultures containing modified DMEM was replaced with CO_2 independent L15 media (Lonza) or FluoroBrite DMEM (Life Technologies) modified with 10% FBS. Media in cultures containing OPTI-MEM was not changed. Nocodazole (Acros Organics) was administered 1h before live imaging. Live cell images were obtained with a 5% CO_2 flow and at 37 °C.

TIRF microscopy was performed using 100x Apo TIRF lens at 37 °C. Images were acquired with 100ms exposure at 15% and 20% 485/594 laser intensity respectively for 60-120 seconds every second using Metamorph software.
With fixed and live epifluorescent microscopy, multiple Z-section Images were acquired on a Deltavision® Elite live cell imaging system (Applied Precision) with an Olympus IX-71 microscope and a CoolSnap HQ2 CCD camera, equipped with a 100×, 1.4 NA Olympus U-PlanApo objective, 1×1 binning. 6–12 *z*-sections were acquired at 0.5- to 1-μm steps. Multi-point images were taken using SoftWoRx, movies were assembled in Image-Pro Plus and processed further in ImageJ.

Adobe illustrator was used to construct figures in conjunction with Adobe Photoshop. Linear changes have been made to all images, consistently within

experiments. Non-linear manipulations are stated in figure legends.

2.5.3 Immunofluorescent staining of tubulin in meiotic S.cerevisiae

Solution	**Reagents**
Sorbitol-citrate:	1.2 M Sorbitol
	0.1 M K_2HPO_4
	36 mM Citric acid
PBS-BSA:	1% (w/v) BSA
	40 mM K_2HPO_4
	10 mM KH_2PO_4
	0.15 M NaCl
	0.1% NaN_3
DAPI mount:	9 mM *p*-phenylenediamine
	40 mM K_2HPO_4
	10 mM KH_2PO_4
	0.15 M NaCl
	0.1% NaN_3
	50 ng/ml DAPI
	90% (w/v) Glycerol
Digestion mix	1.2M Sorbitol-citrate
	10% Glusolate (Perkin Elmer)
	30 µg/ml Zymoylase (AMS

	biotechnology)

Table 2.5-3 Solutions required for immunofluorescent staining of tubulin in meiotic S.cerevisae

200 µl of meiotic culture from meiotic culture was centrifuged at 13000 rpm for 1'. Cell pellets were resuspended in 500 µl of 3.7% formaldehyde in 0.1 M KP_i buffer (pH 6.4) and incubated >24h at 4°C, washed three times in 1 ml 0.1 M KP_i, and 1 ml 1.2M sorbitol-citrate. Cells were the frozen at 20 °C. Immunofluorescent slides were prepared by rinsing with sterile water and treating wells with 5µl 0.1% poly-lysine for 5 minutes. Slides were rinsed again and left to air-dry completely.

Thawed samples were centrifuged at 13000 rpm for 3'. Cells pellets were resuspended in digestion mix and incubated at 30 °C for 2-6h – until cells mostly appeared phase dark with jagged edges under a light microscope. Digested cells were pelleted at 3000rpm for 3' and all but 30 µl supernatant removed. 5 µl of resuspended cell pellet was added to prepared immunofluorescent wells. Cells were allowed to attach to glass slides for 10' before the digestion mix and unbound cells were removed by aspiration. Cells were fixed to slides by submerging slides in methanol for 3' followed immediately by acetone for 10" and allowing slides to completely air-dry. 5 µl of primary antibody solution was added per well and incubated for 2 h at room temperature in a dark moisture chamber. After incubation, cells were washed three times with 5 µl PBS-BSA and then 5 µl of secondary antibody

solution was added per well. Slides were incubated for 2 h in a dark moisture chamber at room temperature. Cells were washed five times with 5 µl PBS-BSA before 3 µl of DAPI-mount was added per well. A glass coverslip was placed on top of each slide and sealed with clear nail polish. Slides were stored at -20°C before and after spindle analysis.

Protein	**Fixation time**	**Primary antibody**	**Secondary antibody**
Tubulin	Overnight (4°C)	rat α-TUB 1:50	α-rat FITC 1:100

Table 2.5-4 Antibody dilutions for tubulin staining in *S.cerevisiae* – Antibodies were dilutes in PBS-BSA

2.5.4 Sample preparation for imaging fixed *S.cerevisiae* throughout meiosis

At time points throughout meiosis, 200 µl of culture was added to 10 µl of 37% formaldehyde and incubated at room temperature for 8-10'. Fixed cells were pelleted at 13000 rpm for 2', washed with 1 ml of 80% ethanol and resuspended in 20 µl of 1 µg/ml DAPI. To view in the microscope, 3-4 µl of cells were mounted onto glass slides under a coverslip.

Imaging of fixed cells or live cells on at isolated time-points, viewed on slides, was carried out using a Zeiss Axio Imager Z1 and a Photometric EMCCD camera. Images were taken using Micro-Manager 1.4 and processed using ImageJ software.

2.5.5 Sample preparation and imaging or live *S.cerevisiae* throughout meiosis

For live cell imaging, cells were released into meiosis in flasks and shaken for 2.5 hours at 250rpm at 30 °C. Meiotic cultures where then transferred to a 35mm 6 well glass bottomed culture dishes (Ibidi) pretreated with Concanavalin A (Scientific laboratory supplies). To treat culture dishes, wells were washed once with sterile water and covered using 90 µl of concanavalin. Dishes were incubated at 30 °C for 15' before the concanavalin was removed and the well was washed with sterile water 3 times. Prophase block-release strains were transferred onto dishes 15 minutes after release from pachytene.

For the generation of movies, a Deltavision® Elite live cell imaging system was employed in a 30 °C heated chamber with an Olympus IX-71 microscope and a Photometric EMCCD Cascade II camera. Multi-point images were taken using SoftWoRx, movies were assembled in Image-Pro Plus and processed further in ImageJ.

Camera, shutters and stage were controlled through the SoftWorx software (Applied precision) on a Linux operating system. Cells were imaged at 15-minute intervals for a total of 12 hours (asynchronous meiotic release cultures) or 6 hours (release from NDT80 block). Typically, 6-8 points were imaged per strain, with 7 z-stacks at each point with 0.85µm spacing. For imaging of TetR-ymEos3.2 only 6 z-stacks were acquired because ymEos3.2

was found to bleach very quickly. Imaging conditions for different proteins are outlined in table 6.7. Images were analyzed and processed using Image Pro Premier (Media Cybernetics) and ImageJ software (National Institutes of Health).

Protein	**Camera gain**	**Exposure time**	**% transmitted light**
TetR-GFP MTW1-tdTomato PDS1-tdTomato	290	0.2 seconds	5%
TetR-tdTomato	290	0.1 seconds	5%
Tub1-GFP	290	0.2 seconds	5%

Table 2.5-5 Typical imaging conditions

2.6 Biochemical assays

2.6.1 Protein Expression and purification of MCAK and its variants from *E.coli.*

Protein expression and purification of MCAK and its variants, including C-terminus and motor domain is described in depth in (Talapatra *et al*, 2015). BL21(DE3) Codon plus cells transformed with HIS-3C-mCherry-CT at OD_{600} of 0.7–0.8 for 16 h at 18°C and harvested at 5000rpm for 20’ at 4°C and snap frozen in liquid nitrogen. Pellets were thawed in lysis buffer (, , , , ,) and sonicated with 3 rounds of 1’20” with 8” bursts at 4°C. Lysates were clarified by centrifugation at 22000rpm for 1h at 4°C. 6% v/v Nickel bead slurry was equilibrated with lysis buffer before addition to clarified lysate and incubation for 1h at 4°C with rotation. Protein bounds beads were washed 3

times with wash buffer, using 25% v/v of the total lysate volume. Bound proteins were eluted with modified wash buffer containing 2300mM Imidazole in 1ml fractions, 5µl of which were analyzed for purity by SDS-PAGE electrophoresis and coomassie staining. Fractions containing purified HIS-mCherry-CT were pooled and incubated >18h with 100µg/ml 3C protease (Purified by Sandeep Talapatra). Protein sample was run through a Nickle bead column (50% v/v bead slurry) at 4°C several times and resulting protein concentration was calculated by NanoDrap using manufacturer's instructions and checked again for size and purity by SDS-PAGE electrophoresis and coomassie.

Solution	**Reagents**
Lysis Buffer:	0.60mg/ml Lysosoyme
	0.2mM PMSF
	0.03mg/ml DNase
	0.4 mM Sodium orthovanadate
	4 mM β-glycerophosphate
	2 mM Sodium pyrosphosphate
	10 mM Sodium fluoride
Wash Buffer:	50 mM Hepes, pH 7.4
	200 mM NaCl
	1 mM $MgCl_2$
	1 mM ATP

Table 2.6-1 Table showing composition of lysis and wash buffers.

2.6.2 Preparation of Human cell extract for biochemical assays

Adhered cells were washed with 10ml DPBS. Cells were incubated ~1' in 1ml TripleE media to dissociate them from the dish, re-suspended and diluted in 1ml modified DMEM and transferred to 50µl of 3x LDS with 5% beta-mercaptoethanol. After 5' boiling at 100°C samples were stored at -80°C until further use.

2.6.3 Protein binding assay

MCAK mCherry tagged C-terminus was added to a reaction tube with HIS tagged MCAK motor domain at equal concentrations and made to a total reaction volume of 30 µl in HIS purification buffer (Talapatra *et al*, 2015). After 30' incubation at room temperature Nickel beads equilibrated in His purification buffer was added to the reaction and rotated at room temperature for 1h. Beads were washed three times in 5x bed volume in HIS wash buffer before bound proteins were removed by boiling the sample in LDS with 5% beta-mercaptoethanol.

2.6.4 Phosphorylation assay using radiolabeled ATP

20 µl Phosphorylation reaction contained 10 µg substrate, 1x Kinase buffer, 100 µM NaATP, 1 µg of Ipl1p kinase (Invitrogen), 5µCi of p32NaATP. GST-CT was acquired from a 10mg/ml stock, GST-CT_{S715E} was acquired from a 10mg/ml stock purified by Sandeep Talapatra as described in (Talapatra *et al*, 2015). Reaction was incubated at 37°C for 30' before addition of 5 µl 4x

LDS 5% beta-mercaptoethanol and boiled for 5’ at 100 °C. Reactions were electrophoresed on 15% SDS-PAGE gels before drying between Whatmann paper (Amersham) and saran wrap using Hoefer Slab Gel Dryer. Dried gel was exposed to Kodak Bio-Max light film and developed using a Konica-Minolta SRX-101A developer.

Solution	**Reagents**
10x Kinase buffer	20mM Hepes (pH7.5)
	10mM $MgCl_2$
	5100mM $MnCl_2$
	250mM β-glycerophosphate
	10mM DTT

2.6.5 TCA protein extraction from *S.cerevisiae*

Trichloroacetic acid (TCA) protein extraction method was used for protein analysis from cell cycle cultures during meiosis. This method of extraction allows for rapid protein precipitation and preserves protein phosphorylation.

Solution	**Reagents**
3x SDS sample buffer:	187 mM Tris (pH 6.8)
	6% (w/v) β-mercaptoethanol
	30% (w/v) Glycerol
	9% (w/v) SDS
	0.05% (w/v) Bromophenol blue

TE (pH 7.5)	10 mM Tris-HCl
	1 mM EDTA

Table 2.6-2 Solutions required for TCA protein extraction

5 ml of *S.cerevisiae* meiotic culture was centrifuged at 4000 rpm for 3 mins. Cell pellets were resuspended in 5 ml of 5% TCA and incubated on ice for 10 mins. Tubes were centrifuged at 4000 rpm for 3 mins at 4°C, the majority of the supernatant was discarded and the remaining used to transfer the pellet to 2 ml FastPrep tubes (MP Biomedicals). Tubes were briefly centrifuged at 14000 rpm and cell pellets were snap-frozen in liquid nitrogen and stored at -80°C until further processing. Pellets were then resuspended in 1 ml of acetone and centrifuged at 14000 rpm for 7'.Cell pellets were air dried in a fume hood for 2-3 h. Dried pellets were resuspended in 100 µl of ice-cold TE with 2.75 µl of 1 M DTT and 1x Roche EDTA-free protease inhibitors and a small quantity of glass beads (Sigma). Cells were disrupted using a Fastprep Bio-pulveriser FP120, subjecting tubes to 3 x 45 secs disruption at speed 6.0. 50 µl of 3x SDS sample buffer was added and extracts boiled at 100°C for 5 mins. Tubes were spun down at 14000 rpm for 5 mins and eluted protein was transferred to a new eppendorf before loading onto a gel.

2.6.6 SDS Polyacrylamide Gel Electrophoresis (SDS-PAGE)

SDS-PAGE gel electrophoresis was used to separate denatures proteins in a protein mixture by size.

Solution	Reagents
4x Separation buffer:	1.5 M Tris
	0.4% (w/v) SDS
	pH adjusted to 8.8 with glacial acetic acid
2x Stacking buffer:	0.25 M Tris
	0.2% (w/v) SDS
	pH adjusted to 8.8 with glacial acetic acid

Table 2.6-3 Buffers required for SDS Polyacrylamide Gel preparation

	10% Resolution buffer	6% Resolution buffer	4% Stacking buffer
30% acrylamide (National Diagnostics)	10ml	6 ml	2 ml
4 x Separation buffer	7.5 ml	7.5 ml	-

2 x Stacking buffer	-	-	7.5 ml
10% APS	450 µl	450 µl	150 µl
TEMED	30 µl	30 µl	15 µl
Water	12.5 ml	16.5 ml	5.3 ml

Table 2.6-4 Recipe for 30ml TRIS-BIS SDS-PAGE resolution and stacking buffers

2.6.6.1 Large SDS-PAGE Gel Electrophoresis

Two glass plates were assembled with 1 .5mm gap and the edges sealed with 1% agarose. Polyacrylamide Resolution gels were prepared, poured between the glass plates and topped with isopropanol. Isopropanol prevents water evaporation from the gel during polymerization and is removed before the addition of stacking gel. 20 well combs were inserted into stacking gel before polymerization to from well for protein samples. Gels were electrophoresed using Biometra V15.17 electrophoresis apparatus in 1 x running buffer at 65 mA until samples migrates past the stacking gel layer into the resolution gel, from which they were then ran at 12mA ~16h.

2.6.6.2 Small SDS-PAGE Gel Electrophoresis

Small SDS-PAGE gels were cast using 5ml of Resolving gel, 2.5ml stacking gel and small 10well combs (All Biorad). Proteins were electrophoresed in Mini Trans-Blot Electrophoretic Transfer Cells (Biorad) at 65 mA for ~3 h. A pre-stained protein marker (GE Healthcare or NEB) was loaded alongside samples to estimate protein sizes in differentially separated bands.

2.6.7 Western blot protein probing

Solution	Reagents
Transfer buffer:	25 mM Tris
	1.5% (w/v) Glycine
	0.02% (w/v) SDS
	10% (v/v) Methanol
Ponceau S:	0.47% (w/v) Ponceau S
	3% (w/v) TCA
	1% (v/v) Acetic acid)
PBS-T:	0.1% Tween-20 in PBS

Table 2.6-5 Buffers required for Western blot protein blotting

To probe for specific proteins in a size separated SDS-PAGE gel, proteins were first transferred into nitrocellulose membrane protran BA 85 nictrocellulous membranes (Whatmann). Large gels were transferred using an Amersham TE70 semi-dry transfer unit and small gels were transferred using a Mini Trans-Blot Electrophoretic Transfer Cells. The membrane and blotting paper (Amersham) were soaked in transfer buffer prior to transfer at 1 mA/cm^2 for 2.5 h. To check for transfer and loading consistency,

membranes were stained with Ponceau S and scanned electronically. Unspecific antibody binding was reduced by blocking the membrane with 2% dry non-fat milk in PBS-T. Membranes were incubated with primary antibody overnight at 4°C (Large gels), or for 1h at room temperature (small gels) with gentle agitation. Between incubation with primary and secondary antibody and after secondary antibody incubations, membranes were given 3 x 15’ washes in PBS-T.

Antibody	**Species**	**Working Conc.**	**Source**
HA.11 (α-HA)	Mouse	1:1000	BioLegend MMS-101R-1000
9E10 (Myc Tag)	Mouse	1:1000	BioLegend - 658502
M2 (FLAG Tag)	Mouse	1:1000	Sigma Aldrich F1804-5mg
α-PAP (TAP Tag)	Mouse	1:1000	Sigma Aldrich P1291
α-PGK1	Rabbit	1:10000	Lab Stock (Colette Connor - custom)
α-Rabbit raised proteins	Donkey	1:5000	VWR NA934-1ml
α-Mouse raised proteins	Sheep	1:5000	VWR

			NXA931-1ml
α-MCAK CT	Rabbit	1:1000	GL Biochem (Custom)

Table 2.6-6 Antibodies used for Western blot probing of protein tags. Antibodies were diluted in 2% non-fat milk powder in PBS-T

With HRP conjugated antibodies ECL (TermoScientific) Pico and Femto reagents were used, as per the kit manual. Membranes were wrapped in Saran wrap and exposed to Kodak Bio-Max light film and developed using a Konica-Minolta SRX-101A developer.

2.6.8 Immunoprecipitation of TAP-tagged CIn8 protein from *S.cerevisiae*

For purification of TAP-tagged expressed proteins at the kinetocho re of *S.cerevisiae* a modified immunoprecipitation protocol was used.

Solution	**Reagents**
Lysis buffer in ‘Eris Buffer’:	2 µM CLAAPE (Chymostatin, Leupeptin, Antipain, Pepstatin A, E-64 Protease inhibitor)
	2 µM AEBSF (Pefabloc)
	0.8 µM Sodium Orthovanadate
	0.2 µM LR Microcystin
	2.5 µM N-ethylmaleimide (NEM)
	0.8 mM Sodium orthovanadate
	8 mM β-glycerophosphate
	4 mM Sodium pyrosphosphate

	20 mM Sodium fluoride
Eris Buffer	25 mM hepes (pH8)
	1 mM $MgCl_2$
	0.5 mM EGTA-KOH (pH8)
	15 % Glycerol
	150 mM KCl
Sodium Phosphate buffer	0.1M Sodium Phosophate (pH7.4)
PBS (pH7.4)	0.1M Sodium Phosphate (pH 7.4)
	150mM NaCl
NuPage Sample Loading Buffer (LDS)	NuPage Sample Loading Buffer
	5% beta-mercaptoethanol

Table 2.6-7 Buffers and inhibitor required for Immunoprecipitation

3L of *S.cerevisiae* cells were released into meiosis in SPO at OD_{600} >2.5. Cells were incubated at 30 °C shaking at 250rpm for 4h before harvesting at 4 °C by centrifugation at 4000rpm for 5'. Cell pellets were washed in sterile water and resuspended in 20% v/v sterile water with 0.2 mM PMSF before drop freezing into liquid nitrogen and storage at -80 °C. Frozen cell beads were ground in a Retch mixer mill MM400 for 5 rounds of 3' at -196 °C with the aid of liquid nitrogen submersion instruments and samples between rounds of shaking. To couple Rabbit IgG into epoxy-activated Dynabeads, 10mg of Dynabeads were washed in phosphate buffer three times and incubated with Rabbit IgG 1mg/ml with rotation for 24h at 37°C. After coupling beads were washed four times in PBS and twice in lysis buffer for

equilibration. Final concentration of beads used per lysed sample was approximately 0.5mg bead slurry per 1g of cell grindate. To lyse cell, frozen grindate was thawed on ice and 1ml/g of lysis buffer was added with 40U/ml benzonase. Lysis mixtures were incubated on ice for 1h and centrifuges at 4000rpm for 10’ at 4°C. Antibody coupled beads were added to cleared lysates and incubated at 4°C for 1.5h with rotations to bind TAP-tagged proteins. Non-specific binding of proteins to the antibody-coupled beads was reduced by three washes of 10’ each with lysis buffer before the remaining bound protein was dissociated from beads by NuPAGE® LDS sample buffer at 100°C for 5 mins. 5 µl of β-mercaptoethanol was added to samples, boiled for another 5 mins then spun down at 13000 rpm for 5 mins at 95°C. Small fractions of samples were tested for protein purity. Small samples were electrophoresed twice onto a precast NuPAGE® 8-12% Bis-Tris gel (Novex. One gel was transferred by Western blotting onto nitrocellulose membrane and probed using antibodies against PAP antigen (See method 2.6.7). The other gel was stained by Silver Staining (see method 2.6.9)

2.6.9 Silver Staining

Silver staining was performed using a Silver Staining kit (Thermo Scientific) according to manufacturer's instructions.

2.6.10 Coomassie Staining

Coomassie staining was performed using a Colloidal Blue Staining kit (Novex) according to manufacturer's instructions.

2.6.11 In-gel tryptic digestion of proteins

Protein bands were excised from Coomassie-stained NuPAGE® 8-12% Bis-Tris gels and washed alternatingly with 50 mM ammonium bicarbonate and acetonitrile solutions until Coomassie staining was removed. Gel pieces were submerged in with 10 mM DTT in 50 mM ammonium bicarbonate for 30 mins at 37°C then washed with acetonitrile. 55 mM iodoacetamide in 50 mM ammonium bicarbonate was added to gel slices and incubated at room temperature in the dark for 20 mins. After washing again with 50 mM ammonium bicarbonate and acetonitrile, gel pieces were incubated with trypsin for 15' at 4 °C and transferred to 37°C for >16h. Digestion reactions were treated with 0.1% (w/v) trifluoroacetic acid, incubated for 15' to allow peptides diffusion from gel. The digestion buffer, now congaing sample peptides, were passed through an equilibrated StageTip consisting of two layers of Empore Disks C18 within a pipette tip. A single StageTip was used per sample. Peptides were later eluted for analysis via Mass Spectrometry.

2.6.12 Mass Spectrometry (MS)

Mass Spectrometry was performed by Christos Spanos in the Juri Rappsilber lab (University of Edinburgh). MS data was compiled in MaxQuant 1.4.1.2 and quantitative analysis was performed using Perseus 1.5.1.6 software.

Chapter 3: Investigating the structure and action of MCAK during human cell mitosis

3.1 Introduction

In general, kinesins have a very distinct protein shape. Visualised by negative stain electron microscopy, most kinesins form an elongated dimer whereby the respective two ATPase domains are in close proximity, the neck region forms a flexible coiled-coil, which is capped by the two globular domains (Moore & Endow, 1996; Lawrence *et al*, 2004). MCAK is a kinesin 13 family member and unlike canonical kinesins, its structure looks closed, compact and globular by EM studies (Noda *et al*, 1995).

Consequently, the domain organisation of MCAK is unlike that of other kinesin families; the MCAK Motor Domain does not reside at the N- or C-terminus, and instead is in the interior of the protein sequence (**Figure 3.2-1**) (Cross & McAinsh, 2014; Maney *et al*, 2001). Whilst the three-dimensional structure of MCAK's highly conserved catalytic motor domain has been resolved to high resolution, full length MCAK, including N and C termini has not, owing to its tendency to precipitate and degrade at high concentrations.

MCAK also uses energy derived from ATP hydrolysis in the catalytic motor domain to initiate microtubule depolymerisation, whereas members of other kinesin families use ATP in the coordinated, progressive movement along microtubule tracks in the cell to act as cargo transporters. Thus, it is predict that MCAK will not hold a similar structure to cargo-transporting kinesins as they have a different domain organisation (Maney *et al*, 2001).

While little is known as to the overall protein folding of MCAK there have been several interesting studies on different MCAK domains. The C terminus of MCAK and its role in MCAK depolymerase activity has been the subject of several studies (Zong *et al*, 2016; Ritter *et al*, 2015; Moore & Wordeman, 2004b).

In Moore & Wordeman, (2004) they removed the C terminus of the mouse MCAK homologue and found that depolymerase activity of the truncation increased. Also in 2008, Zhang and Ems-McClung describe Xenopus MCAK homologue C-terminal phosphorylation by Aurora A, which alters MCAK function (Zhang *et al*, 2008). Research published in 2011 by Zhang et al, describe mouse MCAK homologue C-terminal phosphorylation by Plk1 which promoted its depolymerase activity (Zhang *et al*, 2011).

Together these studies indicate that the C terminus of MCAK could act to inhibit or regulate its depolymerase activity. Correlating MCAK structure and depolymerase activity, Ems-McMclung et al found that Aurora B phosphorylation of MCAK neck domain (S196) causes a conformational switch in the protein, reducing its affinity for microtubules, and thus global microtubule depolymerase activity (Ems-McClung *et al*, 2013).

Dietrich et al, (2008) gave molecular insight into possible C terminal regulation of kinesin activity by similar conformational mechanisms; the ATPase activity of Kinesin 1 is inhibited when one of the two C-termini of the

pair folds over the dimer and binds to an inhibition site between the two ATPase domains (Dietrich *et al*, 2008).Considering evidence of C-terminal phosphorylation, and its effect on MCAK depolymerase activity, I hypothesise that a conformational change in the C-terminus as a result of phosphorylation may also act to regulate MCAK activity.

In detail; I hypothesise that the C terminus of MCAK binds to the Motor Domain, the ATPase domain. Secondly, I hypothesise that binding of MCAK C terminus to the motor ATPase domain inhibits the depolymerase activity of MCAK. Finally, I hypothesise that the binding of MCAK C terminus to the ATPase domain is dependent on phosphorylation of MCAK, potentially on the C terminus itself, and that this phosphorylation regulates MCAK activity during the cell cycle.

3.2 Results

3.2.1 Investigating the molecular arrangement of MCAK domains in cell culture.

The first hypothesis I tested was whether the C terminus of MCAK binds to the ATPase/Motor Domain of MCAK. Sandeep Talapatra, a post-doctoral associate in the lab was trying to address this question *in vitro*, while I tested the relevance of the *in vitro* observations *in vivo,* using cell culture.

3.2.1.1 MCAK C terminus can bind to MCAK ATPase Domain in vitro.

To investigate the possibility that MCAK C terminus can associate with its ATPase domain, I first tested for an interaction between these domains *in vitro*. I collaborated with Sandeep Talapatra, in the Welburn lab to investigate the molecular arrangement of MCAK domains *in vitro*.

Sandeep purified recombinant MCAK Motor Domain, the N-terminus and Motor Domain, and C terminus from bacteria, subcloned in pET3aTr vector (**Figure 3.2-1**). When HIS-tagged MCAK Motor Domain is incubated with GST-tagged MCAK C terminus for 1 hour, a complex of the two can be isolated using Glutathione beads. This shows that *in vitro* at least, MCAK Motor Domain can interact with the C terminus and that the interaction is specific and strong enough to withstand salt washes of 150mM (see materials and methods; Talapatra *et al*, 2015b).

A.

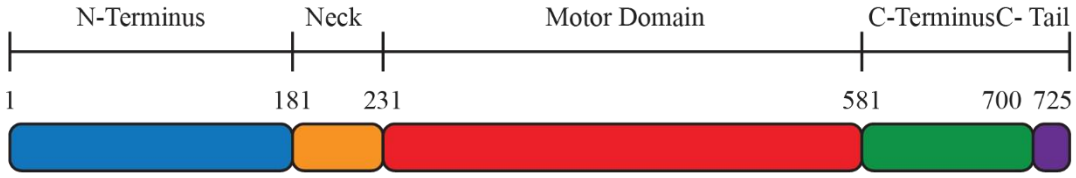

MCAK Domain	Abbreviation	Amino Acids
N-Terminus	N	1-181
N-Terminus and Motor Domain	NM	1-581
Motor Domain	MD	232-581
C-Tail	CT	700-725

B.

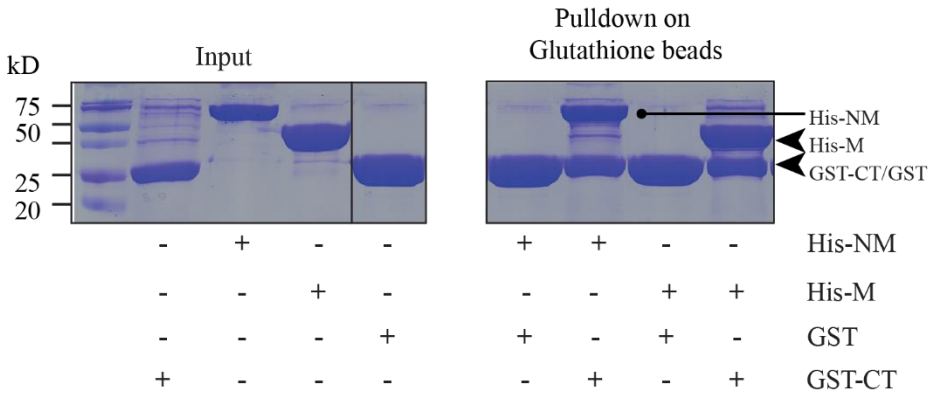

Figure 3.2-1 GST-Tagged MCAK Tail Domain binds to alternate MCAK domains in vitro.

(A) Schematic shows the domain structure of MCAK and the different truncation constructs used in this study, including their abbreviations. (B) Data taken from an experiment performed by Sandeep Talapatra, published in (Talapatra *et al*, 2015). Recombinantly purified MCAK MD or NMD HIS-tagged truncations were incubated with GST-CT or GST. Complexes containing GST were isolated using glutathione beads before electrophoretic separation on a denaturing SDS-Page and stained using coomassie.

To confirm this interaction, Sandeep incubated MCAK Motor Domain with the C terminus in the absence of any protein tags. The protein mixture was separated using size-exclusion chromatography (**Figure 3.2-2**). When MCAK C terminus is present in the protein mixture, it forms a complex with MCAK Motor Domain and as a result elutes earlier from the size-exclusion column. This can be seen clearly when the fractions are run on a denaturing SDS-Page acrylamide gel (**Figure 1.1-1**).

This experiment confirmed that MCAK C terminus can bind to MCAK Motor Domain *in vitro* and that the association is not an artefact of using a GST tag, which itself dimerises.

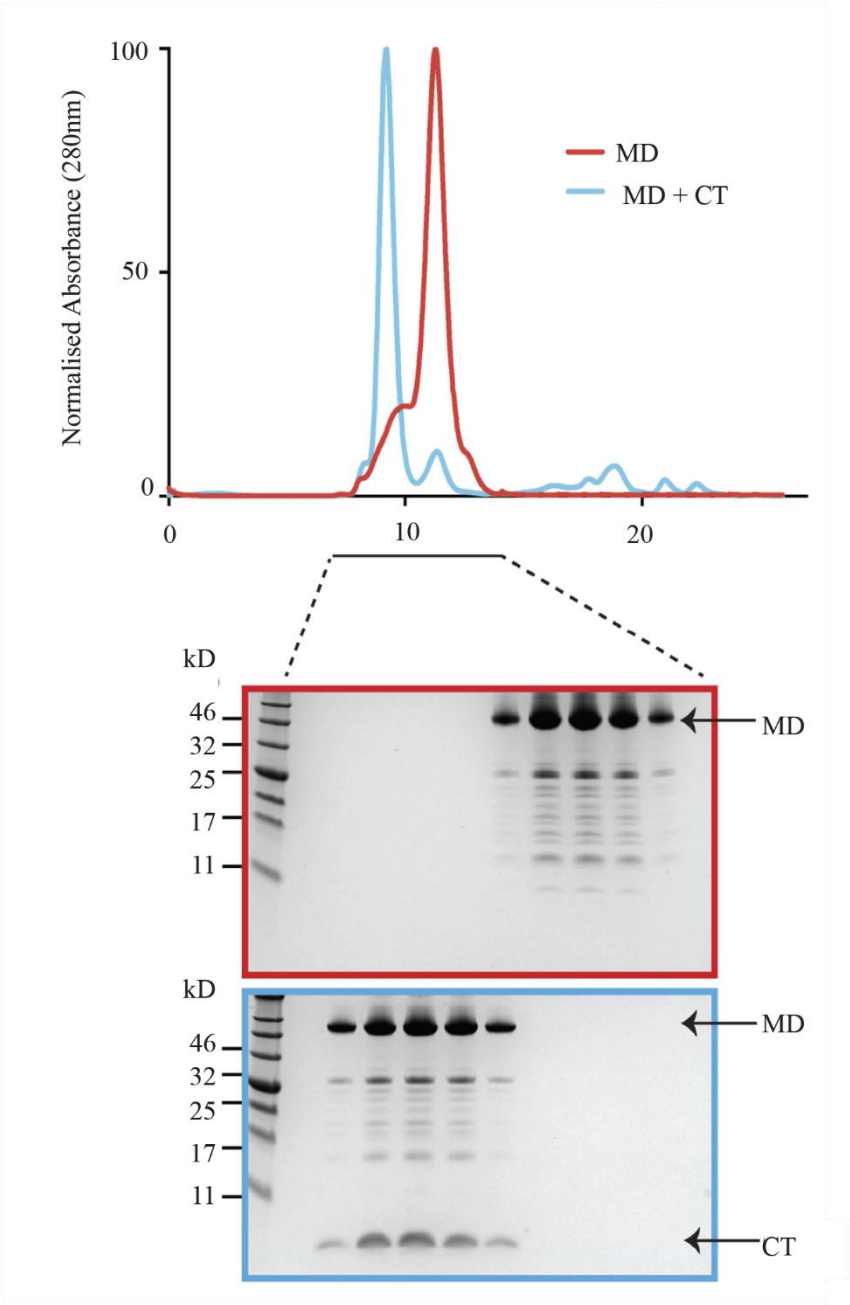

Figure 3.2-2 MCAK TD binds to the motor domain.

Data taken from an experiment performed by Sandeep Talapatra, published in Talapatra et al (2015). Recombinantly purified MCAK MD was pumped through a size exclusion column either alone (MD - Red profile) or after complex formation with MCAK CT (MD + CT - Blue Profile). Elution fractions were separated by protein size by electrophoresis on a denaturing SDS-Page acrylamide gel and stained using coomassie blue.

3.2.1.2 Developing an assay to test MCAK domain binding in cells.

From the studies aforementioned *in vitro* we were able to establish that the Motor Domain of MCAK can bind to its C terminus. However, it was still unclear whether this interaction occurs in cells. To test whether the Motor Domain binds to the C terminus in cells I wanted to develop an assay that would show complex formation in the cell.

A small, twenty amino acid membrane targeting sequence from the protein Neuromodulin (MEM), used in pEYFP-Mem (Clonetech, PT3378-5, Cat#6917-1), was employed to constitutively target a protein to the plasma membrane, N-terminal to a fluorescent mCherry tag. I hypothesised that an MEM-tagged MCAK C terminus should be able to recruit MCAK Motor Domain to the plasma membrane if they interact in cells. To visualise this interaction, I N-terminally tagged MCAK Motor Domain with fluorescent GFP protein (**Figure 3.2-3**).

Upon testing the various constructs required for the assay I found that the MEM tag localises mCherry tagged C terminus to the plasma membrane of the cell, while a diffuse localisation was observed in the absence of the localisation signal. Moreover, the signal is best visualised in HeLa cells in mitosis over those in interphase as the surface area to volume ratio is smaller, concentrating the fluorescent tag within the membrane (**Figure 3.2-4**).

GFP-MCAK Motor Domain also localised as expected to the mitotic spindle, particularly to the plus end of growing microtubules. This shows that the addition of a GFP tag has not perturbed MCAK Motor Domain localisation to microtubules, at least.

All constructs produced localised to their expected localisation after transient transformation and act as promising indicators that using the MEM tethering assay will help us understand MCAK domain interactions in living cells. It is important to note that the expression of MCAK Motor Domain, and in fact all the constructs tested at this point, is in addition to exogenous MCAK in the cell and thus overall, MCAK is in a state of overexpression in the cell.

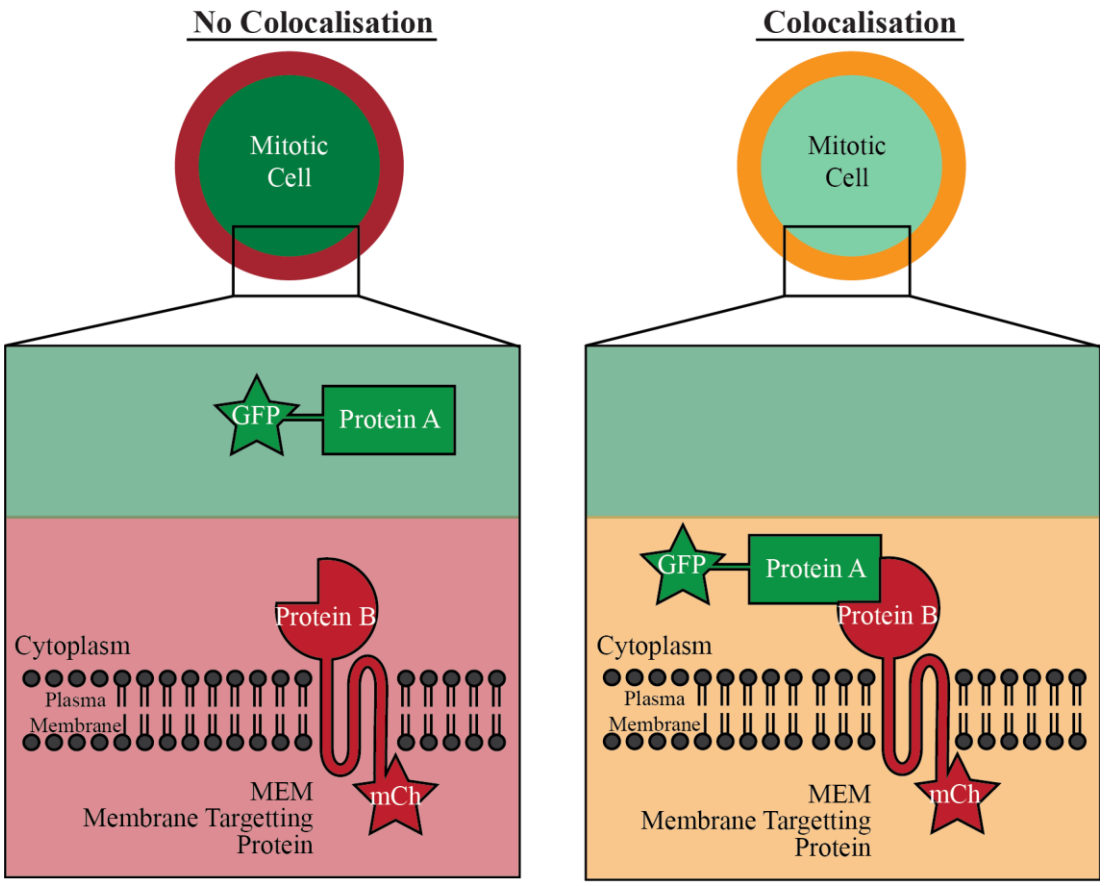

Figure 3.2-3 Development of an assay to test protein interaction *in vivo*.
Schematic showing the mechanisms of a membrane targeting (MEM) 'anchor away' system in vivo. Protein fragment B is tethered to the cell membrane using a short 20 amino acid membrane translocation domain and tagged using a fluorescent GFP. Protein fragment A is tagged with a red fluorescent mCherry (mCh). Complex formation between protein fragment A and B is visualized by dominant colocalization of green and red fluorescent tags at the membrane.

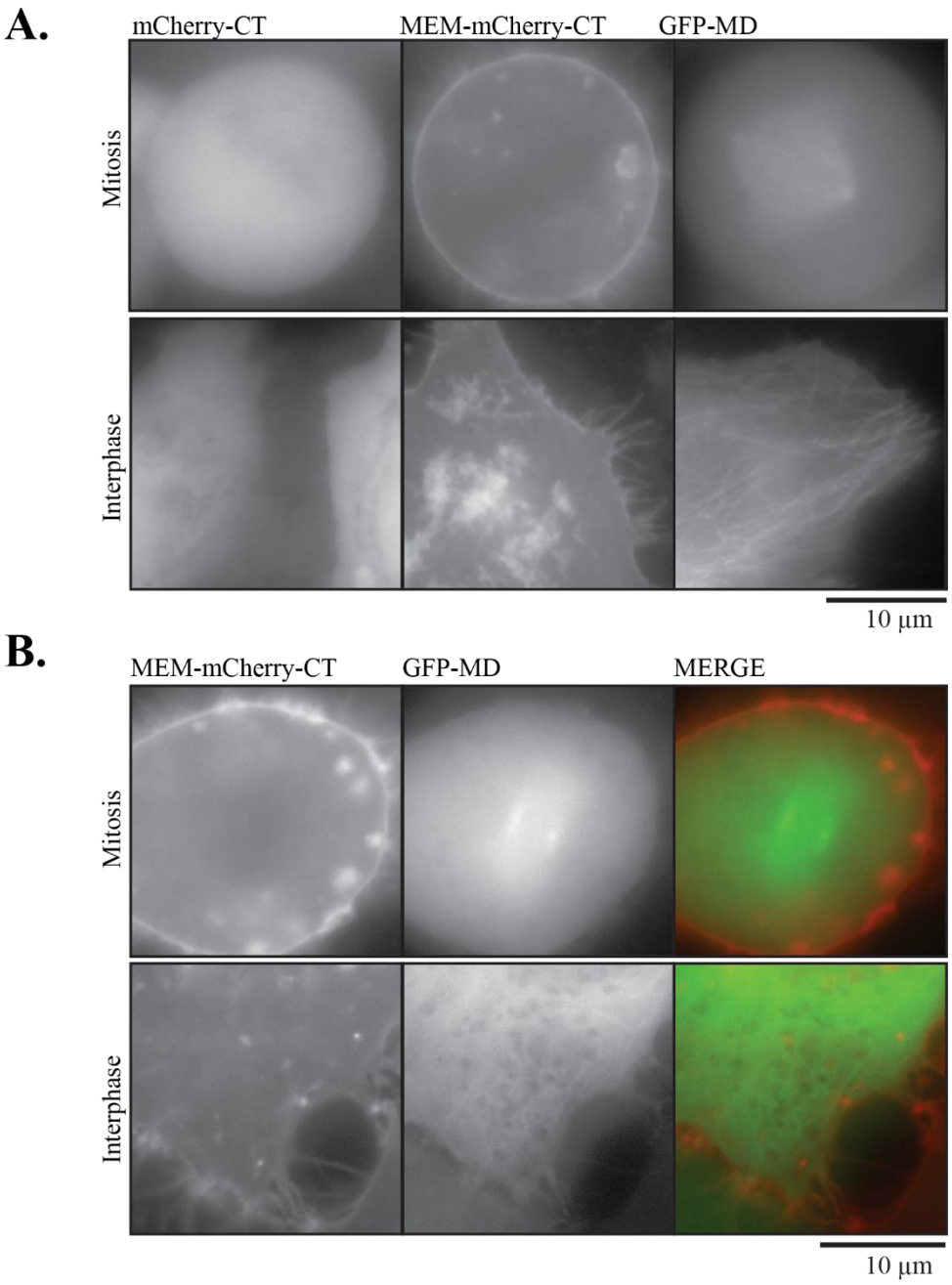

Figure 3.2-4 MCAK 'anchor-away' constructs show expected localizations upon transfection into HeLa cells.

(A) Representative images of mitotic or interphase HeLa cells with a single construct transfection, taken 72h after transient transfection with plasmids coding either mCherry-C terminus MEM-mCherry-CT or GFP-MD. (B) HeLa cells were transiently co-transfected with MEM-mCherry-CT (Red) and GFP-MD (Green) DNA constructs and imaged 72 hours later. Representative images were taken of both interphase and mitotic cells.

3.2.1.3 MEM-mCherry tagged C terminus is unable to recruit GFP-Motor Domain to the cell membrane.

To test the hypothesis that MCAK C terminus binds to the motor domain in cells, I transiently co-transfected MEM-mCherry tagged C terminus and GFP-Motor Domain into HeLa cells using the Lipofectamine transfection method (See 2.3.5).

First, I confirmed that the individual constructs localized in the expected way. Next, I determined if co-transfection of these constructs resulted in the co-localization of MEM-mCherry tagged C terminus and GFP-Motor Domain.

Cells were visualized after 72h and the cells with similar expression levels of each construct were chosen for imaging. Transfected alone, MEM-mCherry tagged C terminus localises to the cell membrane. GFP-Motor Domain localises to the microtubule spindle and astral microtubule +ends during mitosis, but to the microtubule lattice, rather than forming microtubule plus end comets like WT. In cells where GFP-MD signal was brighter, bipolar spindles were shorter, indicating that MD is functional on the spindle, shortening microtubules. (**Figure 3.2-4**).

Both in mitosis and during interphase I was unable to spot any co-localisation between the red MEM-mCherry tagged C terminus and green GFP-Motor Domain (**Figure 3.2-4**), even using intensity level line scans across the entire cell (not shown)**.** In fact, GFP-Motor Domain remained localised on the

mitotic spindle, which looked shorter, probably the result of excess MCAK expression/protein levels in these cells. I conclude that under these conditions, MEM-mCherry tagged C terminus and GFP-Motor Domain do not stably interact in cells.

3.2.1.4 MEM-mCherry tagged C terminus does not recruit GFP-Motor Domain to the cell membrane in the absence of microtubules.

Transfected MCAK-Motor Domain localises to the microtubule spindle, specifically the plus ends of growing microtubules (see Figure 3.2-4). I hypothesise that, in the previously described assay, stable interaction between GFP-Motor Domain and microtubules in the mitotic spindle is more favourable than between GFP-Motor Domain and MEM-mCherry-MCAK at the membrane.

In the even that tubulin is acted as a competitive inhibitor against MEM-mCherry-CT, I repeated the assay in the presence of 2µM Nocodazole, which has been shown to completely depolymerise microtubules (Saxton *et al*, 1984). As a control, I treated cells with DMSO, the solvent used for the Nocodazole stock. In the presence of 2µM Nocodazole, MEM-mCherry-CT was still able to localise to the cell membrane, which indicates a microtubule-independent method of MEM signal transport within the cell. Simultaneously, GFP-Motor Domain no longer localised to the spindle and is expected to be free to bind to MEM-mCherry tagged C-Terminus. Despite the loss of tubulin

as a competitive binding partner I was unable to detect any co-localisation of GFP-Motor Domain with MEM-mCherry tagged C terminus (**Figure 3.2-5**).

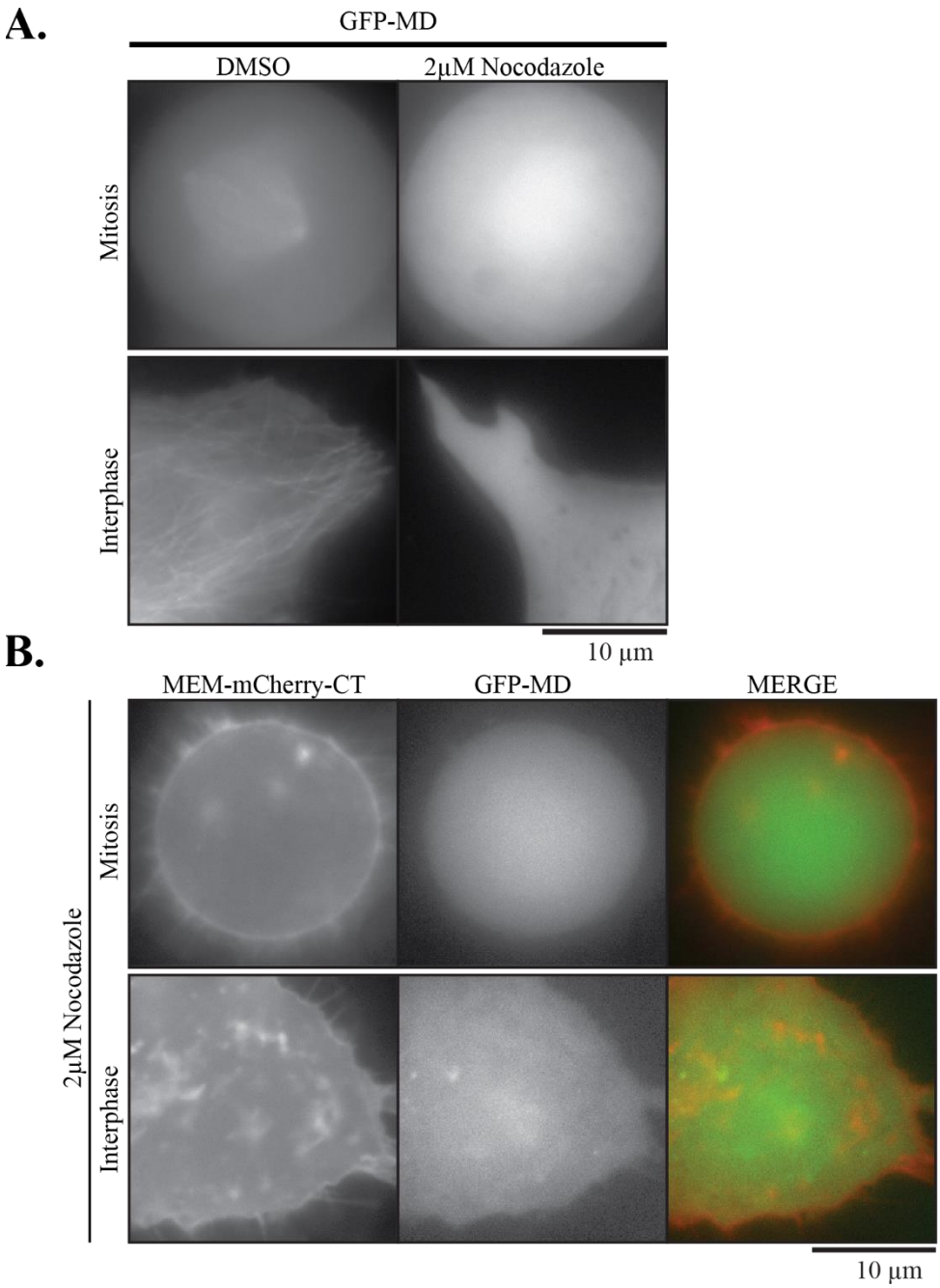

Figure 3.2-5 MEM-mCherry-CT does not recruit GFP-MD to the cell membrane in the absence of microtubules.

(A) HeLa cells were transiently transfected with DNA constructs denoting expression of GFP-MD. After 72h cells were treated with either DMSO or 2µM Nocodazole and imaged live. (B) HeLa cells were transiently co-transfected with DNA constructs denoting expression of both MEM-mCherry-CT (Red) and GFP-MD (Green). After 72h cells were treated with either DMSO or 2µM Nocodazole and imaged live. All images are representative of cell population.

3.2.1.5 MEM-mCherry tagged C terminus was unable to recruit GFP-Motor Domain despite depleting or endogenous MCAK by RNAi.

MCAK forms a homodimer in the cell (Hertzer *et al*, 2006). Another possibility to explain the lack of binding of GFP-Motor Domain to MEM-mCherry tagged C terminus could be that endogenous MCAK acts as a competitive binding partner for GFP-MCAK against MEM-mCherry tagged C-Terminus.

To test this hypothesis, I performed the assay in conjunction with a depletion of endogenous full-length MCAK by RNAi against the N-terminus of MCAK (see **Figure 3.2-6**). Despite depletion of endogenous MCAK, GFP-MCAK was still not recruited to the plasma membrane by MEM-mCherry tagged C-Terminus. To test for RNAi depletion, I probed for MCAK C terminus using a custom-made antibody in cell extract treated with an RNAi oligonucleotide sequence against MCAK N-terminus or non-specific DNA sequence (see **Figure 3.2-6**).

MCAK was depleted 72 hours after RNAi to undetectable levels (see **Figure 3.2-6**). Finally, I added 2µM Nocodazole to depolymerase the spindle (see **Figure 3.2-6**). In the absence of microtubules and endogenous MCAK as competitive binding partners, there is potentially some overlap of fluorescent signal, particularly in interphase cells, but it is impossible to determine with high throughput analysis..

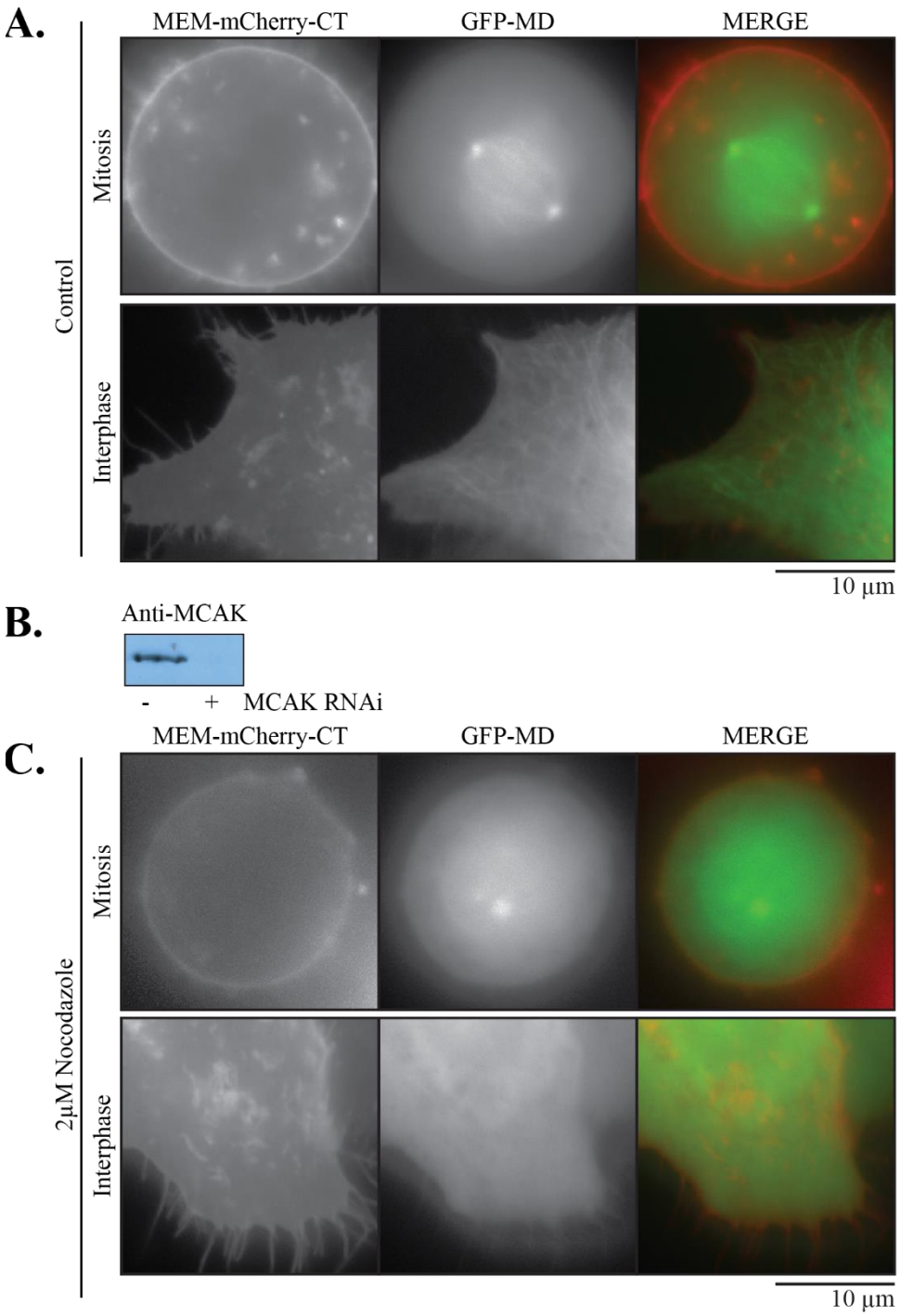

Figure 3.2-6 MEM-mCherry-CT was unable to recruit GFP-MD in in the absence of endogenous MCAK or polymerized microtubules.

(A) RNAi resistant MEM-mCherry-CT was co-transfected with GFP-MD, 24h after RNAi depletion of endogenous MCAK by RNAi. Images show cells in mitosis and interphase. MEM-mCherry-CT = Red whilst GFP-MD = green. (B) Successful RNAi transfection and subsequent endogenous MCAK protein depletion was assayed by western blot against

MCAK in harvested asynchronous cell samples. (C) 2µM of nocodazole or DMSO (DMSO not shown) was added to cell cultures to depolymerize microtubules 2h before imaging. GFP-MD - green; MEM-mCherry-CT = red.

3.2.1.6 GFP-MCAK is not recruited to the cell membrane by MEM-mCherry-MCAK1-700

Having not succeeded to see any MCAK domain binding at the membrane, I hypothesised that perhaps the C terminus alone was not enough for the interaction between the two MCAK domains in cells and that other parts of the protein are necessary to allow proper protein complex conformation. To try to address this I extended the length of MCAK which could be recruited to the membrane to amino acids 1-700. This constitutes all MCAK other than the C-Terminus. In this assay I was still unable to see MCAK1-700 co-localise with MEM-mCherry tagged C terminus at the membrane, even in the presence of 2μM Nocodazole (see **Figure 3.2-7**).

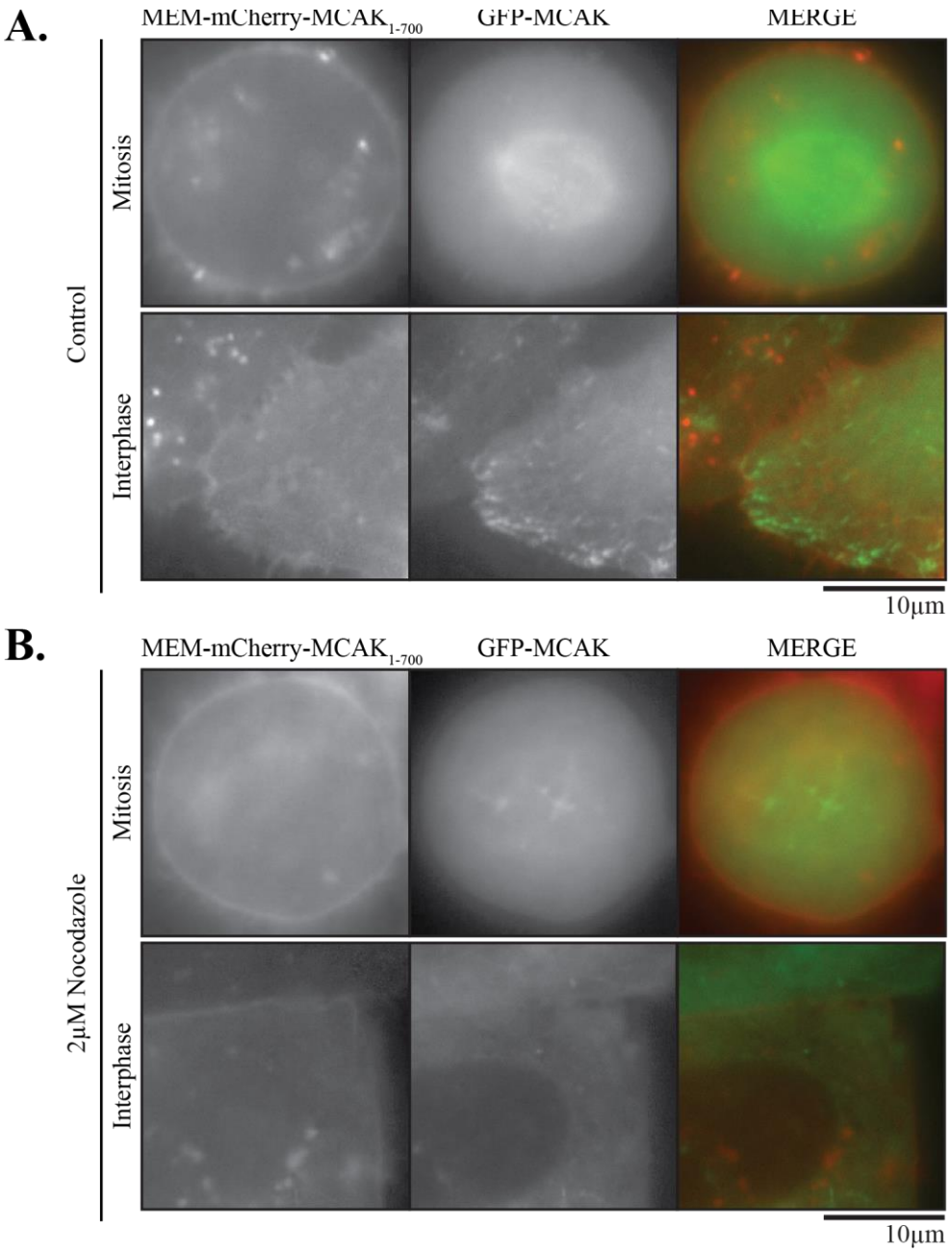

Figure 3.2-7 GFP-MCAK is not recruited to the cell membrane by MEM-mCherry-MCAK1-700

HeLa cells were transiently transfected with DNA constructs denoting ectopic expression of MEM-mCherry-MCAK1-700 and full-length GFP-MCAK. (B) After 72h incubation with DMSO or 2µM of Nocodazole was added to cultures and representative images were taken.

3.2.1.7 MEM-GFP-Motor Domain is unable to recruit mCherry tagged C terminus to the plasma membrane.

Rather than tethering MCAK C terminus at the membrane to recruit MCAK-Motor Domain, which is large by comparison, I hypothesised that tethering MCAK Motor Domain to the membrane and using that to recruit MCAK C terminus to the membrane would be more effective. To test whether membrane-tethered MCAK Motor Domain can recruit MCAK C terminus I transiently transfected MEM-mCherry-Motor Domain with GFP-MCAK C terminus in HeLa cells and looked at the subcellular localisation of the expressed protein, 72h post transfection.

Single transfection of GFP-MCAK C terminus shows diffuse localisation throughout the cell. MEM-mCherry-Motor Domain localises to the cell membrane (see **Figure 3.2-8**). Tethering MCAK Motor Domain to the membrane rather than MCAK C terminus is advantageous to the inverse experimental design as it removes MCAK Motor Domain from binding partners in the cell that may interfere with its stable interactions with free MCAK C terminus in the cytoplasm. However, transient co-transfections of MEM-mCherry-Motor Domain with GFP-MCAK C terminus did not induce GFP-MCAK C terminus localisation to the plasma membrane (see **Figure 3.2-8**).

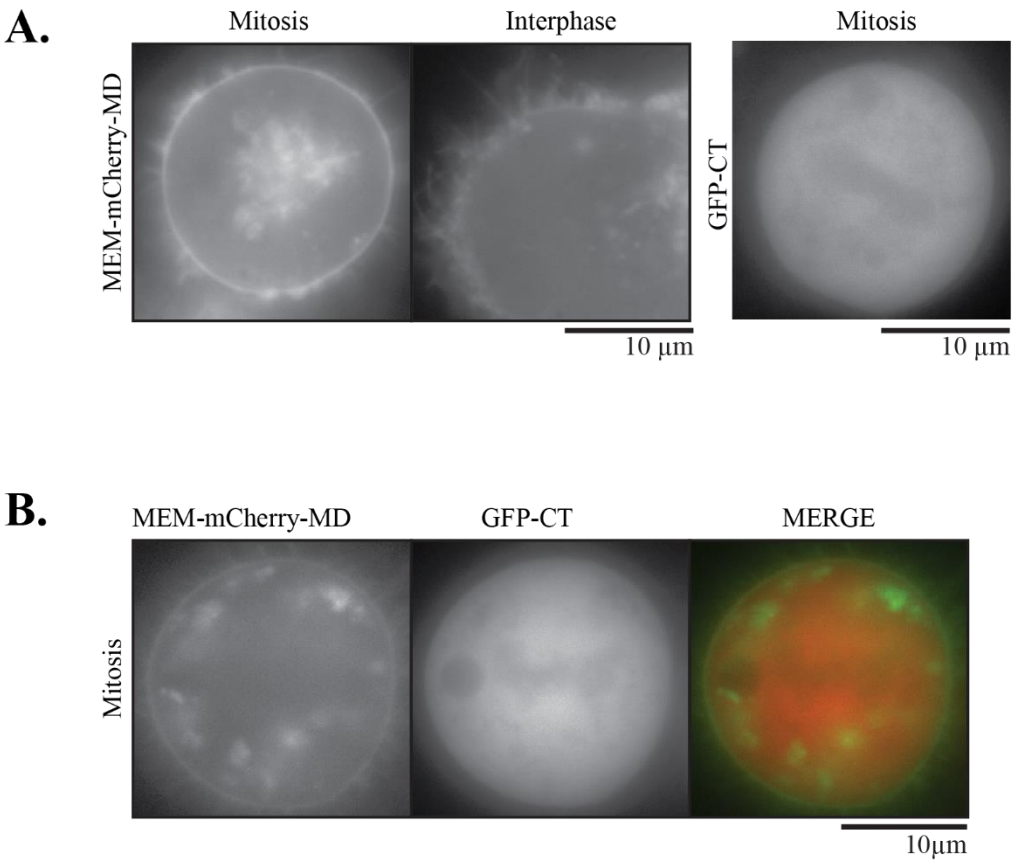

Figure 3.2-8 MEM-mCherry-MD is unable to recruit free GFP-CT to the cell membrane. (A) HeLa cells were transiently transfected with either MEM-mCherry-MD or GFP-CT 48h before live cell imaging. (B) HeLa cells were transiently co-transfected with MEM-mCherry-MD (Red) and GFP-CT (Green) 48h before live cell imaging. Colours have been reversed on merged image to aid visualization of faint mCherry signal.

3.2.1.8 MEM-mCherry-HSET is unable to recruit by dimerization GFP-HSET to the plasma membrane.

A lack of co-localisation of MCAK domains in HeLa cells could be due to a lack of binding or due to interference caused by fusing a fluorescent tag to the protein fragment. To try to distinguish between the two, I designed a positive control. HSET is a microtubule binding kinesin which is shown to form homodimers (Lecland & Lüders, 2014). Upon co-transfecting MEM-mCherry-HSET and GFP-HSET I hoped to observe co-localisation at the plasma membrane, showing that recruitment of kinesins is possible in cells. Whilst MEM-mCherry-HSET is unable to recruit GFP-HSET to the plasma membrane in cells, MEM-mCherry-HSET was recruited to the plasma membrane, both fusion proteins were recruited to the mitotic spindle and MEM-mCherry-HSET was also recruited to spindle poles (see **Figure 3.2-9**) (Chavali *et al*, 2016). Recruitment to the spindle shows that fusion of fluorescent tag did not perturb wildtype localisation. Recruitment of MEM-mCherry-HSET to both the plasma membrane and the spindle could be caused by competitive binding between the two sites; the spindle (4 binding sites) being stronger than at the membrane (1 binding site). In agreement with the latter hypothesis; MEM-mCherry-HSET localises to the spindle poles where tubulin is denser, whereas GFP-HSET is not, and shows only wild type HSET localisation to microtubule lattice.

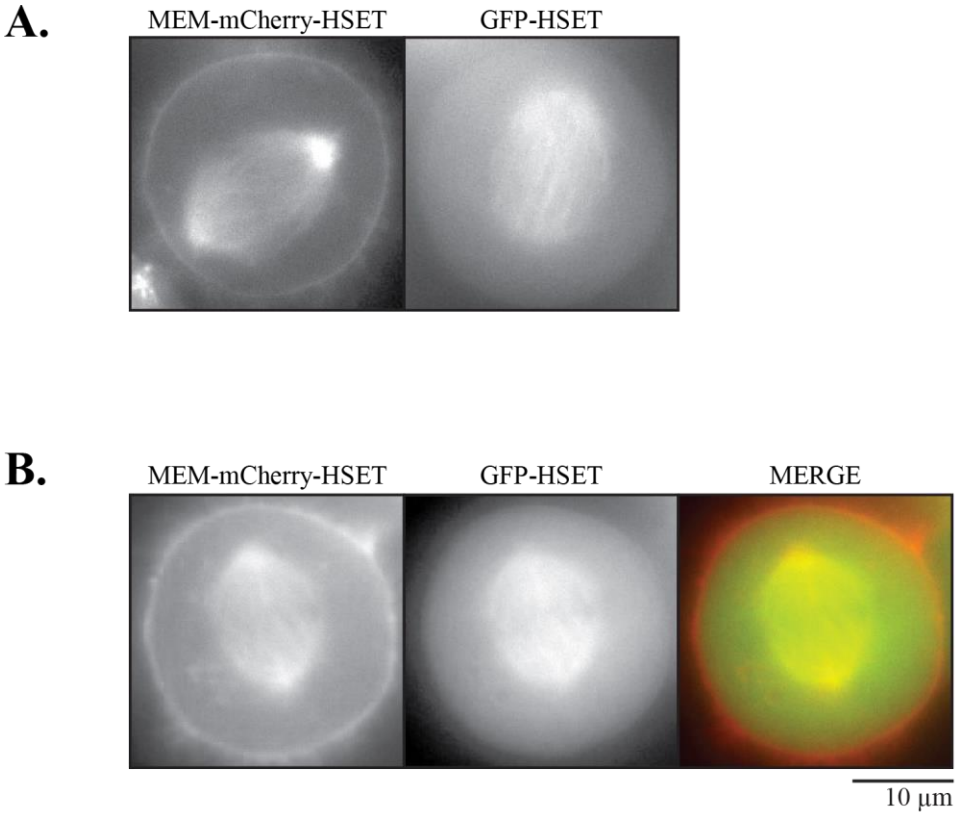

Figure 3.2-9 MEM-mCherry-HSET is unable to dimerise with GFP-HSET after transient co-expression in HeLa cells.

(A) HeLa cells were imaged live 48h after transfection with constructs denoting MEM-mCherry-HSET or GFP-HSET. (B) MEM-mCherry-HSET (Red) and GFP-HSET (Green) coding plasmids were transiently co-transfected into HeLa cells 48h before live cell imaging.

3.2.1.9 The binding of MCAK-Motor Domain to MCAK C terminus is dependent on strict spatial freedom during the binding process.

Following disappointment with the MEM-tethering assay I decided to go back to the *in vitro* work and try it with my own hands. In the methods described by Sandeep Talapatra, MCAK HIS tagged Motor Domain and GST tagged C terminus were recombinantly expressed and purified from *E.coli*. MCAK HIS-Motor Domain was mixed with GST-C terminus and incubated on ice for 1 hour before adding GST beads to isolate GST tagged C terminus and the HIS tagged Motor Domain bound to it.

In vivo, compared to *in vitro*, proteins are folded only as they are translated; so MEM-mCherry tagged C terminus may not be free, in close proximity free in the cytoplasm with GFP tagged Motor Domain for long before it is localised and has spatial restriction placed upon it. At the membrane, the lipid bilayer could hinder access of GFP-MCAK to the C-Terminus. Alternatively; the mCherry tag on MCAK C terminus may restrict Motor Domain binding.

To distinguish between these hypotheses I expressed and purified mCherry tagged C terminus from *E.coli* and repeated a modified protocol of the binding pulldown assays performed by Sandeep Talapatra. Firstly, I incubated HIS tagged Motor Domain with mCherry tagged C Terminus. Whilst GST is similar in molecular size to mCherry, it also dimerises with itself, which could interfere with Motor Domain interactions. mCherry does not dimerise with itself and is also the tag used in the cellular tethering assay.

Secondly, I used the HIS tag on HIS tagged Motor Domain to pull out MCAK complexes in the absence of GST tagged proteins in this experiment. In one reaction I incubated HIS tagged Motor Domain and mCherry tagged C terminus together for one hour on ice before adding nickel beads and purifying HIS tagged Motor Domain and any complexes it had formed.

In a different reaction I bound HIS-Motor Domain to the Nickel beads before adding mCherry C terminus and purifying any HIS tagged Motor Domain complexes. Purified HIS tagged Motor Domain and any bound proteins were separated by size by electrophoresis on a denaturing SDS-PAGE acrylamide gel and stained using Coomassie.

I hypothesise that the latter experimental set up is truer of the cellular environment at the membrane and that this environment is not conducive to MCAK Motor Domain/C terminus complex formation (Methodology explained in **Figure 3.2-10**). When HIS tagged Motor Domain is pre-incubated with, mCherry-tagged C terminus a complex of both proteins is isolated on Nickel beads (see **Figure 3.2-10**).

However, results show that that the spatial restriction imposed on HIS-Motor Domain when bound to beads was sufficient to prevent mCherry tagged C terminus binding and in this reaction, I was unable to detect mCherry tagged C terminus in the HIS tagged Motor Domain purification product.

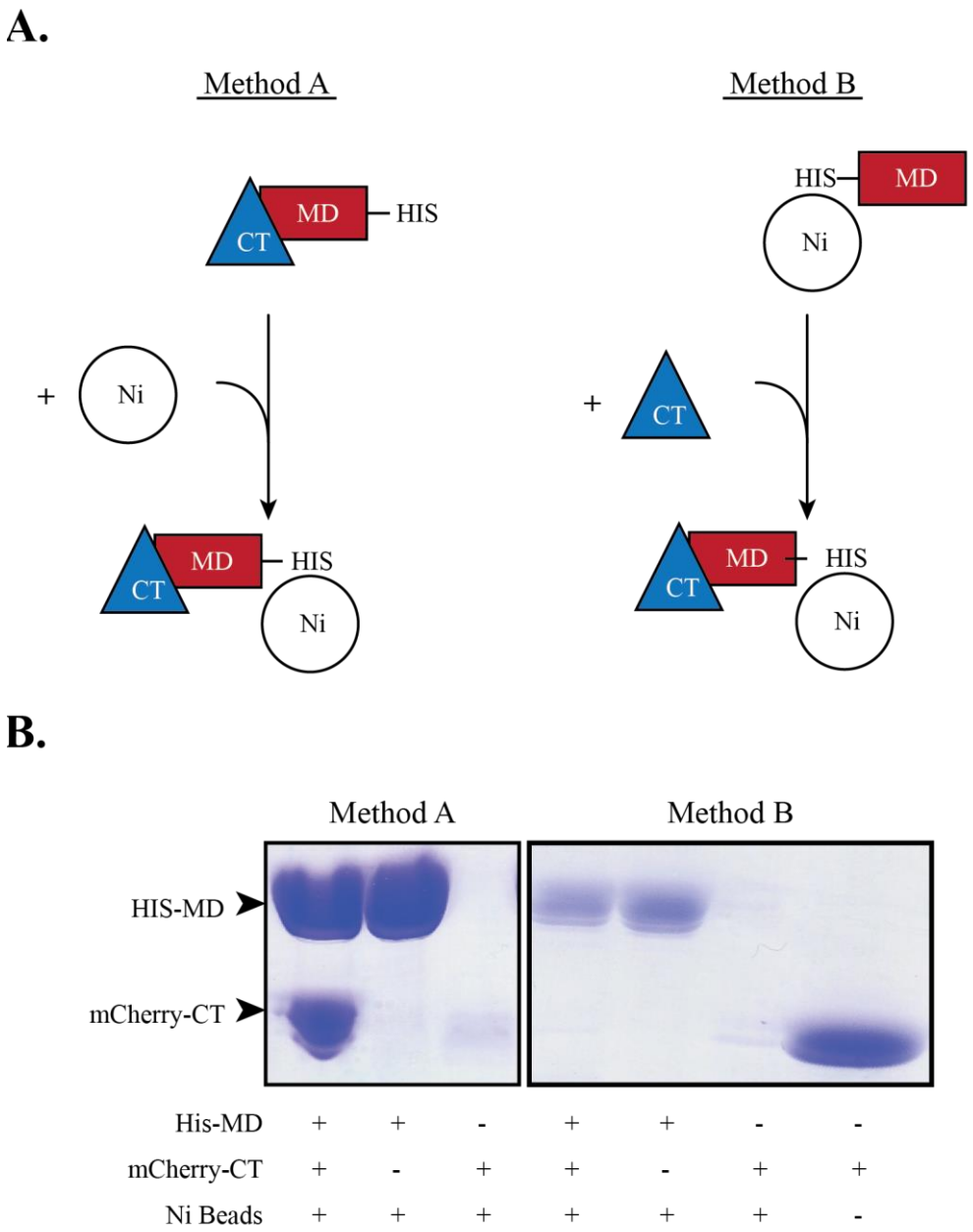

Figure 3.2-10 mCherry-CT is able to bind to MD in vitro under strict *in vivo* conditions .(A) Schematic shows the two different methods that were used to test for mCherry-CT binding to MD. In method A, HIS-tagged MD is incubated with Nickel beads alone. Unbound protein is washed off before mCherry-CT is added to the mix. In method B, HIS-tagged MD is incubated with mCherry-CT alone, then nickel beads are added to purify HIS-MD and any bound mCherry-CT. (B) Purified complexes were electrophoresed on a denaturing SDS-Page acrylamide gel and Coomassie stained to show protein separation.

3.2.2 Investigating the role of MCAK C terminus on MCAK depolymerase activity.

Successful crystallisation of MCAK Motor Domain bound to C terminus revealed the binding interface between the two protein domains. These findings fuelled the design of specific point mutants of MCAK (Sandeep Talapatra), for which this binding site is perturbed and MCAK is forced into what we defined as an ‘open’ conformation (Talapatra et al, 2015). The sites mutated were highly conserved between species.

Evidence supporting an ‘open’ conformation is shown in (see **Figure 3.2-11**) Recombinantly purified GST tagged MCAK C terminus point mutants were used to immunoprecipitate recombinantly purified MCAK Motor Domain in vitro.

Wild type MCAK C terminus bound to MCAK Motor Domain, indicating the possibility of ‘closed’ conformation, binding is lost in all point mutations other than R716A and I718A, suggesting that full length MCAK with the same point mutations would not be able to form the same ‘close’ tertiary confirmation as wild type MCAK.

In parallel, I set out to investigate whether this change in conformation altered MCAK function in the cell.

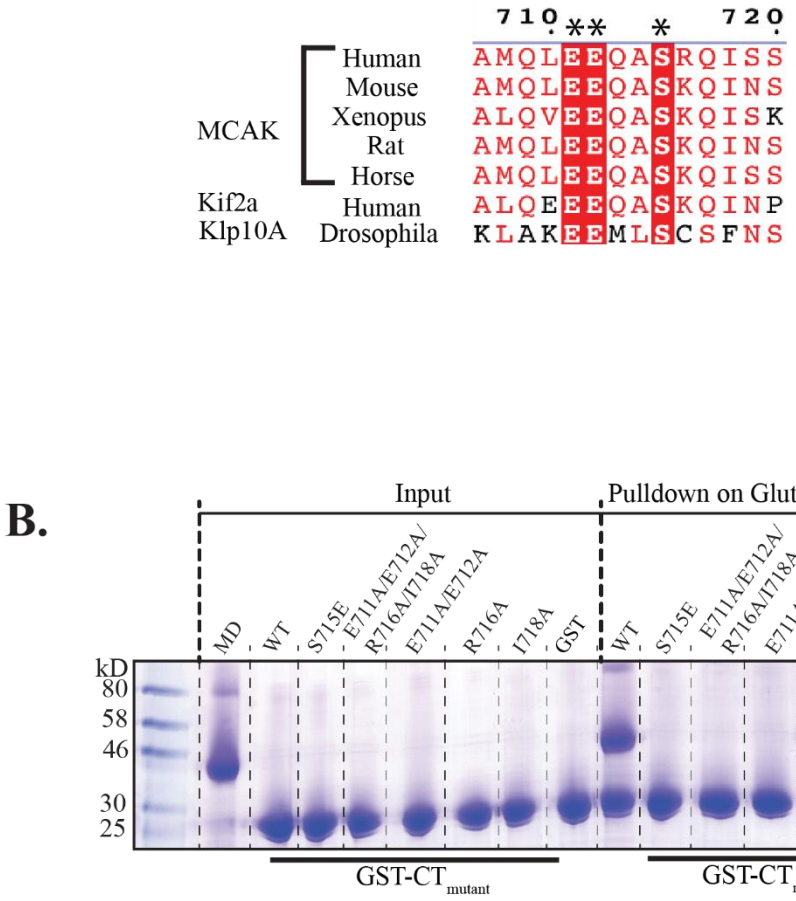

Figure 3.2-11 Specific mutations at the CT/MD interaction site perturbs MCAK-CT binding to MCAK-MD

(A) Amino acid sequence alignment of MCAK homologues is different organisms. Red blocks show amino acids of high sequence conservation between species. (B) Recombinant GST-CT point mutants were incubated with MCAK MD before isolation on Glutathione beads. Coomassie stained SDS-page acrylamide gel shows separation of the proteins isolated on the GST beads by size. Reactions in which MCAK MD bound to GST-CT mutants shows two bands, one at ~46kDa and one at ~27kDa, showing the presence of MCAK MD and CT respectively. This experiment was carried out by Sandeep Talapatra and adapted from (Talapatra *et al*, 2015).

3.2.2.1 Single point mutations in MCAK C terminus perturb its binding to Motor Domain in vitro

In vitro experiments show that R176A or I718A mutations in GST tagged C terminus of MCAK did not interfere with its binding to MCAK Motor Domain (see **Figure 3.2-11**). S715E or E711A and E712A mutations in GST tagged C-terminus, however, prevented it from binding to MCAK Motor Domain (see **Figure 3.2-11**). Following this, I wanted to investigate whether altering MCAK conformation changes its activity.

I hypothesised that a change in conformation will alter MCAK depolymerase activity either indirectly, by changing its localisation and thus access to microtubule substrates; or by directly altering MCAK intrinsic ATPase activity. To test this hypothesis, I generated constructs encoding GFP-MCAK with different point mutations and transiently transfected them into HeLa cells.

I used fixed immunofluorescence microscopy to image GFP-MCAK and stain for proteins which localise to the same mitotic structure as MCAK; EB1, a microtubule +end tracker; or Ndc80, a kinetochore protein. Reassuringly, MCAK localised to microtubule +ends and kinetochores and colocalised with EB1 and Ndc80 (see **Figure 3.2-12** and **Figure 3.2-13**).

In vitro, R716A and I718A mutated MCAK C terminus are still able to bind to Motor Domain and create a ‘closed’ conformation (see **Figure 3.2-11**). In cells, full-length $MCAK_{R716A}$ and $MCAK_{I718A}$ show unchanged microtubule

localisation and still localise to microtubule +ends (see **Figure 3.2-12**). Similarly, full-length MCAK$_{R716A}$ still localises to mitotic kinetochores (see **Figure 3.2-13**).

I was unable to obtain images of full-length MCAK$_{I718A}$ with Ndc80 staining. MCAK C terminus $_{E711A, E712A}$ was unable to bind to MCAK-Motor Domain *in vitro* but *in vivo* full-length MCAK with the same mutations is only weakly able to track microtubule +ends and is detectable at mitotic kinetochores. A combination of all 4 mutations compromises MCAK localisation at microtubule +ends and kinetochores (see **Figure 3.2-12** and **Figure 3.2-13**).

Together, these experiments indicate that mutations causing changes in full-length MCAK structure alter MCAK localisation in the cell, which could decrease net MCAK directed microtubule catastrophe, by reducing MCAK interaction with its substrate.

3.2.2.2 MCAK$_{S715E}$ shows altered localisation at microtubule +ends.

Determining the localisation of MCAK$_{S715E}$ by immunofluorescence was not possible. This could have been due to more transient binding, which is lost during cell fixation. Consequently, the localisation of MCAK$_{S715E}$ was determined through live-cell imaging. I co-transfected GFP-EB3 and mCherry-MCAK or mCherry-MCAK$_{S715E}$ into U2OS cells and imaged them using TIRF microscopy (**Figure 3.2-14**).

(A) I found that while MCAK tracks the microtubule polymerising plus end, $MCAK_{S715E}$ localises along the microtubule lattice and does not show an accumulation at plus ends. I quantified this result by taking line scan along the microtubule and measuring the average fluorescent intensity with one pixel either side of the line. From the line scan the distribution of MCAK is different when S715 is mutated to a negatively charged glutamic acid and that MCAK is more prevalent on the stable microtubule lattice.

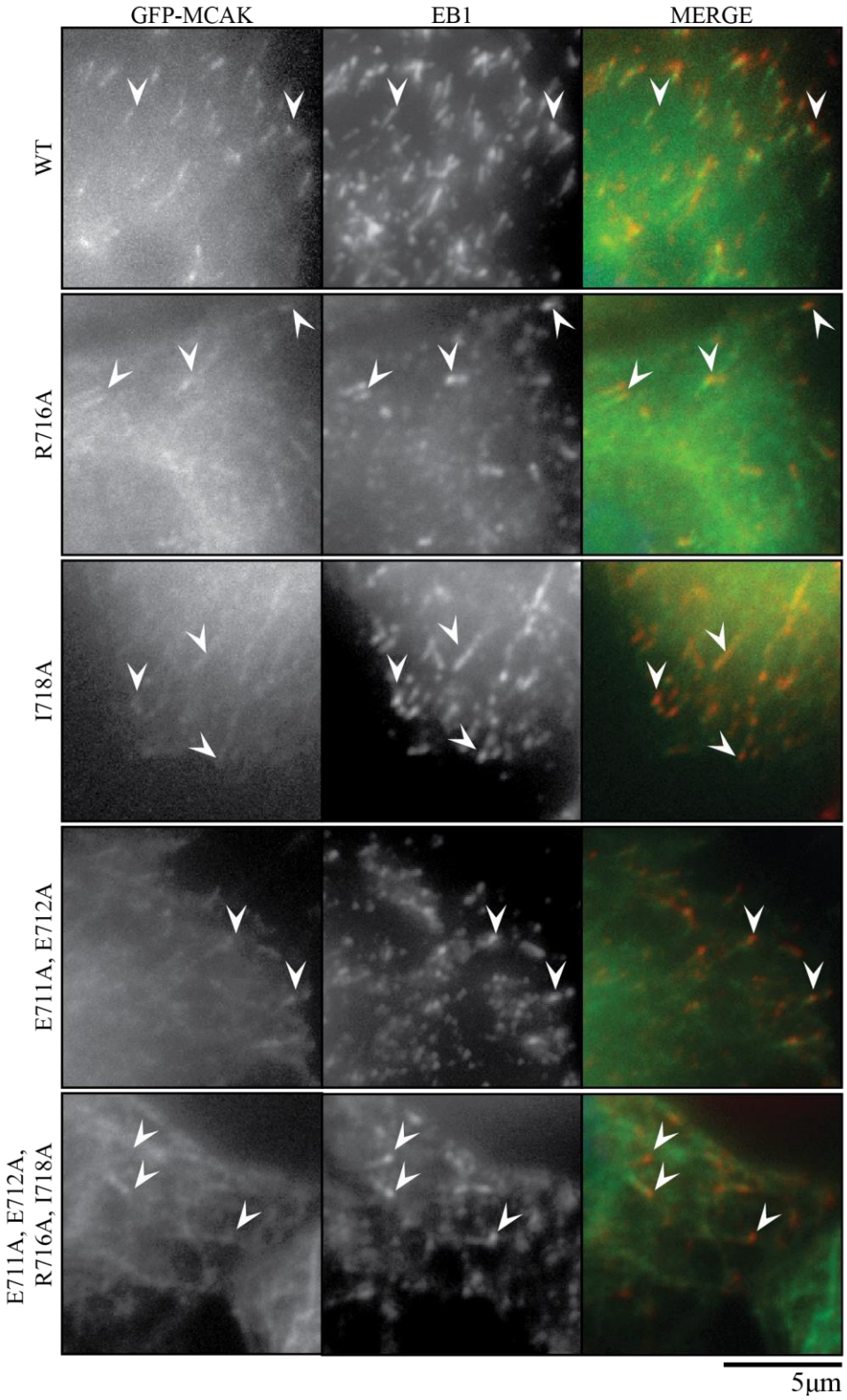

Figure 3.2-12 MCAK CT mutations alter its localization to growing microtubule +ends. HeLa cells were transiently transfected with GFP-MCAK (green) constructs containing point mutations in the CT-terminus. After 48h cells were fixed and EB1 was stained with mCherry (Red). Arrows indicate example growing microtubule +tips.

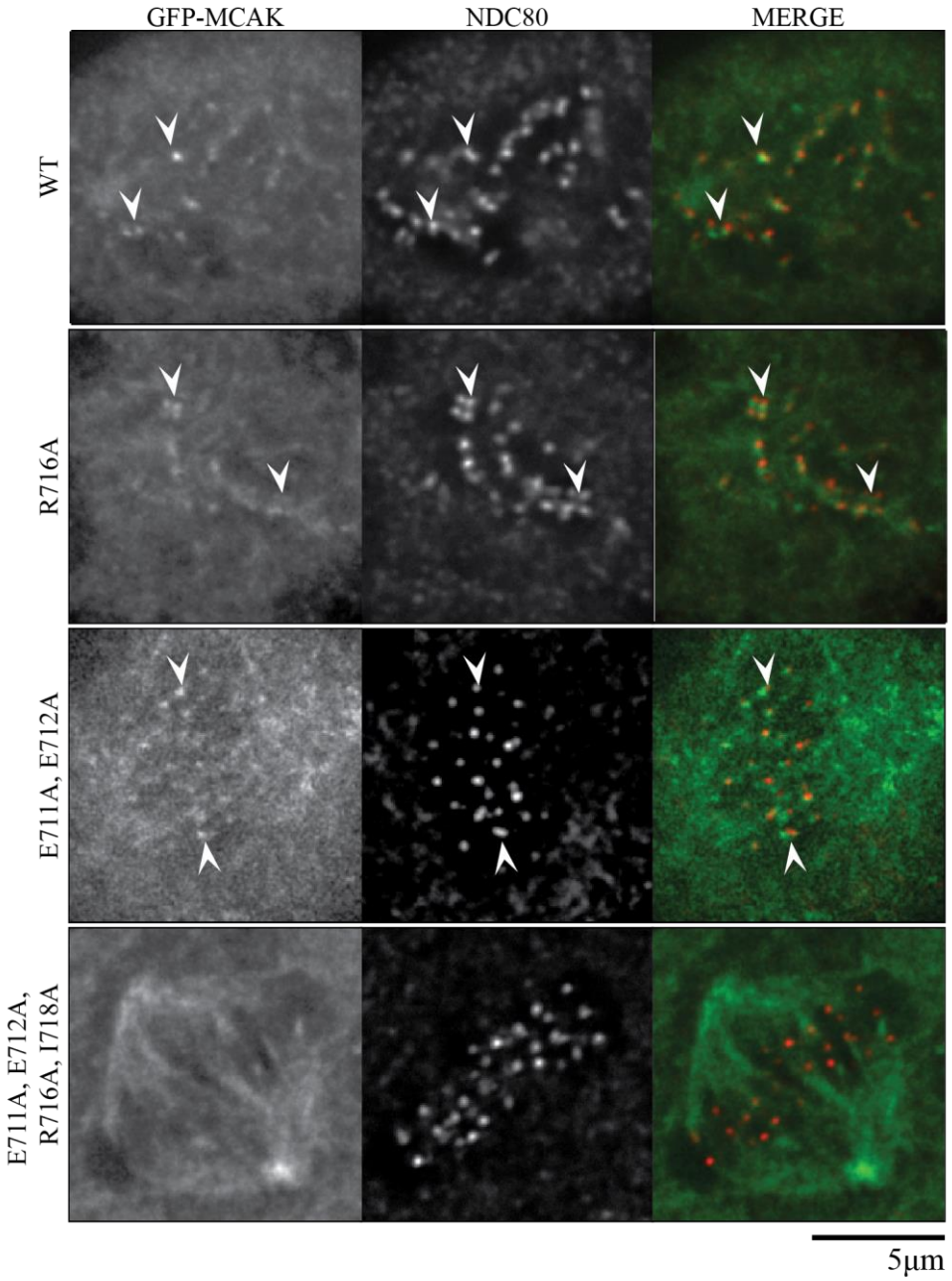

Figure 3.2-13 MCAK CT mutations alter its localization to kinetochores during mitosis. HeLa cells were transiently transfected with GFP-MCAK (green) constructs containing point mutations in the CT-terminus. After 48h cells were fixed and Ndc80 was probed for with mCherry conjugated antibodies (Red). Arrows indicate example kinetochores.

3.2.2.3 MCAK$_{S715E}$ binds to microtubules more stably but shows equal depolymerase activity compared to WT MCAK.

MCAK $_{S715E}$ preferentially binds more on the microtubule lattice than the growing microtubule +end compared to wild type MCAK. Microtubule binding assays (experiments Sandeep Talapatra) confirm this result. MCAK$_{S715E}$ is detected at higher levels on the microtubule lattice pellet in higher concentrations than WT MCAK, even at low tubulin concentrations (Figure 3.2-15). This indicates that MCAK$_{S715E}$ binds to a microtubule lattice with more affinity in an 'open' conformation compared to a 'closed' conformation.

Surprisingly, when ATP was added to a mix of MCAK or MCAK$_{S715E}$ and microtubules, the rate of depolymerisation was equal. Whilst the *in vitro* depolymerase assay may lack sensitivity, the current results indicate that 'open conformation' MCAK binds to microtubule lattices with higher affinity but does not alter its depolymerase activity.

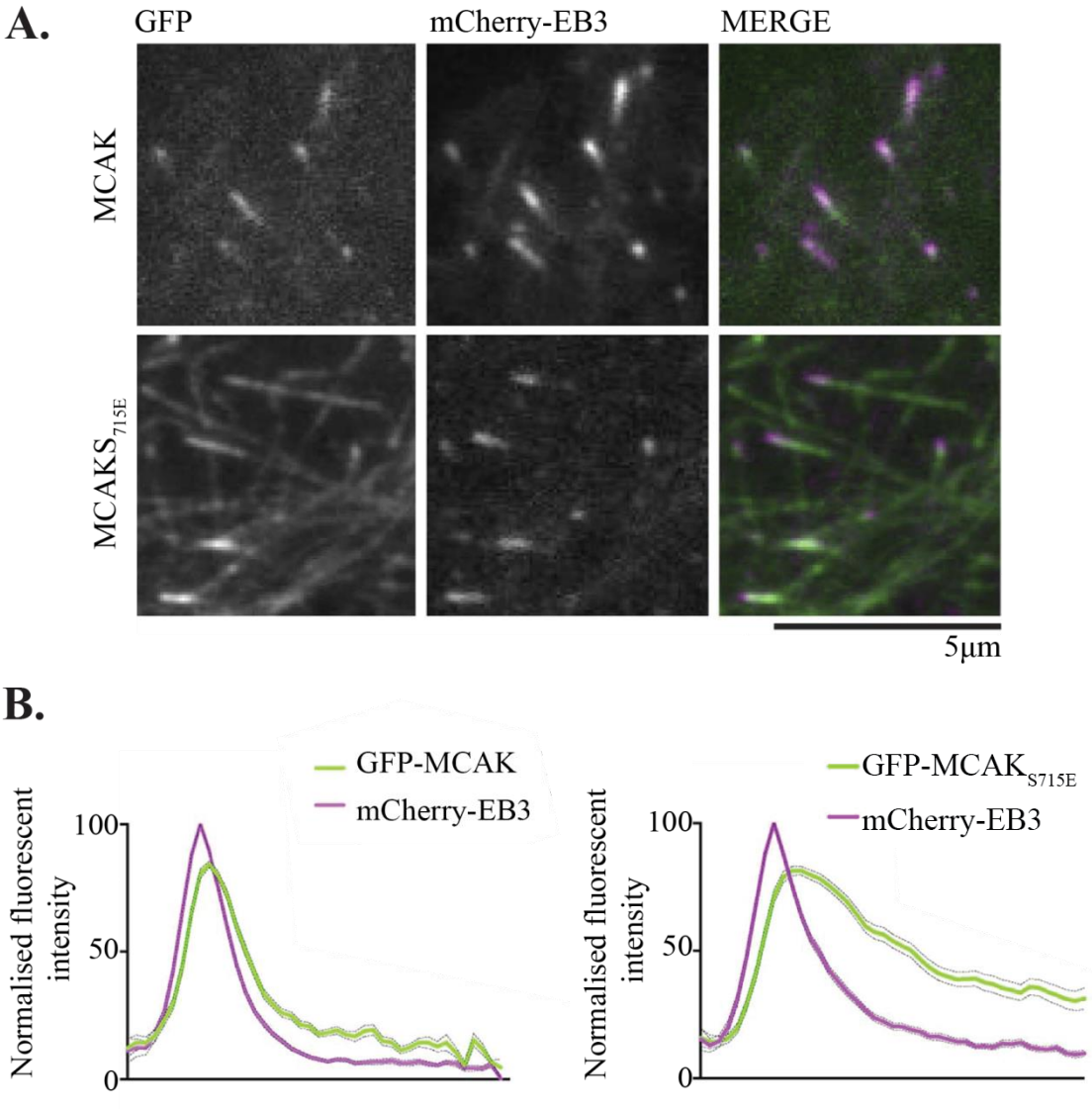

Figure 3.2-14 TIRF microscopy shows MCAK distribution on microtubules

(A) U2OS cell co-transfected with mCherry-EB3 and either GFP-MCAK or GFP-MCAKS715E. After 48h cells were imaged by TIRF microscopy. Representative images are shown and merged in in the final panel. Scale bar shows 5µm.

(B) Normalized fluorescent intensity profiles of line scans, taken along microtubule plus-tips of TIRF images shown in (A). (n=50). Grey shading represents standard error.

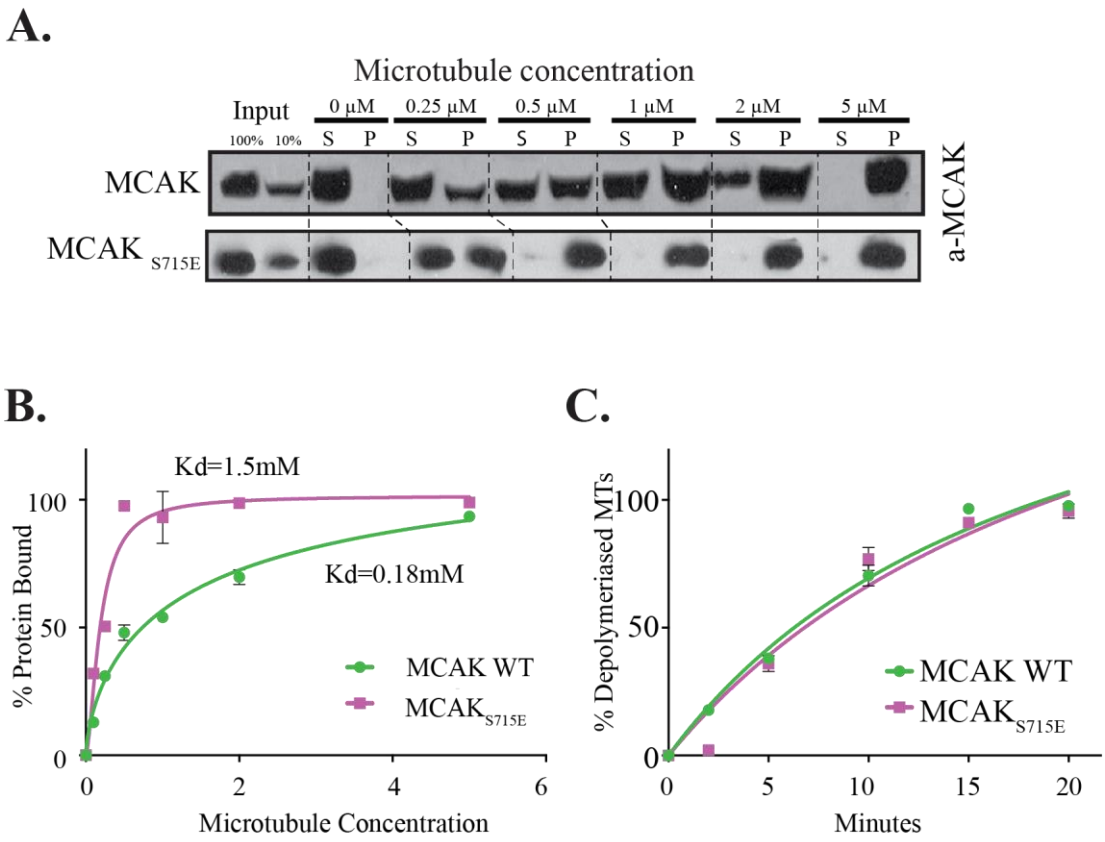

Figure 3.2-15 MT depolymerase activity of MCAK$_{S715E}$ shows the same depolymerase activity as MCAK but binds to microtubules with a stronger affinity.
(A) Recombinantly expressed MCAK and MCAKS715E were incubated with increasing concentrations of purified porcine brain microtubules. Reactions were centrifuged to separate microtubules and any bound proteins from free tubulin and unbound proteins. The pellets were electrophesed on an SDS-Page denaturing acrylamide gel and probed for the MCAK using an antibody raised against the C-terminus. This experiment was performed by Sandeep Talapatra and published in Talapatra et al (2015) (B) Quantification of the percentage of MCAK or MCAKS715E binding to microtubules using ECL signal intensity in pelleted microtubules versus that of free, soluble tubulin in the supernatant. (C) Stable microtubules were incubated with MCAK WT or MCAK$_{S715E}$ full-length proteins and ATP. At regular intervals, reactions were centrifuged and the levels of free 'depolymerized' tubulin was calculated as a measure of depolymerase activity.

3.2.3 Investigating the regulation of MCAK conformation by S715 phosphorylation.

One explanation for a loss of C terminus binding to Motor Domain when S715 is mutated to glutamic acid, is simply that the bulky glutamic acid residue causes steric hindrance and prevents crucial interactions between the C terminus and the Motor Domain which are needed to achieve interaction and maintain robust binding.

Glutamic acid substitution is used to mimic phosphorylation owing to the charge of the residue, therefore the loss of C terminus binding to Motor Domain could be due to the addition of charge to the residue, similar to that created by serine phosphorylation.

Serine 715 (718 in Xenopus) has been reported as a phosphorylation target of Plk1 and Aurora A kinase and is highly conserved across species (Santamaria *et al*, 2011; Zhang *et al*, 2008). I hypothesise that phosphorylation of MCAK at Ser715 regulates MCAK conformation, and that this mechanism could be used to affect microtubule dynamics in defined regions of the cell during mitosis.

3.2.3.1 Quantifying the specificity and efficiency of phospho-specific MCAK Ser715 antibodies on whole cell extract.

To test whether MCAK is phosphorylated at Ser715 in cells, we ordered an antibody against the C terminus of MCAK, and a phospho-specific antibody

against the same Ser715. I first tested the specificity and activity of the antibodies on recombinant MCAK. I used western blotting to transfer GST-tagged C terminus and GST-tagged MCAK C-Terminus$_{S715E}$ proteins, onto nitrocellulose membrane and probed them with both WT and MCAK$_{pS715}$ antibodies (see **Figure 3.2-16**).

Despite glutamic acid only having one negative charge rather than two, like a phospho-group, I hoped that MCAK$_{S715E}$ would be close enough to MCAKpS715 in negative charge to act as a positive control for the phospho-specific antibody. The antibody against MCAK C terminus was able to detect both phospho-mimetic and WT C terminus of MCAK while the phospho-specific antibody only recognised the phospho-mimetic C terminus peptide (see **Figure 3.2-16**).

To test the specificity of the antibody against WT MCAK, I probed for MCAK C terminus in a whole cell extract that had either been depleted of endogenous MCAK by RNAi using oligos against MCAK N terminus, or scrambled oligos (see B of **Figure 3.2-16**). The MCAK C terminus antibody was able to detect one band of protein, with a size corresponding to MCAK C terminus in cells which received the scrambled oligos, but not the cells depleted of MCAK. This indicated that the antibodies are specific for MCAK C terminus.

Following these promising results, I probed the whole cell extract for MCAK-$_{pS715}$. As a positive control for the antibody I transiently expressed GFP-MCAK or GFP-MCAK$_{S715E,}$ both of which are silently mutated to give resistance to the RNAi oligos (see C in **Figure 3.2-16**). The MCAK C terminus antibody recognised the GFP-MCAK and the endogenous MCAK, indicated by bands 30kDa apart at ~100kDa and 70kDa.

Unfortunately, the phospho-specific antibody did not detect any proteins from the whole cell extract, even the transfected GFP-MCAK$_{S715E}$ phospho-mimetic positive control. I repeated the experiment several times, with newly prepared antibody but was not able to detect phosphorylated S715 in whole cell extract.

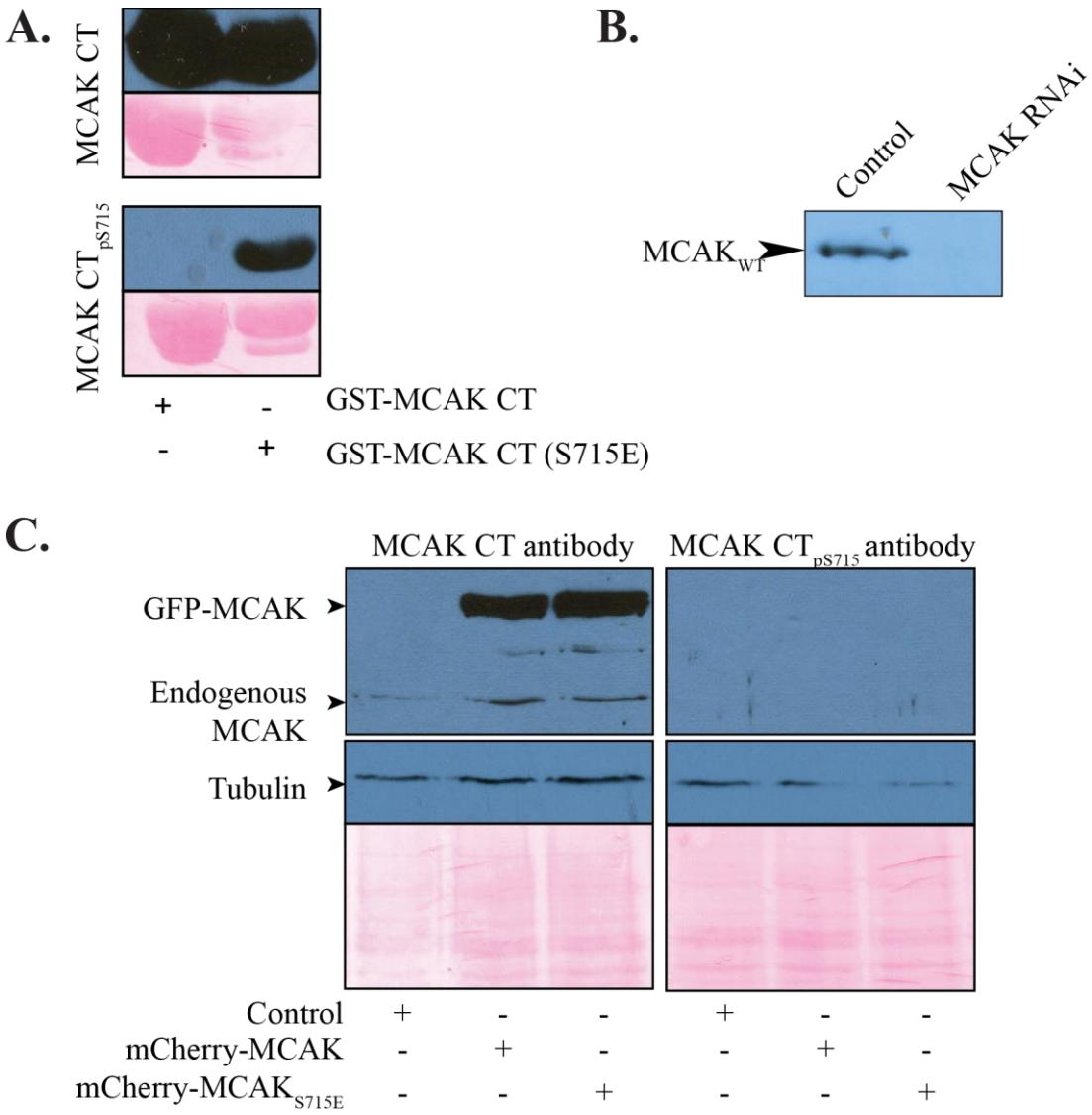

Figure 3.2-16 An assay to test the effectiveness of anti-MCAK and phosphorylated MCAK$_{S715}$ using recombinant protein and cell cultures.

(A) New anti-MCAK CT and anti-MCAK CTP715 antibodies were tested for accuracy and affinity by probing against recombinant, purified GST-CT and GST-CT$_{S715E}$. Experiment performed with first batch of diluted of antibody.(B) HeLa cell extract was probed for MCAK using the new antibody. Cells were transfected with either random oligos sequence or against MCAK N-terminus 72h before harvesting. (C) HeLa cells were transiently transfected with constructs coding for GFP-MCAK and harvested 72h later. Extracts were separated by size using denaturing SDS-Page electrophoresis. The same sample was split between two gels, each probed with a different antibody. Membranes were probed using antibody against MCAK-CT or MCAK-CTpS715. Ponceau staining of the membrane was used as a loading control. This experiment was performed using the second batch of diluted antibody,

3.3 Discussion

During mitosis, MCAK initiates microtubule catastrophe and is an important kinesin for regulating spindle length and microtubule dynamics (Moore & Wordeman, 2004a). In the absence of MCAK, cells demonstrate increased chromosome missegregation and DNA chromosome instability (CIN) (Maney *et al*, 1998; Moore & Wordeman, 2004a).

MCAK regulation is complex and multifaceted with both intrinsic and external modes of regulation (Yount *et al*, 2015). Spatial regulation of MCAK provides one layer of MCAK activity regulation. Regulated localisation within the cell can put MCAK within reach of its microtubule substrate to indirectly influence MCAK activity, or within the reach of other protein modifiers or binding partners; which directly alter MCAK activity (Tanenbaum *et al*, 2011a; van Heesbeen *et al*, 2016; Lee *et al*, 2008).

For example, kinetochore localisation is achieved via a localisation signal in the N-terminus of MCAK (Welburn & Cheeseman, 2012; Ems-McClung *et al*, 2007). At the kinetochore, MCAK is close to microtubule +ends, its substrate, and in the vicinity of Aurora B and Plk1 kinase activity, both of which have been shown to phosphorylate MCAK to directly alter its depolymerase activity (Andrews *et al*, 2004; Ems-McClung *et al*, 2013; Hood *et al*, 2012; Zhang *et al*, 2011; Shao *et al*, 2015).

Sub-spindle localisation of MCAK could be an additional, fine tuning method of MCAK regulation (Zhang *et al*, 2008, 2011; Shao *et al*, 2015; Zong *et al*, 2016). I hypothesised that, like the N terminus of MCAK, the C terminus also regulates MCAK in cells, by binding to the catalytic motor domain and altering either localisation of MCAK, its catalytic activity, or both.

Both the Welburn and Walzcak lab propose that MCAK can switch from 'open' to 'closed' conformations during its catalytic cycle (Ems-McClung *et al*, 2007; Talapatra *et al*, 2015). I was unable to definitively show that MCAK C terminus binds to the Motor Domain in cells using an adapted 'anchor-away' assay. However, with further optimisation I believe it could be possible.

One caveat of the experimental design is that the localisation signal is active as soon as the tagged protein is translated and folded into its tertiary structure. I have shown with *in vitro* assays that the complex of Motor Domain and C terminus requires spatial freedom in order to assemble, and without it the two proteins cannot be co-purified using immuno-precipitation. I propose that the same principle applies in the cell.

Using the current assay design, one of the tethered complex components is restricted to the membrane, imposing steric hindrance and limiting protein movement and conformation. An alternate method design would be to employ an inducible tethering assay PICT (Protein interactions from imaging

of complexes after translocation), which utilises a modified rapamycin induced FBP/FKBP ‘anchor-away’ technique (Gallego *et al*, 2013).
In this assay one of the complex partners is tagged with FRB, a small peptide which binds strongly to FKBP (which itself is constitutively recruited to the plasma membrane) but only upon the addition of rapamycin. In this system, complex components are free to bind and localise in the cells without steric interference before Rapamycin addition, after which the movement of protein/complex is more easily measured.

Successfully used in the Wordeman lab to rapidly relocalise MCAK to the plasma membrane within 3 minutes, I envision that this experimental approach would recreate the conditions required for complex formation *in vitro*, in a cell biochemical background (Wordeman *et al*, 2016).

Without definitively knowing the molecular arrangement of MCAK in cells, I proceeded to assess potential roles for MCAK C terminus on localisation and activity regulation, assuming that our hypothesis derived from in vitro data holds true in cells. I have shown that preventing the C terminus interacting with its Motor Domain alters MCAK sub-spindle localisation on microtubules.

Compared to WT MCAK conformations, ‘open’ conformation is less concentrated at growing microtubule tips and binding persists on newly incorporated tubulin, even after GTP hydrolysis to GDP. *In vitro*, an ‘open’ conformation translates to a stronger binding affinity for the stable

microtubule lattice. In cells, qualitative microtubule depolymerisation assays have been published using immunofluorescent labelling of tubulin in cells transiently transfected with modified MCAK (Shao *et al*, 2015; Moore & Wordeman, 2004b).

I performed these assays but found them very inconsistent and hard to draw conclusions from, based on the variable levels of transient protein expression in transiently transfected cells. However, from the same TIRF videos used to assess MCAK localisation qualitatively, improved +tip tracker software may be able to measure global microtubule dynamics in cells to correlate sub-spindle localisation of MCAK with local microtubule dynamics (Applegate *et al*, 2011; Matov *et al*, 2010; Braun *et al*, 2016; Stout *et al*, 2014).

I hypothesise that global rates of microtubule depolymerisation will be reduced in cells transfected with MCAK 'open' conformation, owing in part to a reduced availability of microtubule +end substrates.

Before completing my research, Plk1 had been shown to interact with human MCAK at the C terminus both in vitro and in vivo, and to phosphorylate MCAK in *in vitro* (Zhang *et al*, 2011). In *Xenopus*, Aurora A had both been implicated in phosphorylating MCAK at S715 equivalent residues (Zhang *et al*, 2008), and deletion of MCAK C terminus shows elevated levels of depolymerase activity using the aforementioned depolymerase assays (Moore & Wordeman, 2004b).

Drawing on these previous findings I hypothesised that phosphorylation of human MCAK at serine 715 could be a mechanism for regulating MCAK C terminus with its catalytic domain, altering its sub-spindle localisation and depolymerase activity.

Firstly, I attempted to confirm human $MCAK_{S715}$ phosphorylation in vitro. Using recombinant MCAK truncations I was unable to show MCAK phosphorylation at S715 by Plk1, I hypothesised that this lack of phosphorylation could have been limited by the size of the MCAK truncations used. Plk1 phosphorylation can be dependent on a post-translational modification on itself by another kinase and in fact, Shoa et al have shown that Plk1 is phosphorylated by Aurora B at kinetochores and that this phosphorylation is responsible for Plk1 phosphorylation of MCAK on S715 (Shao *et al*, 2015).

Using a 25-amino acid peptide as my substrate, in a minimal reaction containing only MCAK C terminus and Plk1 would not have allowed these modification prerequisites. To test these findings in my assay and accommodate for Aurora B activation of Plk1 phosphorylation of MCAK Serine 715, I could repeat the assay with the addition of in human cell extract.

To investigate MCAK serine 715 phosphorylation in cells, I ordered phospho-specific antibodies, to recognise the phospho site. Initially, the antibody showed promise in its specificity by recognising $MCAK_{S715E}$ truncations in vitro. Disappointingly, the antibody was unable to recognise full-length $MCAK_{S715E}$ from cell extracts, by immunofluorescence and western blotting.

This leads me to believe that unfortunately, the antibody efficacy had declined over time and, upon repeating *in vitro* assays, newly prepared antibody from powder stock was now unable to recognise even truncated $MCAK_{S715E}$. Since this study, an effective phospho-specific S715 antibody has been synthesised and with it insight has been gained into to the temporal regulation of MCAK activity at the kinetochore (Shao *et al*, 2015).

In vitro, anti-pS715 antibody recognised a decrease of phosphorylation in cells treated with inhibitors against Aurora B, Aurora A and Plk1, consolidating previous studies which described C terminus phosphorylation by either Plk1 or Aurora A (Shao *et al*, 2015; Zhang *et al*, 2011, 2008). In cells, the phosphospecific antibody shows MCAK S715 phosphorylation at centromeres, owing to a described Aurora B/Plk1 signalling cascade (Shao *et al*, 2015).

At centrosomes, a study using *Xenopus* MCAK C terminus depicts a similar signalling cascade at centrosomes, initiated by active Aurora A (Zong *et al*, 2016; Shao *et al*, 2015). Together these papers demonstrate regulation of

MCAK conformation on a sub-spindle level. In addition, complimentary *in vitro* studies by Sandeep Talapatra, link ‘open’ conformation of MCAK with increased depolymerase activity (Talapatra *et al*, 2015; Shao *et al*, 2015).

Chapter 4: Studying kinesin function for proper meiosis in *S.cerevisiae*

4.1 Introduction

For proper reductive chromosome segregation during meiosis, newly duplicated homologous chromosome pairs must bivalently attach to a microtubule spindle and separate to opposite poles of the cell. In a second round of division sister chromatids are segregated, forming 4 separate masses of DNA (Potapova & Gorbsky, 2017; Petronczki *et al*, 2003). To orchestrate this elegant series of events, the mitotic spindle is constantly remodelled and regulated (Gadde & Heald, 2004; Kapoor & M., 2017). Firstly, the interphase spindle must be disassembled, and the spindle pole bodies must be duplicated. In *S.cerevisiae* mitosis, newly duplicated spindle poles are separated by a bridge structure, which is severed to release spindle poles, allowing them to migrate to opposite sides of the nuclear membrane. Migration to opposite poles and maintenance of the interdigitated antiparallel microtubule array, which keeps them apart, is orchestrated in part by kinesin proteins (Lim *et al*, 1996; Byers & Goetsch, 1975; Saunders, 1993). After successful metaphase chromosome orientation, coordinated microtubule dynamics pull chromatid pairs to opposite spindle poles. Between the first round of division and second round of division the meiotic spindle is disassembled and the two SPBs are duplicated (Stern, 2003). This process in part utilises the Cdc14 regulated FEAR pathway, (Marston *et al*, 2003; Ruthnick & Schiebel, 2016; Fox *et al*, 2017). Different from meiosis I, two distinct microtubule spindles must form in the same nucleus and orchestrate chromosome segregation in the same cell.

Human cells contain a large number of kinesins with varied structure and function (Miki *et al*, 2005). With large numbers of kinesins, comes a large scope for functional redundancy and interdependency, which has made studying individual contributions of each kinesin during cell division difficult, particularly *in vivo*. In comparison to human cells, *S.cerevisiae* only has 6 kinesins; Kip1, Kip2, Kip3, Cin8, Kar3 and Smy1, which presents itself as a useful tool for studying individual kinesin contributions to cell division *in vivo* (McAinsh *et al*, 2003). Moreover, for the purpose of studying meiosis in vivo, rather than mitosis, *S.cerevisiae* exists as either a haploid or diploid, and readily switches between the two by mating and meiotic sporulation, providing a great opportunity to study kinesin roles in meiosis cheaply and quickly.

Currently, there is void of knowledge on the role of the 6 kinesins in *S.cerevisiae* meiosis compared to mitosis, and considering the vast biochemical and physical differences between mitosis and meiosis; I hypothesis that the function and importance of each kinesin for proper mitosis is not directly translated from mitosis to meiosis.

To approach the question unbiasedly, I decided to first assay the importance of each kinesin for proper meiotic progression and chromosome segregation in meiosis before endeavouring to ascertain their function.

4.2 Results

4.2.1 Initial screening shows that Cin8 and Kar3 are more important for meiosis than other kinesins but not essential.

For screening purposes, I replaced each kinesin gene with a drug resistance marker *S.cerevisiae* in haploid cells, mating them to generated diploids homozygous for the mutation of interest and assessed 4 parameters after Kip3 and Kar3. I did not analyse cells lacking Smy1 because the literature suggests that it is not involved in mitosis, but in the transport of secretory vesicles (Lillie & Brown, 1994, 1998, 1992; Lwin *et al*, 2016).

It is important to note that Kar3 is essential for karyogamy during strain mating (Polaina & Conde, 1982; Meluh & Rose, 1990) and as such, generating diploid cells from haploid strains lacking *KAR3* is not possible. To overcome this problem, I exchanged the promoter of *KAR3* with the *CLB2* promoter (Lee & Amon, 2003) . Since Clb2 is expressed during mitosis, but not during meiosis, this should result in the meiosis-specific depletion of Kar3. Kar3 in this construct is also tagged at its N terminus with 3HA epitopes. To confirm that Kar3 was not produced in meiosis, I probed for Kar3 throughout meiosis and in an asynchronous mitotic culture using anti-HA antibodies (**see Figure 4.2-1D**). While Kar3 was not completely absent in meiosis its levels were dramatically reduced.

Having generated yeast strains in which kinesins were absent or depleted during meiosis, I went on to characterise their phenotype. First, I assayed was the rate of meiotic progression. If chromosome segregation is perturbed

the cell employs certain checkpoints to arrest the cell cycle and allow for correction. This translates to a measurable delay in the time taken to finish meiosis with 4 segregated Dapi stained masses (Allshire, 1997). To test whether the absence of kinesins resulted in a meiotic delay, I induced diploid cells lacking (or depleted for) each of the kinesins into meiosis and counted Dapi stained masses in the cell at regular intervals (see **Figure 4.2-1** A). Wild type cells show an increase of 4 Dapi stained masses over time, particularly between 6-8 hours, with ~ 70% of cells finishing meiosis in the first 10 hours. Cells lacking Kip1, Kip2 and Kip3 all perform meiosis at a similar rate to wildtype. However, only ~25% of cells lacking Cin8 completed meiosis within 10 hours, and only a few cells with reduced levels of Kar3 formed 4 DAPI stained masses. I conclude that both Cin8 and Kar3 are required for successful meiosis.

To determine whether the lack of cells with 4 DAPI stained masses seen in *cin8Δ* and *pCLB2-3HA-KAR3* strain is due to a failure to enter or complete meiosis or whether meiosis is completed but chromosomes are missegregated, I surveyed >100 cells 10 hours after inducing sporulation and scored the shape and segregation pattern of DNA (Left graph in Figure 4.2-1A). If cells are delayed in meiosis I would expect an accumulation of cells with 1 or 2 Dapi stained masses, accounting for cells stuck in earlier stages of meiosis. This is the case for *pCLB2-3HA-KAR3* cells, 79 % of cells had only one dapi mass, indicating an arrest in early meiotic events. A sizeable fraction (24.5%) of *cin8Δ* cells showed undistinguishable DAPI

masses, suggesting that *cin8Δ* potentially causes chromosome segregation and meiotic defects.

To visualise chromosome segregation in *cin8Δ* cells, I crossed haploid strains carrying the deletion with those containing a *tetO* repeat array integrated close to the centromere on chromosome V, and expressing GFP-TetR, then made diploid cells homozygous for the *cin8Δ* deletion and for the GFP-labelled chromosome. The resulting strains display a GFP dot on chromosome 5, which is replicated during DNA replication and can be followed through segregation (**See Figure 4.2-1B**). After meiosis I, two GFP dots should be observed: one in each of the segregated DAPI-stained masses. After meiosis II, cells show four GFP dots, one in each of the four DAPI-stained masses. Screening within the population of cells with 4 DAPI-stained masses, I found that 29% of *cin8Δ* cells had more than 4 GFP dots, suggesting either improper number of ChrV in the cell or overduplication of DNA. However, those with 4 GFP dots segregated them at a similar efficiency to wild type cells, one into each Dapi stained mass. Upon examination, *kip1Δ, kip2Δ* and *kip3Δ* cells showed unperturbed chromosome segregation of ChrV, like wild type strains. I attempted the same assay with a *pCLB2-3HA-KAR3* strain but was unable to create the strain in the available time, owing to difficulty generating spores by dressing the stains.

S. cerevisiae have 16 chromosomes. A caveat of looking at the segregation patterns of one chromosome over the course of meiosis is that you are

unable to visualise or measure the frequency of segregation defects in the other 15 chromosomes. In addition, this experiment is unable to measure the importance of any chromosome segregation defects without knowing the long-term viability of the cells. To screen the viability of strains lacking kinesins, I performed spore viability assays. Cultures were induced to undergo meiosis on solid agar –containing sporulation (SPO) media (See Methods 2.2.2.6). The resulting tetrad spores were dissected into their constituent haploids and grown on 2% glucose (rich) solid Agar media to allow them to germinate (see Figure 4.2-1C). Spore viability assays show that while *kip1Δ* cells show normal ChrV segregation and meiotic progression there is a reduced spore viability compared to wild type. Also, *cin8Δ* results in a large decrease in spore viability, potentially due to chromosome polyploidy and aneuploidy defects observed above. Additionally, only 59% of *pCLB2-3HA-KAR3* spores were viable. It should be noted, however, that due to the very poor sporulation efficiency of *pCLB2-3HA-KAR3* cells, this is a highly selected population since finding 100 tetrads in spore cultures expressing *pCLB2-3HA-KAR3* was very difficult and required a larger culture of cells compared to wild type cells.

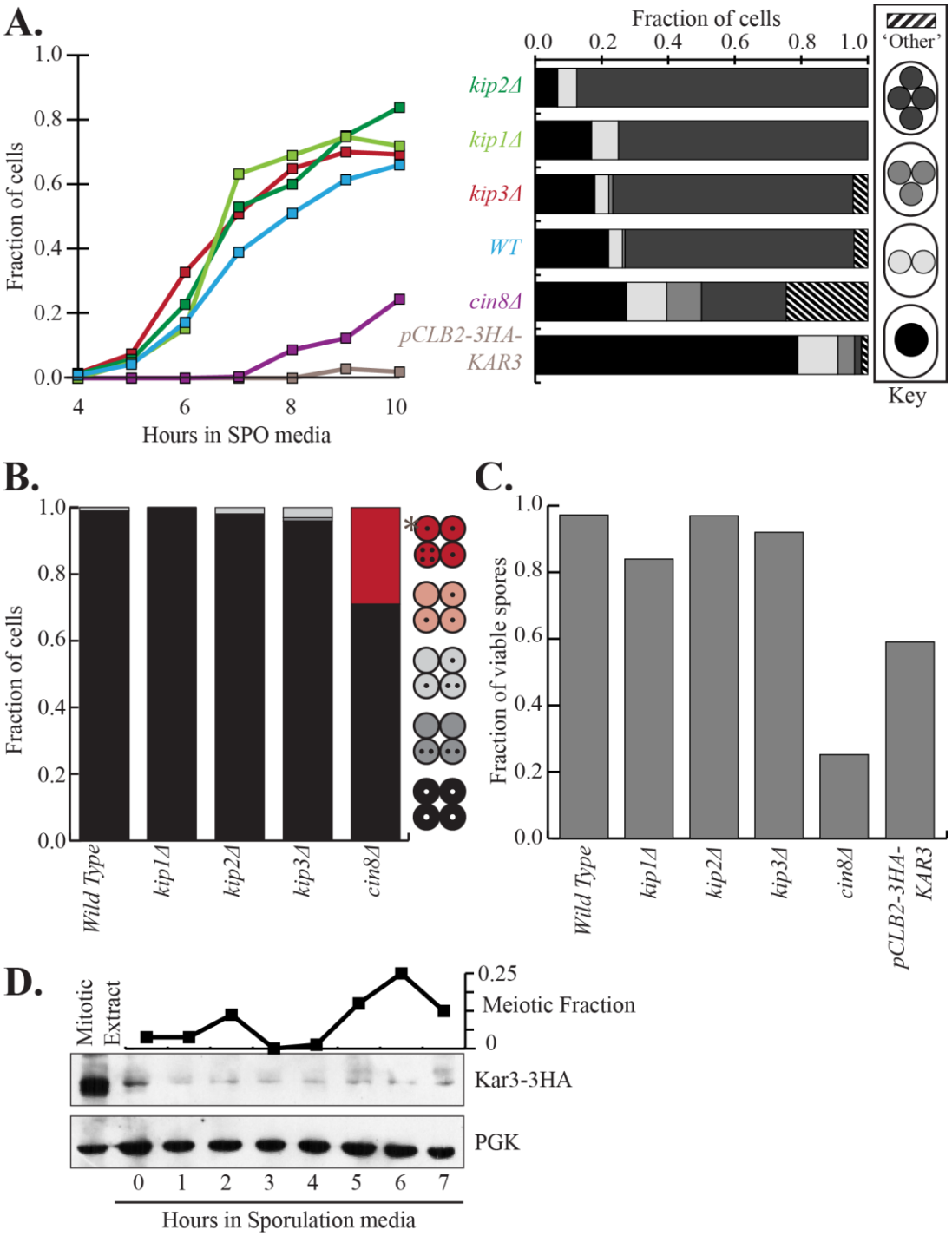

Figure 4.2-1. A screen to estimate the contributions of different kinesins on proper meiotic chromosome segregation.

Stationary phase *S.cerevisiae* cultures were released into meiosis and samples collected every hour. (A) Meiotic samples were fixed in methanol and stained with Dapi to count chromosome masses. Left graph shows the fraction of 100 cells counted with 4 Dapi stained masses over the course of the experiment; right graph displays the fraction of cells after 10

hours with 1, 2, 3, 4 or ‘other’ undistinguishable Dapi stained masses. (B) Chromosome segregation after 10h was assessed using strains expressing Tet-O arrays on CenV, recording the segregation pattern of CenV in cells with 4 segregated Dapi strained masses (Methods 2.2.2.6). * represents extra GFP dots (>4) caused by polyploidy. (C) 100 tetrads, sporulated on agar media, were isolated and dissected. The viability of individual spores was scored on their ability to grow on 2% glucose YPDA agar media. (D) Kar3 endogenous promotor was replaced with pClb2 and HA tagged. Conditional protein depletion during meiosis was confirmed by probing for HA on TCA extracted protein samples, separated by SDS-PAGE and transferred onto nitrocellulose by Western Blot (See 2.2.2.1).

4.2.2 Conditional meiosis-specific depletion of Cin8 reveals greater importance in meiosis than mitosis.

Cin8 has no recorded function in DNA replication and as such it was surprising to see more than 4 ChrV *tetO* foci during meiosis, which would normally suggest over duplication for chromosomes. Removal of Cin8 during mitosis however is described to cause chromosome missegregation, resulting in an accumulation of chromosome instability and abnormal chromosome numbers. I hypothesis that the severe meiotic defects are caused by a combination of losing Cin8 function in meiosis, but also the cumulative effect of not having Cin8 during the mitotic divisions prior to meiosis. To dissect Cin8 importance in mitosis and meiosis I swapped the *CIN8* promoter for that of *CLB2*, verifying meiosis specific depletion of Cin8 by Western Blot (Figure 4.2-2A). Upon further assay, cells lacking Cin8 in meiosis only show a normal number of chromosomes and thus I can trust that any meiotic defects see are henceforth a result of Cin8 in meiosis and not carried over from aberrant mitosis (see Figure 4.2-2C).

4.2.3 Cells depleted of Cin8 during meiosis generally segregate chromosomes properly but fail to package them properly in spores.

Using conditional Cin8 meiosis-specific protein depletion I proceeded to assay potential defects in meiosis (see **Figure 4.2-2**). Initially the rate of meiotic progression appears slower in *pCLB2-3HA-CIN8* strains compared to wild type strains, with lower frequency of tetranucleates 10h after sporulation

induction. However, under closer inspection, the rate of progression is not notably different; cells complete meiosis in 10h but form an elevated number of trinucleate rather than tetranucleate cells (see **Figure 4.2-3**B). GFP-TetR on ChrV segregates as well as wild type strains in *pCLB2-3HA-CIN8* strains, but globally spore viability after chromosome segregation is 21.7% less than wild type strains. I was curious to know whether triad formation was a result of chromosome missegregation. Therefore, I analysed GFP-*tetO* segregation patters after 10 hours. Over 80% of triad spores lacking Cin8 during meiosis contained 4 distinct *tetO* arrays, with two in one spore. This suggests that the cycle of cohesin loss on chromosomes may occur normally, but that nuclear division fails in meiosis II.

4.2.4 Meiosis specific depletion of Cin8 in combination with Kip3 deletion exacerbates meiotic defects.

In cycling cells, it has been reported that combining a *cin8* deletion with a *kip1* deletion is lethal (Geiser *et al*, 1997; Hoyt *et al*, 1992; Roof *et al*, 1992). Consistent with this, I was unable to make a strain, diploid or haploid, by transformation or mating, lacking both Cin8 and Kip1. To study the combined importance of Kip1 and Cin8 for proper meiosis, I also tried to combine *kip1Δ* with *pCLB2-3HA-CIN8* but any spore containing both genetic changes was inviable (Data not shown). Kip3 has also been reported to share some functional redundancy with Cin8 during mitosis and acts antagonistically to Cin8 at certain stages of mitosis (Roof *et al*, 1992; Hoyt *et al*, 1992). To

examine functional redundancy during meiosis, I designed a strain lacking Kip3 and conditionally depleted for Cin8 during meiosis. Together these mutations massively perturbed meiotic progression, more so than either protein compromised alone, with few cells going through meiosis over the course of 10h. Over 60% of cells were still mononucleate while about 20% were binucleate at 10h (see **Figure 4.2-2**B). Cells that had completed meiosis had strange phenotypes, making them hard to classify, with DNA fragments outside of the pre-spore walls, seemingly not encased in a spore. Combined with a resulting spore viability of 34%, I hypothesise that combining *kip3Δ* with *pCLB2-3HA-CIN8* causes aneuploidy and chromosome instability (see **Figure 4.2-2**D). In fact, looking at GFP-*tetO* arrays on ChrV, over 20% of tetrads show chromosome missegregation, and 10% of tetrads have spores completely lacking ChrV. The same is true for chromosome segregation in triads, with almost 40% of triads having missegregated chromosomes and ~30% having improper ChrV number, some of which are outside of the pre-spore walls, in small DNA fragments scattered in the ascus (see **Figure 4.2-2**C). It is important to note that it's possible to mistake two ChrV dots for one when looking by eye on an epifluorescent microscope if they are in very close proximity. Together this data suggests that there is functional redundancy between Cin8 and Kip3 during meiosis but also that neither Cin8 or Kip3 are individually essential for proper meiosis.

4.2.5 Cin8 alone, without Kip1 and Kip3, is sufficient for proper chromosome segregation and meiotic progression.

Neither Cin8 meiotic depletion, Kip1 deletion or Kip3 deletion causes meiotic lethality, indicating that none of them are uniquely essential for proper meiosis. However, Cin8 meiotic depletion in combination with Kip3 deletion had detrimental effects on meiosis and chromosome segregation, while Cin8 meiotic depletion in combination with Kip1 deletion becomes lethal even in mitosis. Together this data leads me to hypothesise that Cin8, Kip1 and Kip3 all share functional redundancy to some extent; however, I cannot tell where these functional redundancies overlap and for what purpose. Above, in 4.2.4, I describe data that describes Kip1 as sufficient for meiosis without Cin8 and Kip3, albeit with some aberrations. Also, I have shown that Kip3, in the absence of Kip1 and Cin8 is insufficient even during vegetative growth Next, to test whether Cin8, in the absence of Kip1 and Kip3, is sufficient for proper meiosis and to what extent its functions are unique, I designed a strain lacking both Kip1 and Kip3 in *S.cerevisiae* and repeated screen assays. In all assays, the *kip1Δ* and *kip3Δ* strains behaved like wild type strains. This data supports a hypothesis that of Kip1, Kip3 and Cin8, Cin8 or Kip1 alone are sufficient for proper meiosis. but not necessary, unlike Kip3, which cannot support proper meiosis in the absence of either Kip1 or Cin8 (see **Figure 4.2-2**).

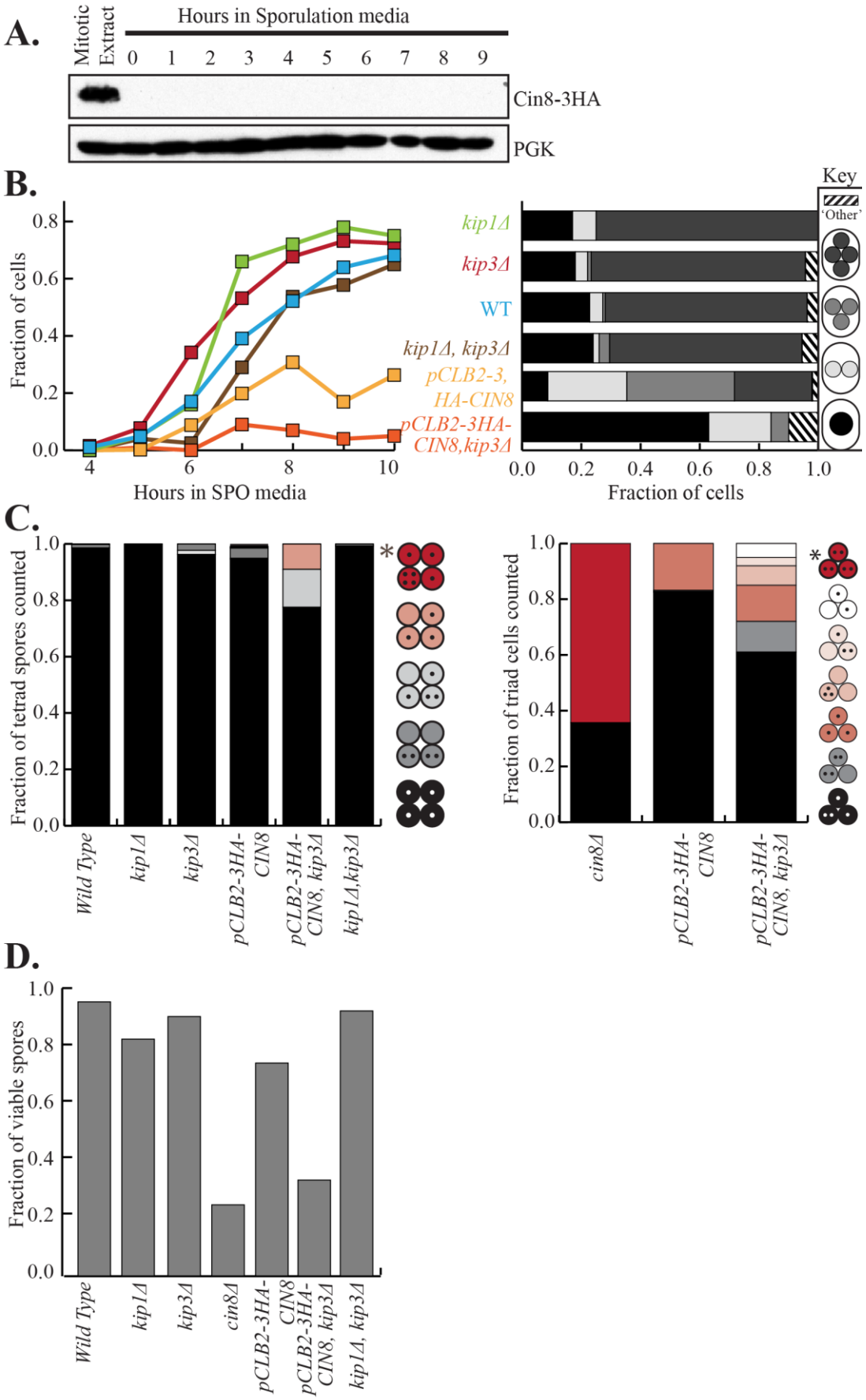
A.
Mitotic Extract
Hours in Sporulation media
0 1 2 3 4 5 6 7 8 9
Cin8-3HA
PGK
B.
Fraction of cells
Hours in SPO media
kip1Δ
kip3Δ
WT
kip1Δ, kip3Δ
pCLB2-3, HA-CIN8
pCLB2-3HA-CIN8,kip3Δ
Key
'Other'
Fraction of cells
C.
Fraction of tetrad spores counted
Wild Type
kip1Δ
kip3Δ
pCLB2-3HA-CIN8
pCLB2-3HA-CIN8, kip3Δ
kip1Δ,kip3Δ
Fraction of triad cells counted
cin8Δ
pCLB2-3HA-CIN8
pCLB2-3HA-CIN8, kip3Δ
D.
Fraction of viable spores
Wild Type
kip1Δ
kip3Δ
cin8Δ
pCLB2-3HA-CIN8
pCLB2-3HA-CIN8, kip3Δ
kip1Δ, kip3Δ

Figure 4.2-2. An in-depth screen to assess contributions and functional redundancy between Kip1, Kip3 and Cin8 for proper chromosome segregation.
Asynchronous *S.cerevisiae* samples were released into meiosis and samples were collected every hour. (A*) CIN8* endogenous promotor was replaced with *pCLB2* and tagged with HA (see Methods 2.2.2.1). Conditional protein depletion during meiosis was confirmed by probing for HA by Western Blot on TCA extracted protein samples, separated by SDS-PAGE and transferred onto nitrocellulose. (B) Meiotic samples were fixed in methanol and stained with DAPI to count chromosome masses. Left graph shows the fraction of 100 cells counted that have 4 Dapi masses over the course of the experiment; right graph displays the fraction of cells after 10 hours with 1, 2, 3, 4 or 'other' undistinguishable Dapi masses. (C) Chromosome segregation after 10h was assessed using strains expressing Tet-O arrays on CenV, recording the segregation pattern of CenV in cells with 4 segregated Dapi masses (Left) or 3 Dapi masses (Right) (see methods 2.2.2.6). * represents extra GFP dots (>4) caused by polyploidy. (D) 100 tetrads, sporulated on agar media, were isolated and dissected. The viability of individual spores was scored on their ability to grow on 2% glucose YPDA agar media.

4.2.6 Conditional depletion of Cin8 during meiosis results in shorter microtubule spindles during meiosis I and meiosis II.

As described above; Cin8 conditional depletion during meiosis results in lower spore viability and spore formation defects. The literature describing studies carried out in mitosis suggests that cells lacking Cin8 in mitosis experience spindle collapse and as a result frequently carry aneuploidy through mitosis, making cultures sick over time (Hoyt *et al*, 1990). To test whether the same is true in meiosis, I created an *S.cerevisiae* strain with *pCLB2-3HA-CIN8*, in combination with Tub1-GFP fluorescent tubulin (see **Figure 4.2-3**A). Using fluorescent tubulin as a marker for the meiotic spindle, I performed live cell imaging of cells progressing through meiosis, measuring spindle length when at its longest, just before spindle breakdown at both meiosis I and meiosis II. As well as visualising spindle break and rescue in real time, I found that spindles in both anaphases of meiosis were significantly shorter in Cin8-depleted cells, measuring 5.38µm ±0.15 vs. 6.14 µm ±0.10 in Wild Type cells (see **Figure 4.2-3**B). This data indicates that like mitosis, Cin8 is important for meiotic spindle maintenance.

4.2.7 Conditional depletion of Cin8 during meiosis Results in triads, containing mainly sister homologues.

Using fluorescent microscopy to image DNA mass and TetO ChrV segregation, cells expressing pCLB2-3HA-Cin8 appear to complete meiosis within the 10h of meiotic release, and segregate chromosomes to form 4

distinct TetO ChrV arrays, however when the spores are counted there is a high frequency of triads and dyads rather than tetrads. Viability of tetrad spores is partially compromised but not compared to *Cin8Δ* strains which show high aneuploidy. I hypothesized that the chromosomes are segregated properly but spore formation is partially compromised. To test this, I dissected pCLB2-CIN8 triad spores and tested their mating type by replica plating the dissected spore colonies onto agar plates covered with wild type haploids of either mating type. Upon triad ascus dissection, 62% were viable, 14% less than tetrads of the same strain indicating a higher level of chromosome instability but less than the aneuploidy caused by *cin8Δ.* In 34% of triads dissected, all three spores of the triad were viable.

Following meiosis II, the central plaque of each SPB is modified for form the spore plaque, at which point It is able to assimilate membranous vesicles and form prespore walls around newly segregated DNA masses (Neiman, 2005). Under certain conditions, such as delayed meiosis >10h, carbon starvation or sporulation in water, only one SPB per meiosis II spindle is modified, resulting in non-sister dyad (Neiman, 2005). Non-sister dyads are haploid, in that they contain homologues which were segregated from their sisters in meiosis I, and are a single mating type as a result. Of the 29 triads consisting of three viable spores (87 spores in total), 92% (80 spores) had a single mating type, and only 8% (7 spores) were a:α:diploid. This indicated that Cin8 contributes to spore formation in meiosis and could prove topic for an interesting route of investigation.

4.2.8 Deletion of Kip3 has no significant effect on meiotic spindle length during meiosis I but spindles are shorter during meiosis II.

In meiosis, Cin8 has been described to work in synergy with Kip3 to maintain spindle length during metaphase, and extend meiosis during anaphase (Su *et al*, 2013). In addition, cells lacking Kip3 have been described to have a 'lasso' microtubule phenotype in mitosis, caused by longer buckled spindle microtubules when spindle midzone microtubule elongation is no longer supressed by Kip3 (Straight *et al*, 1998; Cottingham & Hoyt, 1997; Rizk *et al*, 2014). Considering this, and that cells depleted for Cin8 in meiosis are shorter, I hypothesised that cells lacking Kip3 would have significantly longer spindles. However, there is no significant increase in spindle length in *kip3* mutants during meiosis and in fact, surprisingly, spindles are significantly shorter during anaphase of meiosis II at 6.06 µm ± 0.18 and 3.88 µm ±0.14 respectively, compared to 6.31 µm ± and 4.68 µm ±0.13 in wildtype for meiosis I and II respectively (see **Figure 4.2-3**).

4.2.9 Deletion of Kip3 in combination with Cin8 meiotic deletion results in significantly longer spindles during both meiosis I and II.

Based on the literature (Su *et al*, 2013; Rizk *et al*, 2014) I initially hypothesised that *Cin8Δ* during meiosis in combination with *Kip3Δ* would result in longer spindle lengths compared to wild type. However, after measuring spore viability, and chromosome segregation, I rejected my hypothesis. Depletion of Cin8 during meiosis results in shorter spindles

during both meiosis I and II. Deletion of Kip3 has no significant effect on meiotic spindles during anaphase I but significantly decreases spindle length during anaphase II (see **Figure 4.2-3**). Based on this data I hypothesised that a combination of the two mutations could result in smaller spindles throughout meiosis. In fact, cells depleted of Cin8 and lacking Kip3 during meiosis had significantly longer spindles than WT during anaphase I and II, with 7.63 µm ±0.11 and 6.62 µm ±0.1 respectively (see **Figure 4.2-3**). It is possible that this phenotype is a result of spindle checkpoint activation, which would cause longer spindle, and would have to be investigated further.

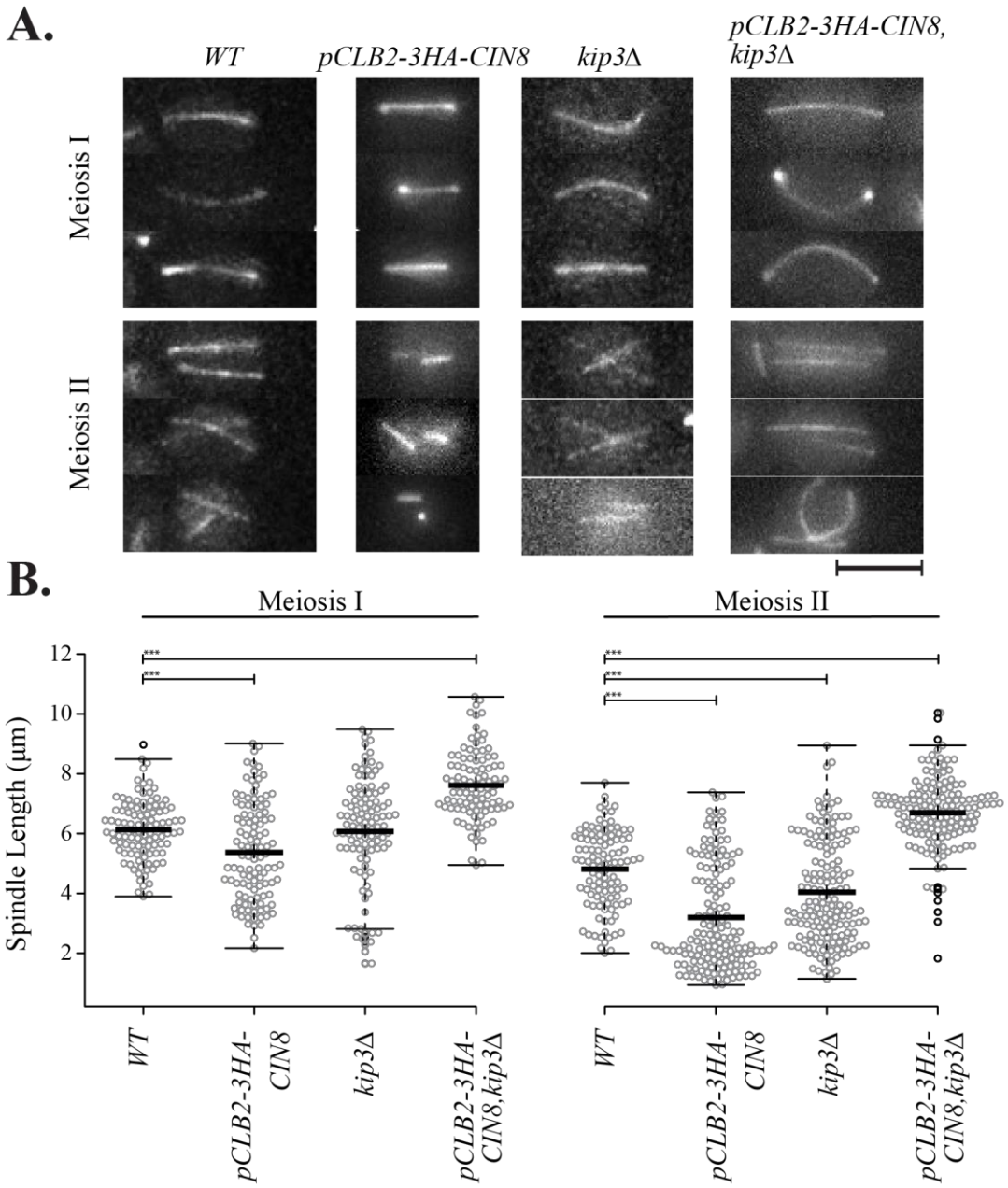

Figure 4.2-3 Meiotic depletion of Cin8 during meiosis causes shorter spindles, while additional deletion of Kip3 has the opposite effect.

Asynchronous *S.cerevisiae* cultures expressing GFP-TUB1 were released into meiosis in glass bottom dishes (See Methods 2.2.2.6) and imaged by epifluorescence microscopy at 15 minute intervals. (A) Representative images of cells in anaphase of meiosis I or II demonstrate different spindles that were analyzed. (B) Line scans were drawn to measure spindle length, using GFP-TUB1 as a reference of both spindle length and morphology. Graph bold, center lines show the sample means; box limits indicate the 25th and 75th percentiles as determined by R software; whiskers extend 1.5 times the interquartile range from the 25th and 75th percentiles, outliers are represented by dots; data points are plotted

as open circles. One way ANOVA followed by a Bonferroni and Holm multiple comparison test was performed (n>100 per sample) and significance is shown by * in the graph (*** = p<0.001). Scale bar represents 5µm.

4.2.11 Cin8-GFP is transiently translocated from the spindle pole bodies to spindle midzone during meiosis I and again during meiosis II.

Deletion of Cin8 causes spindle collapse during mitosis and consequently cells develop aneuploidy over time (Hoyt *et al*, 1990). If Cin8 depletion causes greater meiosis II spindle length disparity compared to meiosis I, it is possible that Cin8 function is more important during establishment of a second meiotic spindle during meiosis II. Following this question, I set about to answer a question not yet addressed in the kinesin field; the role of Cin8 during meiosis and how its function is regulated. Points of this question include; whether it is the same as mitosis, and if function is constant throughout meiosis. To start answering this question I fluorescently labelled Cin8 with GFP fluorophore, and imaged cells live, progressing through meiosis. Also, in cells, I tagged Spc42 with tdTomato, as a marker of the spindle poles (SPBs) and thus the theoretical end of spindles. During metaphase I, Cin8 is largely localised to SPBs. As cells enter anaphase I, Cin8 translocates to the spindle midzone and then promptly localises back to spindle poles upon spindle breakdown and onset of metaphase II. The same is repeated for meiosis II; Cin8 first localises to the spindle pole bodies at metaphase but then transiently locates to the spindle midzone during anaphase II (see **Figure 4.2-4**). To confirm that Cin8 is in fact localising to the spindle midzone, I should repeat the experiment with additional fluorescently labelled Ase1 in cells, a protein that crosslinks microtubules, and thus localises to antiparallel microtubules, at spindle midzones during anaphase (Tanenbaum *et al*, 2013; Su *et al*, 2013).

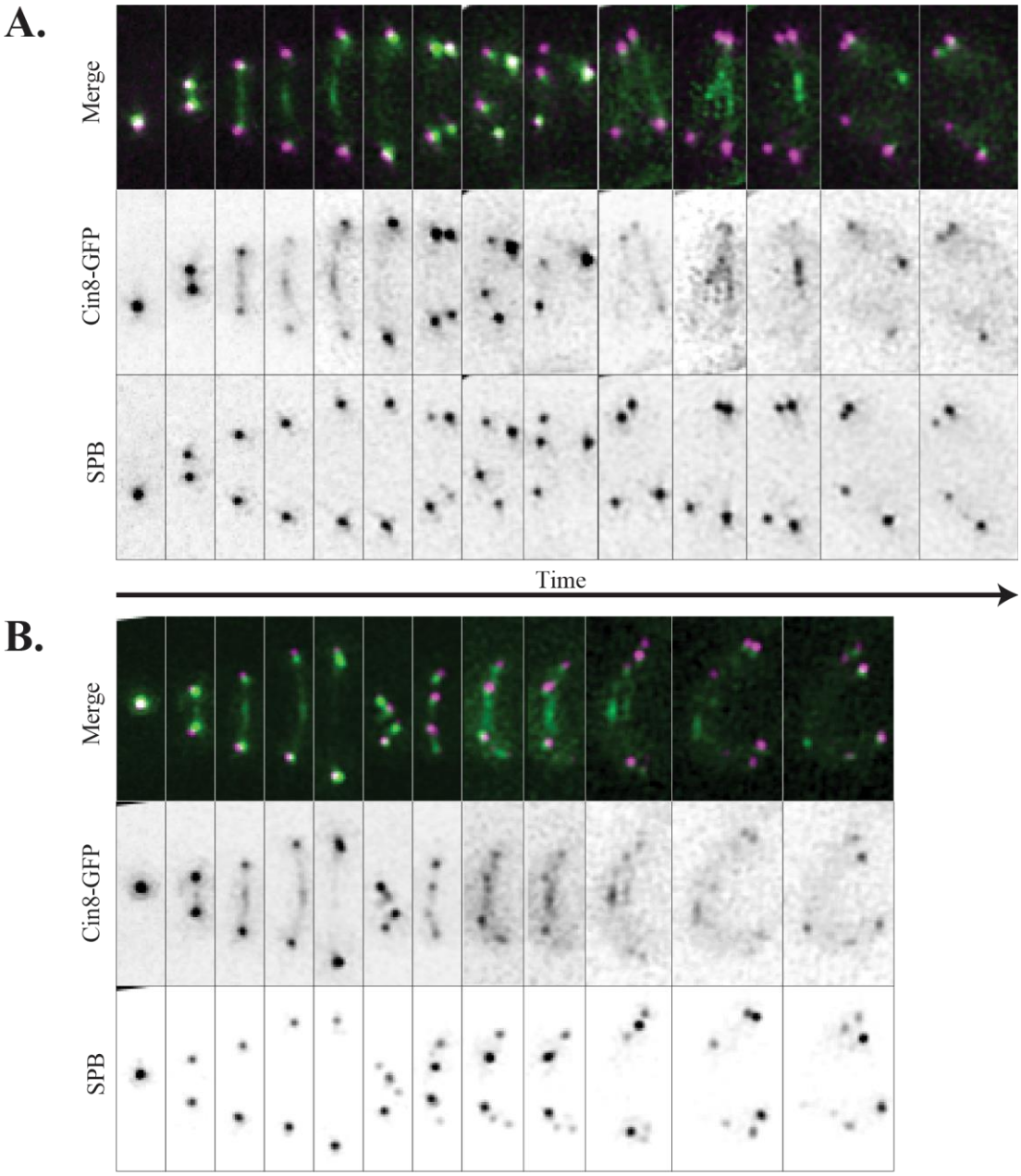

Figure 4.2-4. Cin8 localisation shifts from the spindle poles to the spindle midzone upon anaphase onset and back upon anaphase exit.

S.cerevisiae cultures were arrested in prophase by preventing NDT80 expression under the inducible pGAL promotor. Cultures were released into meiosis in glass bottomed dishes and imaged using an epifluorescent microscope at 5-minute intervals. Spindle pole bodies are marked by SPC42-tdTomato expression. A and B show two different, representative cells progressing through meiosis, showing spindle pole location and Cin8-GFP localisation throughout meiosis. Green signal is Cin8-GFP whilst purple signal is SPC42-tdTomato.

4.2.12 Cin8 protein levels increase over the course of meiosis but is rapidly degraded upon meiotic exit at the time of spindle disassembly.

Based on the hypothesis that Cin8 could be more important for the establishment of anaphase II spindles than anaphase I spindles, I hypothesise that there could be measurable differences in Cin8 activity. To investigate this, I decided to first look at protein levels throughout meiosis to test whether levels were different between anaphase I and II. Higher protein levels in the cell could equate to higher protein activity. Unfortunately, measuring protein levels during meiosis is limited by the variation in meiotic entry. To control this, I reversibly arrested cells in prophase I, before pachytene stage. The gene for NDT80 is placed under the GAL1-10 promotor. Addition of β-oestradiol stimulates production of Ndt80, which triggers simultaneous entry into meiosis. Samples were collected every 15 minutes and probed for Cin8-3HA protein levels. Concomitantly, samples were harvested for anti-tubulin immunofluorescence, as a marker for meiotic progression I found that Cin8 protein levels are low at the onset of meiosis and rise as cells progress through meiosis I and II, being highest during meiosis II. Protein levels are dramatically reduced after anaphase II, at the time of spindle breakdown. From the graph, you could argue that Cin8-3Ha protein levels decrease slightly at 105 minutes after anaphase I onset but should be confirmed by more precise methods of measuring band intensity measurements, such as Licor® imaging (see **Figure 4.2-5**A). From this experiment and repetitions, it appears that Cin8 protein levels are high during meiosis II compared to meiosis I, which could explain why depleting the

protein during meiosis perturbs meiosis II progression more than meiosis I. Also, Cin8 protein levels are very low in mitotic cycling cells, presumably because most cells in a cycling *S. cerevisiae* population are in G1.

4.2.13 Kip1 protein levels increase upon meiotic onset, in low levels throughout meiosis and persists after meiotic exit.

Kip1 has been reported as a binding partner of Cin8, working in a complex to achieve kinesin function during meiosis (Hildebrandt & Hoyt, 2000). Curious to know whether the proteins level of Kip1 could be higher in meiosis II and thus directly regulate Cin8 activity, I repeated the experiment described in 4.2.11 (see **Figure 4.2-5**A) I estimate that Kip1 protein levels are low during meiosis, making it hard to detect Kip1-HA by Western Blot (see **Figure 4.2-5**B). Despite this, it is evident that protein levels are almost undetectable at the beginning of meiosis, increase over the course of meiosis 1 and decrease upon meiotic exit but is not completely degraded. While it is hard to say conclusively, it could be argued that Kip1 protein levels drop between anaphase I and metaphase II and are generally lower in meiosis II, directly opposite to Cin8 protein levels. Finally, although not quantitative, Kip1 levels appear higher during meiosis than in mitotic cell cultures (see **Figure 4.2-5**B).

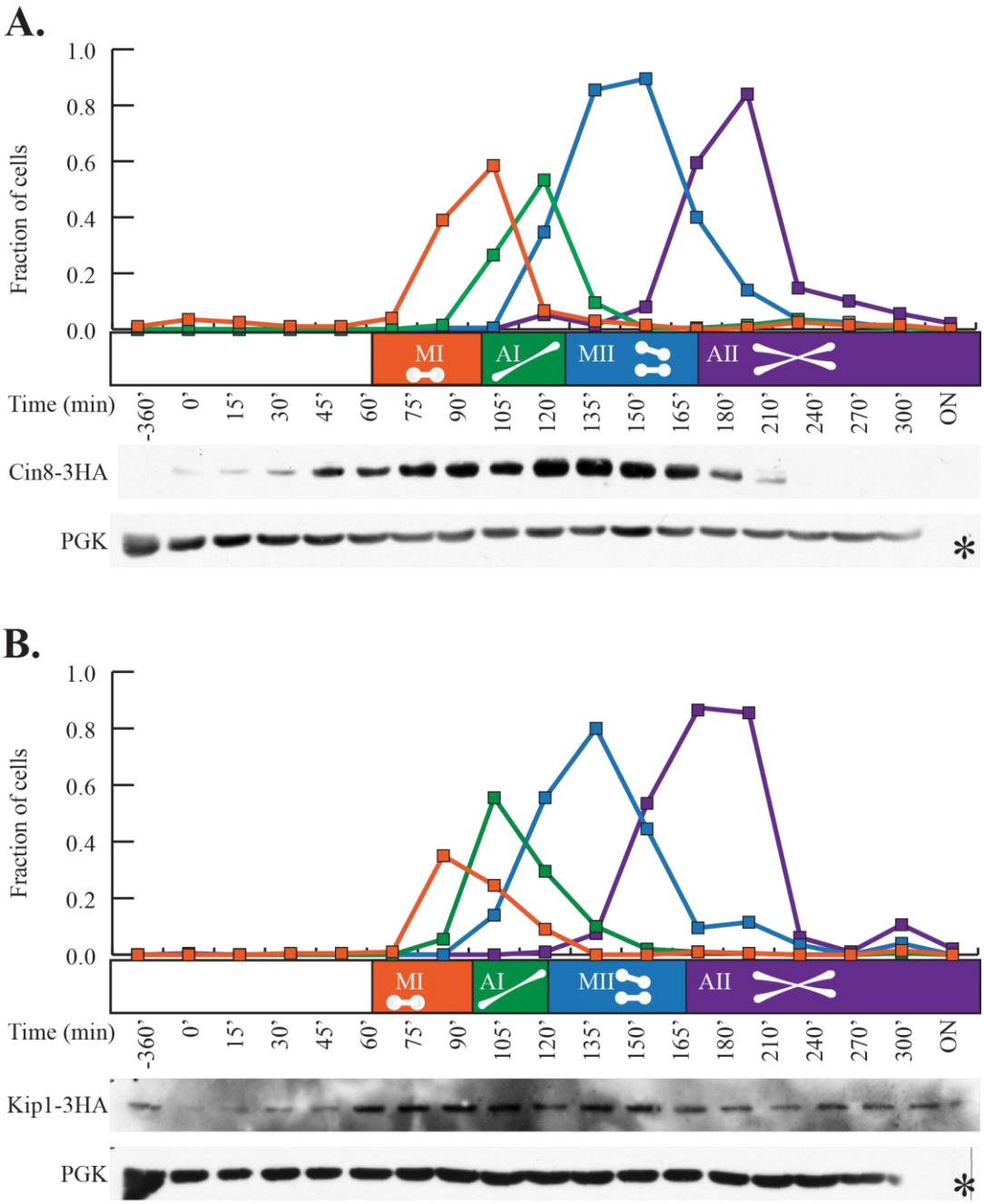

Figure 4.2-5. Cin8 and Kip1 protein levels increase during meiosis and degraded upon anaphase onset

Cin8-HA (A) or Kip1-HA (B) *S.cerevisiae* samples were arrested in prophase using a modified NDT80 inducible promotor. After release from arrest, meiotic culture samples were collected every 15'. Lower Western blots show protein levels of either Cin8-3HA or Kip1-3HA at each timepoint, tested by probing for HA tag in protein extracts. * denotes a lane from the blot which failed to transfer correctly. Meiotic samples were also fixed by formaldehyde and stained for tubulin to score progression through meiosis. Each graph shows the fraction of cells in each stage of meiosis over the time course. AII spindles and 'dotty' degraded spindles were scored under the same category to indicate completion of meiosis.

4.2.14 Mass Spectrometry data indicated that Cin8 may be localised to sub-spindle components via recruitment from site specific proteins.

Other than elevating protein levels, global protein activity levels can also be regulated by binding partner proteins, altering the kinetics of individual proteins. One advantage of this method of protein activity control is that it can be very precisely regulated depending on the localisation of the binding partner and accessibility of its substrate. To screen for potential unknown Cin8 binding partners I isolated TAP-tagged Cin8, hopefully with its binding partners still bound, from asynchronous meiotic cell cultures (4h after meiotic release). Proteins samples were trypsinized in gel and processed for mass spectrometry. **Figure 4.2-6**A shows a silver stained gel of the protein sample that was processed along with a BSA protein standard to estimate the amount of sample. A summarised table of proteins detected by the mass spectrometer and the number of peptides found is found in **Figure 4.2-6**B. Proteins with a high number of peptide hits compared to control samples were grouped by their known function or localisation but none of the results have been confirmed by repeating the same experiment tagging the reciprocal protein.

A.

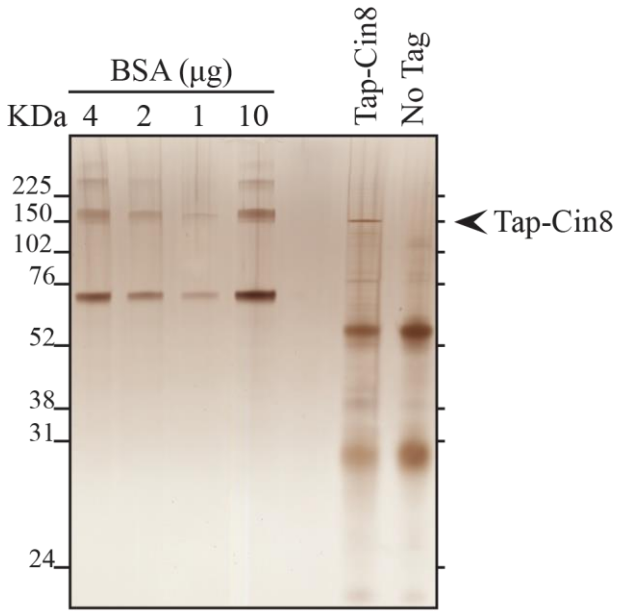

B.

Protein	Control (No Tag)	Cin8-HA	Function
Cin8	4	73	Kinesin protein (Tagged protein)
Act1	3	11	Cytoskeletal Component
Arp3	0	2	Cytoskeletal Component
Tub1	0	7	Spindle Component
Tub2	1	6	Spindle Component
Stu1	0	1	Regulation of Spindle Dynamics
Cdc48	0	7	Regulation of Spindle Disassembly
Cst9	0	3	Meiotic Recombination
Dmc1	0	2	Meiotic Recombination
Zip1	0	4	Chromsome Segreation in M1 Meiotic Recombination
Smc3	0	6	Chromosome Cohesion
Smc1	1	5	Chromosome Cohesion
Rec8	0	3	Chromosome Cohesion (Meiosis Specific)
Spc110	2	10	SPB Component
Cnm67	2	4	SPB Component
Nud1	2	4	SPB Component
Spc42	0	3	SPB Component
Spc29	0	2	SPB Component
Ady3	1	8	Sporulation
Hho1	3	5	Sporulation
Vtc2	0	6	Membrane Trafficking
Wtm1	0	5	Meiotic Regulation and Silencing
Pil1	1	9	Episome Component
Eis1	0	5	Episome Component

Figure 4.2-6. Mass spectrometry of Cin8 bound proteins during meiosis show potential interaction partners

Asynchronous S.cerevisiae samples were released into meiosis for 4 hours before harvest (See Methods 2.2.2.7). Cin8-HA bound proteins were purified using Nickel beads and underwent in-gel trypsinization before being loaded on a mass spectrometer. (A) Silver stain gel shows the purified protein sample, alongside NSA standards to estimate protein concentration. (B) Table shows a highlight of proteins identified in the mass spectrometry sample in wildtype cultures and those containing Cin8-HA. Numbers represent the number of peptides from that protein detected by the mass spectrometry machine.

4.2.15 Spindle assembly is frequently compromised after depletion of Kar3 during meiosis, resulting in short microtubules and failure to properly segregate chromosomes.

Going back to the initial screen, I decided to investigate Kar3 function during meiosis. Kar3 has not been studied thoroughly during meiosis but has a previously described function in karyogamy (Gibeaux *et al*, 2013). For this process, Kar3; a minus end directed protein and microtubule depolymerase like MCAK in human cells, depolymerizes microtubules to aid in pulling the nuclei of newly fused cells of opposite mating type together. When *KAR3* is deleted, cells are unable to fuse nuclei and can neither progress with meiosis or mitotic cell growth as a diploid (Gibeaux *et al*, 2013). Owing to its essential function in nuclear fusion I constructed a strain that was unable to express Kar3 during meiosis, under the *CLB2* promotor. In this strain, the only Kar3 available would be that already translated and not degraded, which as it turns out, is very low amounts (see Figure 4.2-1A). The initial screen time courses indicate that very few cells enter meiosis, or at least not in the first 24 hours after meiotic release. Following this, performing a spore viability assay proved difficult, as simply finding 100 tetrad spores was hard. Of these 100 tetrads only 59% segregated chromosome efficiently enough to allow spore growth on 2% glucose agar media (see Figure 4.2-1). To investigate why 41% of cells were unable to properly segregate chromosomes or form viable spores I created a strain with fluorescently labeled kinetochores, to visualize their segregation/alignment, and fluorescently labelled tubulin, expressing pClb2-Kar3. I imaged these cells live as they progressed through meiosis

(see **Figure 4.2-7**). In 65% of cells observed (n>100) spindle organization appeared normal and kinetochores were segregated like wild type cells. In 35% of cells observed however, cells appear to be stuck in prophase of meiosis I. The spindle does not separate or form a bipolar structure and instead small mitotic like spindles emanate from each other. The kinetochores start unfocussed and then focus around the origin of the spindle. They generally do this twice over the course of a normal meiosis in wild type cells, spreading and refocusing, potentially indicating that meiosis is progressing biochemically, but the spindle is not segregating chromosomes as it should.

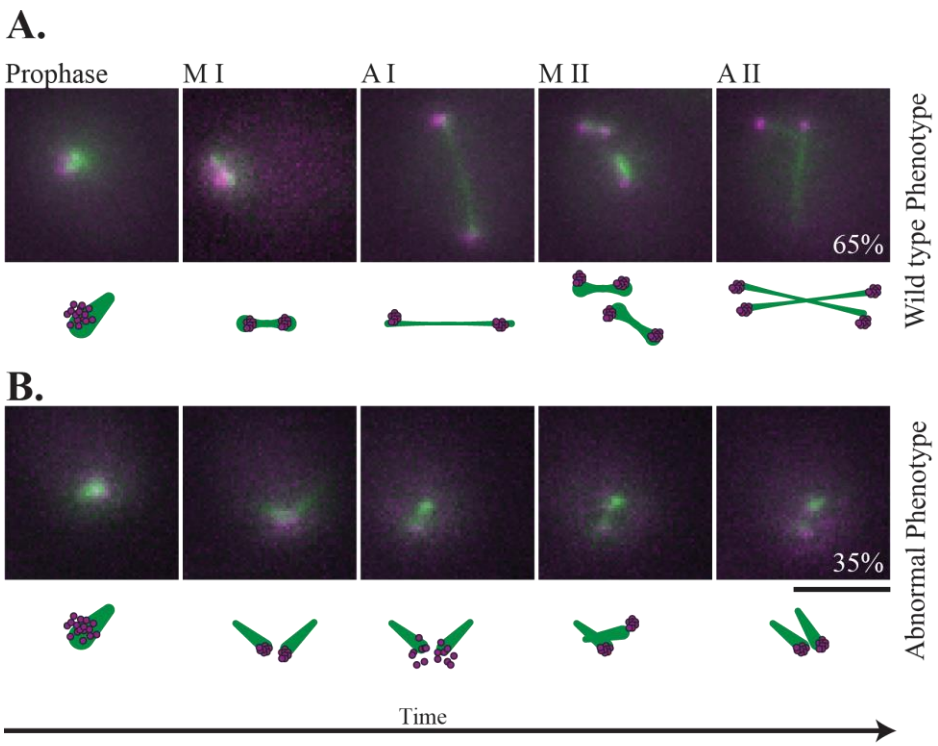

Figure 4.2-7. Cells with depleted Kar3 protein levels frequently fail to form proper bipolar spindles during meiosis I and as a result fail successfully to segregate chromosomes

S.cerevisiae samples expressing Mtw1-mCherry and Tub1-GFP were imaged live through asynchronous meiosis, images were taken at 5' intervals. Cells were scored based on meiotic progression, falling into two categories, shown above. Cells which did not enter meiosis were discarded. Scale represents 5µm.

4.3 Discussion

To ascertain whether kinesin function is the same between mitosis and meiosis I set out to systematically study kinesin function in yeast meiosis. Firstly, I deleted each kinesin and assayed the rate of meiotic progression. *kip1Δ, kip2Δ, kip3Δ* strains were able to progress at similar rates to wildtype cells. Deletion of cin8 showed delayed meiotic phenotypes. Further inspection revealed abnormal dapi stained DNA mass segregation and aneuploidy of individual chromsomes. Aneuploidy is a phenotype associated with vegetative mitotic growth of *cin8Δ* mutants (Saunders & Hoyt, 1992). Consequently, it is most likely that the aneuploidy observed during meiosis is a cumulation of failed mitotic segregation during vegetative growth and in fact, not a result of improper meiotic function. In verification, placing cin8 expression under the Clb2 promotor, which is downregulated in meiosis but not mitosis, restored proper cell ploidy. For the rest of the study, I used *pCLB2-3HA-Cin8*, not *cin8Δ,* to observe and measure Cin8 functions uniquely during meiosis.

Depletion of Cin8 during meiosis resulted in a large proportion of dyad and triad spores (See **Figure 4.2-2** and section 4.2.7). I hypothesized that triad formation was a consequence of short and collapsed meiosis II spindles (See Figure 4.2.6), non-permissive to distinct membrane prespore wall formation. If SPBs (and thus MPs) and DNA masses are too close membranes from opposite poles might merge fuse rather than self-fusing. The higher frequency of triad mating types being a:a:α or α:α:a supports the hypothesis

but is by no means comprehensive. The phenotype observed could indeed be a result of DNA mass consolidation, after a compromised or absent anaphase II spindle. Alternatively, Cin8 could play a role in preparing the SPB for transformation into a meiotic plaque and prespore membrane assembly. Before MPs are created, γ-tubulin and Spc71 must be removed from the central plaque. Failure to remove tubulin or disassemble one of the 4 SPB central plaques could prevent meiotic plaque formation and result in that meiosis II spindle producing just one spore, resulting in 3 spores overall (Taxis *et al*, 2005; Neiman, 2005) (See Figure Figure 4.3-1). If dyad and triad formation in *pCLB2-3HA-Cin8* strains is caused by mis-assembly of 2/3 of the SPB, viable spores should be haploid a/α and spore ratio should be 2a:α or 2α:a per triad. Preliminary data is supportive of the above. Further, Cin8p immunoprecipitated with several SPB proteins, indicating proximity (See Figure 4.2.14), however, cultures were asynchronous, and not uniformly arrested in, or undergoing, meiosis II. To test whether the triad formation is caused by improper MP assembly I could tag one of the structural components of the MP (Mpc54p) and quantitively correlate the number of MPs activated, and number of spores formed in *pCLB2-3HA-Cin8* strains. Alternatively, triad formation could result from incomplete nuclear formation, resulting in a spore containing two SPB and both homologues. In this case I would observe triad spores to express a:α:diploid. Finally, it should not be ignored that Cin8p levels are dramatically reduced upon anaphase onset (see **Figure 4.2-2**A), and may not play a role in spore formation, and the phenotype observed is a downstream effect of earlier meiotic events.

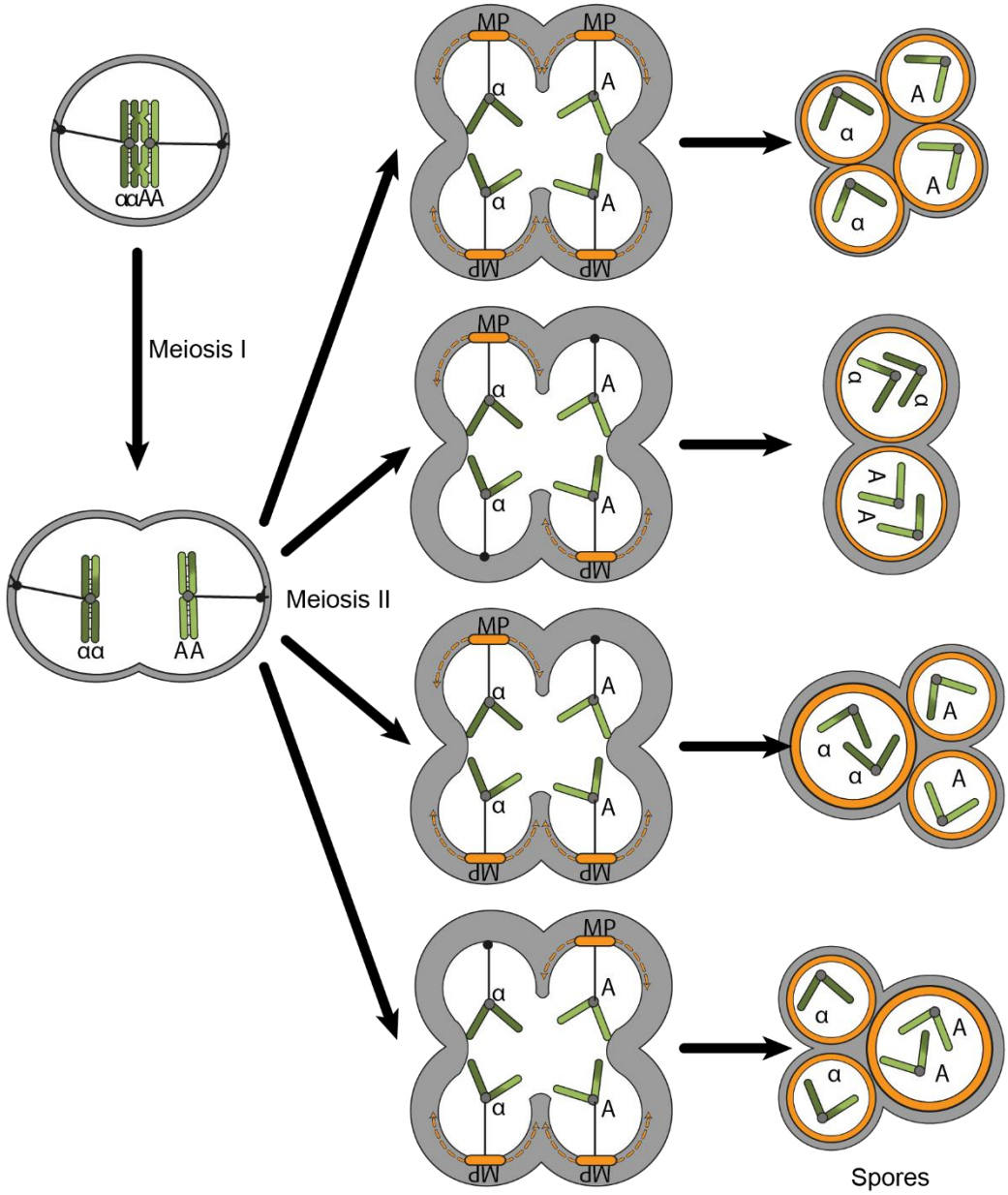

Figure 4.3-1 A diagram to represent various ways cin8Δ may cause dyad and triad formation over tetrad

During meiosis I homologue chromosome pairs are segregated one a meiosis I spindle to opposite poles of the cell. During meiosis II, the central plaque of he SPB is transformed into a meiotic plaque, which can assimilate membrane vesicles and form a prespore membrane, which is alter adapted into a full spore wall. One hypothesis is that only the two, newly replicates central plaques are transformed, leading to a haploid dyad, containing two copies of the same mating gene. Alternatively, 3 of the 4 centrals plaques are transformed, leading to 2 spores with one copy of each gene, and 1 spore with two copies of the same mating type gene. Finally, an alternative, no shown hypothesis is that shorter spindles prevent prespore membrane fusion within each spore, forcing spores to fuse together, leaving 2/3 spores, but 4 meiotic plaques.

During mitosis, Cin8 and Kip1 show to be functionally redundant, with Cin8 playing the more important role, making *cin8Δ* phenotypes more severe than *kip1Δ* (Hoyt *et al*, 1993). Mechanistically, Kip1 and Cin8 are proposed to work antagonistically to Kip3, where kip1/cin8 heterodimers crosslink and slide interdigitated antiparallel microtubules of the mitotic spindle to lengthen it, whilst Kip3 prevents overextension of the spindle by depolymerizing +end microtubules (Cottingham & Hoyt, 1997; Rizk *et al*, 2014). In meiosis, preliminary results suggest that the same is true in meiosis (See Figure 4.2-3). *pCLB2-3HA-Cin8* showed shorted spindles and frequent collapse but was still able to form a bipolar spindle (see **Figure 4.2-3**). This is presumably due to redundant function of Kip1, without which the cells are unviable and indicates that Cin8 still performs a spindle lengthening role during meiosis. Kip3Δ have longer spindles during meiosis, significantly so during meiosis II, supporting a microtubule depolymerase function. Surprisingly, *pCLB2-3HA-CIN8 kip3Δ* mutations result in even longer spindles, whereas I would have expected them to be longer, but shorter than *kip3Δ* alone, without the crosslinking and sliding function of Cin8 to lengthen the spindle. A potential explanation for this phenotype is a spindle checkpoint arrest, caused by unstable spindles, potentially lacking tension across kinetochores without Kip3 function.

Cin8 function at the midzone of the meiotic spindle is supported by fluorescent imaging of CIn8-GFP (see **Figure 4.2-4**). During establishment of the meiotic I spindle Cin8 is strongly localized at the SPB but then migrates to the spindle midzone. The same fluorescence can be see migrating back to the SPB before the process is repeated during meiosis II. This indicates that Cin8 plays a

similar role for both meiosis I and meiosis II spindles, but measurements of spindles formed after Cin8 depletions (*pCLB2-3HA-CIN8*) indicate that the difference in spindle length as a result of depletion is more sever during meiosis II (see **Figure 4.2-3**). In this case, the functional redundancy between Kip1 and Cin8 may lead towards Kip1 being more important for meiosis I, and Cin8 being more important during meiosis II.

During mitosis, *Cin8Δ* and *Kip1Δ* double delete mutants are unable to separate spindle poles bodies and show a mitotic lethal phenotype (Saunders, 1993; Saunders & Hoyt, 1992; Roof *et al*, 1992). Deletion of Kar3 in addition to Cin8 and Kip1 can partially rescue the lethal phenotype, indicating antagonistic force generating functions of Cin8/Kip1 against Kar3 (Hoyt *et al*, 1993).

Kar3 has known functions in spindle development in the nucleus and without Kar3, cells arrest before anaphase I (Meluh & Rose, 1990; Roof *et al*, 1992). During meiosis, Kar3 is essential for karyogamy, the coalescence of two nuclei from fused cells of opposite mating type (Polaina & Conde, 1982; Meluh & Rose, 1990). Further work into Kar3 function during meiosis has found that Kar3 is a more versatile protein and is also essential for progression through meiosis I. Absence of Kar3 triggers a prophase I arrests by preventing heteroallelic recombination. The arrest is strangely reversible and cells can return to vegetative growth (Bascom-Slack & Dawson, 1997). The difference in arrest timing between mitotic and meiotic Kar3 mutants indicates different Kar3 functions dependent on the type of division. Using

Fluorescent and live cell microscopy I was able to visualize this prophase arrest and observe spindle formation and maintenance in *pCLB2-3HA-KAR3 mutants*. I found that 35% of spindles remained short and non-polar, but also that the kinetochores periodically disbursed from and recompressed at presumably the spindle poles (Further experiments are needed to confirm SPB location) (see **Figure 4.2-7**). During the course of imaging, the two small microtubule projections change orientation with respects to each other, and do not look resemble common bush like rosettes attributes to prophase I arrests (Alani *et al*, 1990). It would be interesting to test whether the arrest is due to spindle abnormalities, by deleting spindle checkpoint proteins, or an earlier, prophase arrest cause by failed synaptonemal complexes.

It should be noted however that the imagine experiments were completed with *pCLB2-3HA-KAR3* strains, whose protein levels were largely diminished, but not completely depleted. In the process of making strain containing Kar3-GFP (not shown) I assayed mitotic Kar3 protein levels under its endogenous promotor by Western Blot and found it to be lower during vegetative growth, than under the CLB2 promoter. This test was qualitative and not comparable to the Western Blot shown in **Figure 4.2-1**A, and would require further controlled, qualitative assays for confirmation, however if turnover of Kar3 is slow, residual protein may have been enough to overcome Kar3 requirements in synaptonemal complex formation, but not for spindle establishment or maintenance.

I initially set out to investigate kinesin functions during meiosis and compare them to the functions played out during mitosis. Functional studies of nuclear kinesins in budding yeast is complicated owing to their involvement in multiple processes either individually or in combination. This multiplicity of function creates complex loss-of-function phenotypes which require further investigation. I have identified meiotic functions of Cin8 and Kip1 which are similar to those in mitosis but indicate that their relative functional contributions in meiosis I and II may differ, giving interesting scope to future investigations. To aid in future endeavors, I have developed strains which will are viable under vegetative growth conditions, without accumulating chromsomes instability, and can be tested for meiosis specific deficiencies caused by kinesin depletion.

Bibliography

Alani E, Padmore R & Kleckner N (1990) Analysis of Wild-Type and r&50 Mutants of Yeast Suggests an Intimate Relationship between Meiotic Chromosome Synapsis and RecombMtion. *Cell* **61:** 419–436

Allshire RC (1997) Centromeres, checkpoints and chromatid cohesion. *Curr. Opin. Genet. Dev.* **7:** 264–73

Amos L & Klug A (1974) Arrangement of subunits in flagellar microtubules. *J. Cell Sci.* **14:** 523–49

Andrews PD, Ovechkina Y, Morrice N, Wagenbach M, Duncan K, Wordeman L & Swedlow JR (2004) Aurora B Regulates MCAK at the Mitotic Centromere. *Dev. Cell* **6:** 253–268

Applegate KT, Besson S, Matov A, Bagonis MH, Jaqaman K & Danuser G (2011) plusTipTracker: Quantitative image analysis software for the measurement of microtubule dynamics. *J. Struct. Biol.* **176:** 168–84

Barrett JG, Manning BD & Snyder M (2000) The Kar3p Kinesin-related Protein Forms a Novel Heterodimeric Structure with Its Associated Protein Cik1p. *Mol. Biol. Cell* **11:** 2373–2385

Bascom-Slack CA & Dawson DS (1997) The yeast motor protein, Kar3p, is essential for meiosis I. *J. Cell Biol.* **139:** 459–67

Baudat F, Imai Y & de Massy B (2013) Meiotic recombination in mammals: localization and regulation. *Nat. Rev. Genet.* **14:** 794–806

Bischoff JR, Anderson L, Zhu Y, Mossie K, Ng L, Souza B, Schryver B, Flanagan P, Clairvoyant F, Ginther C, Chan CS, Novotny M, Slamon DJ & Plowman GD (1998) A homologue of Drosophila aurora kinase is oncogenic and amplified in human colorectal cancers. *EMBO J.* **17:** 3052–65

Borisy GG, Olmsted JB, Marcum JM & Allen C (1974) Microtubule assembly in vitro. *Fed. Proc.* **33:** 167–74

Boyle J (2008) Molecular biology of the cell, 5th edition by B. Alberts, A. Johnson, J. Lewis, M. Raff, K. Roberts, and P. Walter. *Biochem. Mol. Biol. Educ.* **36:** 317–318

Braun A, Caesar NM, Dang K & Myers KA (2016) High-resolution Time-lapse Imaging and Automated Analysis of Microtubule Dynamics in Living Human Umbilical Vein Endothelial Cells. *J. Vis. Exp.*

Brawley SH & Robinson KR (1985) Cytochalasin treatment disrupts the endogenous currents associated with cell polarization in fucoid zygotes: studies of the role of F-actin in embryogenesis. *J. Cell Biol.* **100:** 1173–84

Brouhard GJ & Rice LM (2014) The contribution of αβ-tubulin curvature to microtubule dynamics. *J. Cell Biol.* **207:** 323–334

Burns KMM, Wagenbach M, Wordeman L & Schriemer DCC (2014) Nucleotide exchange in dimeric MCAK induces longitudinal and lateral stress at microtubule ends to support depolymerization. *Structure* **22:** 1173–1183

Byers B & Goetsch L (1975) Behavior of spindles and spindle plaques in the cell cycle and conjugation of Saccharomyces cerevisiae. *J. Bacteriol.* **124:** 511–23

Carlile TM & Amon A (2008) Meiosis I Is Established through Division-Specific Translational Control of a Cyclin. *Cell* **133:** 280–291

Cassimeris L & Spittle C (2001) Regulation of microtubule-associated proteins. *Int. Rev. Cytol.* **210:** 163–226

Chan YW, Jeyaprakash AA, Nigg EA & Santamaria A (2012) Aurora B controls kinetochore-microtubule attachments by inhibiting Ska complex-KMN network interaction. *J. Cell Biol.* **196:** 563–71

Chavali PL, Chandrasekaran G, Barr AR, Tátrai P, Taylor C, Papachristou EK, Woods CG, Chavali S & Gergely F (2016) A CEP215–HSET complex links centrosomes with spindle poles and drives centrosome clustering in cancer. *Nat. Commun.* **7:** 11005

Cheeseman IM & Desai A (2005) A Combined Approach for the Localization and Tandem Affinity Purification of Protein Complexes from Metazoans. *Sci. Signal.* **2005:** pl1-pl1

Chretien D (1995) Structure of growing microtubule ends: two-dimensional sheets close into tubes at variable rates. *J. Cell Biol.* **129:** 1311–1328

Cimini D, Wan X, Hirel CB & Salmon ED (2006) Aurora kinase promotes turnover of kinetochore microtubules to reduce chromosome segregation errors. *Curr. Biol.* **16:** 1711–8

Cottingham FR & Hoyt MA (1997) Mitotic Spindle Positioning in Saccharomyces cerevisiae is accomplished by antagonistically acting microtubule motor proteins. *Cell* **138:** 1041–1053

Cross RA & McAinsh A (2014) Prime movers: the mechanochemistry of mitotic kinesins. *Nat. Rev. Mol. Cell Biol.* **15:** 257–271

Desai A & Mitchison TJ (1997) Microtubule polymerization dynamics. *Annu. Rev. Cell Dev. Biol.* **13:** 83–117

Desai A, Verma S, Mitchison TJ & Walczak CE (1999) Kin I kinesins are

microtubule-destabilizing enzymes. *Cell* **96:** 69–78

DeZwaan TM, Ellingson E, Pellman D & Roof DM (1997) Kinesin-related KIP3 of Saccharomyces cerevisiae is required for a distinct step in nuclear migration. *J. Cell Biol.* **138:** 1023–40

Dietrich KA, Sindelar C V., Brewer PD, Downing KH, Cremo CR & Rice SE (2008) The kinesin-1 motor protein is regulated by a direct interaction of its head and tail. *Proc. Natl. Acad. Sci.* **105:** 8938–8943

Domnitz SB, Wagenbach M, Decarreau J & Wordeman L (2012) MCAK activity at microtubule tips regulates spindle microtubule length to promote robust kinetochore attachment. *J. Cell Biol.* **197:** 231–237

Duro E & Marston AL (2015) From equator to pole: Splitting chromosomes in mitosis and meiosis. *Genes Dev.* **29:** 109–122

Ems-McClung SC, Hertzer KM, Zhang X, Miller MW & Walczak CE (2007) The interplay of the N- and C-terminal domains of MCAK control microtubule depolymerization activity and spindle assembly. *Mol. Biol. Cell* **18:** 282–94

Ems-McClung SCC, Hainline SGG, Devare J, Zong H, Cai S, Carnes SKK, Shaw SLL & Walczak CEE (2013) Aurora B inhibits MCAK activity through a phosphoconformational switch that reduces microtubule association. *Curr. Biol.* **23:** 2491–9

Endow SA, Kang SJ, Satterwhite LL, Rose MD, Skeen VP & Salmon ED (1994) Yeast Kar3 is a minus-end microtubule motor protein that destabilizes microtubules preferentially at the minus ends. *EMBO J.* **13:** 2708–2713

Fernius J & Hardwick KG (2007) Bub1 kinase targets Sgo1 to ensure efficient chromosome biorientation in budding yeast mitosis. *PLoS Genet.* **3:** e213

Fox C, Zou J, Rappsilber J & Marston AL (2017) Cdc14 phosphatase directs centrosome re-duplication at the meiosis I to meiosis II transition in budding yeast. *Wellcome open Res.* **2:** 2

Fu J, Bian M, Jiang Q & Zhang C (2007) Roles of Aurora kinases in mitosis and tumorigenesis. *Mol. Cancer Res.* **5:** 1–10

Gadde S & Heald R (2004) Mechanisms and Molecules of the Mitotic Spindle. *Curr. Biol.* **14:** R797–R805

Gallego O, Specht T, Brach T, Kumar A, Gavin A-C & Kaksonen M (2013) Detection and characterization of protein interactions in vivo by a simple live-cell imaging method. *PLoS One* **8:** e62195

Ganguly A, Yang H & Cabral F (2011a) Overexpression of mitotic centromere-associated Kinesin stimulates microtubule detachment and confers resistance to paclitaxel. *Mol. Cancer Ther.* **10:** 929–37

Ganguly A, Yang H, Pedroza M, Bhattacharya R & Cabral F (2011b) Mitotic centromere-associated kinesin (MCAK) mediates paclitaxel resistance. *J. Biol. Chem.* **286:** 36378–84

Garcia MA, Koonrugsa N & Toda T (2002) Two Kinesin-like Kin I Family Proteins in Fission Yeast Regulate the Establishment of Metaphase and the Onset of Anaphase A. **12:** 610–621

Gardner MK, Haase J, Mythreye K, Molk JN, Anderson M, Joglekar AP, O'Toole ET, Winey M, Salmon ED, Odde DJ & Bloom K (2008) The microtubule-based motor Kar3 and plus end-binding protein Bim1 provide structural support for the anaphase spindle. *J. Cell Biol.* **180:** 91–100

Gassmann R, Carvalho A, Henzing AJ, Ruchaud S, Hudson DF, Honda R, Nigg EA, Gerloff DL & Earnshaw WC (2004) Borealin: a novel chromosomal passenger required for stability of the bipolar mitotic spindle. *J. Cell Biol.* **166:** 179–91

Geiser JR, Schott EJ, Kingsbury TJ, Cole NB, Totis LJ, Bhattacharyya G, He L & Hoyt MA (1997) Saccharomyces cerevisiae genes required in the absence of the CIN8-encoded spindle motor act in functionally diverse mitotic pathways. *Mol. Biol. Cell* **8:** 1035–50

Gibeaux R, Politi AZ, Nedelec F, Antony C & Knop M (2013) Spindle pole body-anchored Kar3 drives the nucleus along microtubules from another nucleus in preparation for nuclear fusion during yeast karyogamy. *Genes Dev.* **27:** 335–349

Grishchuk EL, Molodtsov MI, Ataullakhanov FI & McIntosh JR (2005) Force production by disassembling microtubules. *Nature* **438:** 384–388

Heald R, Tournebize R, Blank T, Sandaltzopoulos R, Becker P, Hyman A & Karsenti E (1996) Self-organization of microtubules into bipolar spindles around artificial chromosomes in Xenopus egg extracts. *Nature* **382:** 420–5

van Heesbeen RGHP, Raaijmakers JA, Tanenbaum ME, Halim VA, Lelieveld D, Lieftink C, Heck AJR, Egan DA & Medema RH (2016) Aurora A, MCAK, and Kif18b promote Eg5-independent spindle formation. *Chromosoma***:** 1–14

Helmke KJ, Heald R & Wilbur JD (2013) Interplay Between Spindle Architecture and Function. *Int. Rev. Cell Mol. Biol.* **306:** 83–125

Hepperla AJ, Willey PT, Coombes CE, Schuster BM, Gerami-Nejad M, McClellan M, Mukherjee S, Fox J, Winey M, Odde DJ, O'Toole E & Gardner MK (2014) Minus-end-directed Kinesin-14 motors align antiparallel microtubules to control metaphase spindle length. *Dev. Cell* **31:** 61–72

Hertzer KM, Ems-McClung SC, Kline-Smith SL, Lipkin TG, Gilbert SP & Walczak CE (2006) Full-length dimeric MCAK is a more efficient microtubule depolymerase than minimal domain monomeric MCAK. *Mol. Biol. Cell* **17:** 700–10

Hildebrandt ER & Hoyt MA (2000) Mitotic motors in Saccharomyces cerevisiae. *Biochim. Biophys. Acta* **1496:** 99–116

Hillers KJ & Villeneuve AM (2003) Chromosome-Wide Control of Meiotic Crossing over in C. elegans. *Curr. Biol.* **13:** 1641–1647

Honnappa S, Gouveia SM, Weisbrich A, Damberger FF, Bhavesh NS, Jawhari H, Grigoriev I, van Rijssel FJA, Buey RM, Lawera A, Jelesarov I, Winkler FK, Wüthrich K, Akhmanova A & Steinmetz MO (2009) An EB1-binding motif acts as a microtubule tip localization signal. *Cell* **138:** 366–76

Hood EA, Kettenbach AN, Gerber SA & Compton DA (2012) Plk1 regulates the kinesin-13 protein Kif2b to promote faithful chromosome segregation. *Mol. Biol. Cell* **23:** 2264–74

Hoyt M a & Geiser JR (1996) Genetic analysis of the mitotic spindle. *Ann. Rev. Genet.* **30:** 7–33

Hoyt MA, He L, Loo KK & Saunders WS (1992) Two Saccharomyces cerevisiae kinesin-related gene products required for mitotic spindle assembly. *J. Cell Biol.* **118:** 109–20

Hoyt MA, He L, Totis L & Saunders WS (1993) Loss of function of Saccharomyces cerevisiae kinesin-related CIN8 and KIP1 is suppressed by KAR3 motor domain mutations. *Genetics* **135:** 35–44

Hoyt MA, Stearns T & Botstein D (1990) Chromosome instability mutants of Saccharomyces cerevisiae that are defective in microtubule-mediated processes. *Mol. Cell. Biol.* **10:** 223–234

Hunter AW, Caplow M, Coy DL, Hancock WO, Diez S, Wordeman L & Howard J (2003) The kinesin-related protein MCAK is a microtubule depolymerase that forms an ATP-hydrolyzing complex at microtubule ends. *Mol. Cell* **11:** 445–57

Hyman AA, Chretien D, Arnal I & Wade RH (1995) Structural changes accompanying GTP hydrolysis in microtubules: Information from a slowly

hydrolyzable analogue guanylyl-(α,β)-methylene- diphosphonate. *J. Cell Biol.* **128:** 117–125

Hyman AA, Salser S, Drechsel DN, Unwin4 N & Mitchison TJ (1992) Role of GTP Hydrolysis in Microtubule Dynamics: Information from a Slowly Hydrolyzable Analogue, GMPCPP. *Mol. Biol. Cell* **3:** 1155–1167

Kapoor T & M. T (2017) Metaphase Spindle Assembly. *Biology (Basel).* **6:** 8

Katayama H & Sen S (2010) Aurora kinase inhibitors as anticancer molecules. *Biochim. Biophys. Acta* **1799:** 829–39

Katis VL, Lipp JJ, Imre R, Bogdanova A, Okaz E, Habermann B, Mechtler K, Nasmyth K & Zachariae W (2010) Rec8 Phosphorylation by Casein Kinase 1 and Cdc7-Dbf4 Kinase Regulates Cohesin Cleavage by Separase during Meiosis. *Dev. Cell* **18:** 397–409

Kiyomitsu T & Cheeseman IM (2012) Chromosome- and spindle-pole-derived signals generate an intrinsic code for spindle position and orientation. *Nat. Cell Biol.* **14:** 311–7

Kline-Smith SL, Khodjakov A, Hergert P & Walczak CE (2004) Depletion of centromeric MCAK leads to chromosome congression and segregation defects due to improper kinetochore attachments. *Mol. Biol. Cell* **15:** 1146–59

Koshland DE & Guacci V (2000) Sister chromatid cohesion: the beginning of a long and beautiful relationship. *Curr. Opin. Cell Biol.* **12:** 297–301

Kull FJ, Sablin EP, Lau R, Fletterick RJ & Vale RD (1996) Crystal structure of the kinesin motor domain reveals a structural similarity to myosin. *Nature* **380:** 550–5

Kumar A, Rajendran V, Sethumadhavan R & Purohit R (2013) Evidence of Colorectal Cancer-Associated Mutation in MCAK: A Computational Report. *Cell Biochem. Biophys.* **67:** 837–851

Lan W, Zhang X, Kline-Smith SL, Rosasco SE, Barrett-Wilt GA, Shabanowitz J, Hunt DF, Walczak CE & Stukenberg PTT (2004) Aurora B phosphorylates centromeric MCAK and regulates its localization and microtubule depolymerization activity. *Curr. Biol.* **14:** 273–86

Lawrence CJ, Dawe RK, Christie KR, Cleveland DW, Dawson SC, Endow SA, Goldstein LSB, Goodson H V., Hirokawa N, Howard J, Malmberg RL, McIntosh JR, Miki H, Mitchison TJ, Okada Y, Reddy ASN, Saxton WM, Schliwa M, Scholey JM, Vale RD, et al (2004) A standardized kinesin nomenclature: Table I. *J. Cell Biol.* **167:** 19–22

Lecland N & Lüders J (2014) The dynamics of microtubule minus ends in the

human mitotic spindle. *Nat. Cell Biol.*

Lee BH & Amon A (2003) Role of Polo-like kinase CDC5 in programming meiosis I chromosome segregation. *Science* **300:** 482–6

Lee T, Langford KJ, Askham JM, Brüning-Richardson a & Morrison EE (2008) MCAK associates with EB1. *Oncogene* **27:** 2494–500

Li H, DeRosier DJ, Nicholson W V., Nogales E & Downing KH (2002) Microtubule Structure at 8 Å Resolution. *Structure* **10:** 1317–1328

Lillie SH & Brown SS (1992) Suppression of a myosin defect by a kinesin-related gene. *Nature* **356:** 358–361

Lillie SH & Brown SS (1994) Immunofluorescence localization of the unconventional myosin, Myo2p, and the putative kinesin-related protein, Smy1p, to the same regions of polarized growth in Saccharomyces cerevisiae. *J. Cell Biol.* **125:** 825–42

Lillie SH & Brown SS (1998) Smy1p, a kinesin-related protein that does not require microtubules. *J. Cell Biol.* **140:** 873–83

Lim HH, Goh PY & Surana U (1996) Spindle pole body separation in Saccharomyces cerevisiae requires dephosphorylation of the tyrosine 19 residue of Cdc28. *Mol. Cell. Biol.* **16:** 6385–97

Longtine MS, Mckenzie III A, Demarini DJ, Shah NG, Wach A, Brachat A, Philippsen P & Pringle JR (1998) Additional modules for versatile and economical PCR-based gene deletion and modification in Saccharomyces cerevisiae. *Yeast* **14:** 953–961

Lwin KM, Li D & Bretscher A (2016) Kinesin-related Smy1 enhances the Rab-dependent association of myosin-V with secretory cargo. *Mol. Biol. Cell* **27:** 2450–62

Maiato H, Sampaio P & Sunkel CE (2004) Microtubule-associated proteins and their essential roles during mitosis. *Int. Rev. Cytol.* **241:** 53–153

Maney T, Hunter AW, Wagenbach M & Wordeman L (1998) Mitotic centromere-associated kinesin is important for anaphase chromosome segregation. *J. Cell Biol.* **142:** 787–801

Maney T, Wagenbach M & Wordeman L (2001) Molecular dissection of the microtubule depolymerizing activity of mitotic centromere-associated kinesin. *J. Biol. Chem.* **276:** 34753–8

Manning BD, Barrett JG, Wallace JA, Granok H & Snyder M (1999) Differential regulation of the Kar3p kinesin-related protein by two associated proteins, Cik1p and Vik1p. *J. Cell Biol.* **144:** 1219–33

Marston AL (2014) Chromosome segregation in budding yeast: sister chromatid cohesion and related mechanisms. *Genetics* **196:** 31–63

Marston AL & Amon A (2004) Meiosis: cell-cycle controls shuffle and deal. *Nat. Rev. Mol. Cell Biol.* **5:** 983–997

Marston AL, Lee BH & Amon A (2003) The Cdc14 phosphatase and the FEAR network control meiotic spindle disassembly and chromosome segregation. *Dev. Cell* **4:** 711–26

Matos J, Lipp JJ, Bogdanova A, Guillot S, Okaz E, Junqueira M, Shevchenko A & Zachariae W (2008) Dbf4-Dependent Cdc7 Kinase Links DNA Replication to the Segregation of Homologous Chromosomes in Meiosis I. *Cell* **135:** 662–678

Matov A, Applegate K, Kumar P, Thoma C, Krek W, Danuser G & Wittmann T (2010) Analysis of microtubule dynamic instability using a plus-end growth marker. *Nat. Methods* **7:** 761–8

Mayr MI, Hümmer S, Bormann J, Grüner T, Adio S, Woehlke G & Mayer TU (2007) The human kinesin Kif18A is a motile microtubule depolymerase essential for chromosome congression. *Curr. Biol.* **17:** 488–98

Mayr MI, Storch M, Howard J & Mayer TU (2011) A non-motor microtubule binding site is essential for the high processivity and mitotic function of kinesin-8 Kif18A. *PLoS One* **6:** e27471

MAZIA D (1961) Mitosis and the Physiology of Cell Division. In *The Cell* pp 77–412. Elsevier

McAinsh AD, Tytell JD & Sorger PK (2003) Structure, Function, and Regulation of Budding Yeast Kinetochores. *Annu. Rev. Cell Dev. Biol.* **19:** 519–539

McDonald HB, Stewart RJ & Goldstein LSB (1990) The kinesin-like ncd protein of Drosophila is a minus end-directed microtubule motor. *Cell* **63:** 1159–1165

Melbinger A, Reese L & Frey E (2012) Microtubule length regulation by molecular motors. *Phys. Rev. Lett.* **108:** 258104

Meluh PB & Rose MD (1990) KAR3, a kinesin-related gene required for yeast nuclear fusion. *Cell* **60:** 1029–41

Michaelis C, Ciosk R & Nasmyth K (1997) Cohesins: chromosomal proteins that prevent premature separation of sister chromatids. *Cell* **91:** 35–45

Miki H, Okada Y & Hirokawa N (2005) Analysis of the kinesin superfamily: insights into structure and function. *Trends Cell Biol.* **15:** 467–76

Miller RK, Heller KK, Frisèn L, Wallack DL, Loayza D, Gammie AE & Rose MD (1998) The kinesin-related proteins, Kip2p and Kip3p, function differently in nuclear migration in yeast. *Mol. Biol. Cell* **9:** 2051–68

Moore A & Wordeman L (2004a) The mechanism, function and regulation of depolymerizing kinesins during mitosis. *Trends Cell Biol.* **14:** 537–46

Moore A & Wordeman L (2004b) C-terminus of mitotic centromere-associated kinesin (MCAK) inhibits its lattice-stimulated ATPase activity. *Biochem. J.* **383:** 227–35

Moore AT, Rankin KE, von Dassow G, Peris L, Wagenbach M, Ovechkina Y, Andrieux A, Job D & Wordeman L (2005) MCAK associates with the tips of polymerizing microtubules. *J. Cell Biol.* **169:** 391–7

Moore JD & Endow SA (1996) Kinesin proteins: A phylum of motors for microtubule-based motility. *BioEssays* **18:** 207–219

Morgan DO (2012) The cell cycle : principles of control Oxford University Press

Nasmyth K, Tanaka T, Fuchs J & Loidl J (2000) Cohesin ensures bipolar attachment of microtubules to sister centromeres and resists their precocious separation. *Nat. Cell Biol.* **2:** 492–499

Neiman AM (2005) Ascospore Formation in the Yeast Saccharomyces cerevisiae. **69:** 565–584

Newton CN, Wagenbach M, Ovechkina Y, Wordeman L & Wilson L (2004) MCAK, a Kin I kinesin, increases the catastrophe frequency of steady-state HeLa cell microtubules in an ATP-dependent manner in vitro. *FEBS Lett.* **572:** 80–84

Nicklas RB (1983) Measurements of the force produced by the mitotic spindle in anaphase. *J. Cell Biol.* **97:** 542–8

Noda Y, Sato-Yoshitake R, Kondo S, Nangaku M & Hirokawa N (1995) KIF2 is a new microtubule-based anterograde motor that transports membranous organelles distinct from those carried by kinesin heavy chain or KIF3A/B. *J. Cell Biol.* **129:** 157–67

Nogales E (2000) Structural insights into microtubule function. *Annu. Rev. Biochem.* **69:** 277–302

Nogales E (2003) Tubulin rings: which way do they curve? *Curr. Opin. Struct. Biol.* **13:** 256–261

Nogales E & Wang H-W (2006) Structural intermediates in microtubule assembly and disassembly: how and why? *Curr. Opin. Cell Biol.* **18:**

179–84

Ogawa T, Nitta R, Okada Y & Hirokawa N (2004) A common mechanism for microtubule destabilizers-M type kinesins stabilize curling of the protofilament using the class-specific neck and loops. *Cell* **116:** 591–602

Ohi R, Sapra T & Howard J (2004) Differentiation of cytoplasmic and meiotic spindle assembly MCAK functions by Aurora B-dependent phosphorylation. *Mol. Biol. Cell* **15:** 2895–2906

Ohkura H (2015) Meiosis: an overview of key differences from mitosis. *Cold Spring Harb. Perspect. Biol.* **7:**

Orr B, Talje L, Liu Z, Kwok BH & Compton DA (2016) Adaptive Resistance to an Inhibitor of Chromosomal Instability in Human Cancer Cells. *Cell Rep.* **17:** 1755–1763

Page SL & Hawley RS (2003) Chromosome Choreography: The Meiotic Ballet. *Science (80-.).* **301:** 785–789

Paliulis L V & Nicklas RB (2000) The reduction of chromosome number in meiosis is determined by properties built into the chromosomes. *J. Cell Biol.* **150:** 1223–32

Perou CM, Jeffrey SS, van de Rijn M, Rees C a, Eisen MB, Ross DT, Pergamenschikov a, Williams CF, Zhu SX, Lee JC, Lashkari D, Shalon D, Brown PO & Botstein D (1999) Distinctive gene expression patterns in human mammary epithelial cells and breast cancers. *Proc. Natl. Acad. Sci. U. S. A.* **96:** 9212–9217

Petronczki M, Siomos MF & Nasmyth K (2003) Un ménage à quatre: the molecular biology of chromosome segregation in meiosis. *Cell* **112:** 423–40

Picard D (1999) eEgulation of heterologous proteins by fusion to a hormone binding domain. In *In Nucelar Receptors: a practical approach.* pp 261–274. Oxford University Press

Pines J & Rieder CL (2001) Re-staging mitosis: a contemporary view of mitotic progression. *Nat. Cell Biol.* **3:** E3-6

Polaina J & Conde J (1982) Genes involved in the control of nuclear fusion during the sexual cycle of Saccharomyces cerevisiae. *Mol. Gen. Genet.* **186:** 253–8

Potapova T & Gorbsky G (2017) The Consequences of Chromosome Segregation Errors in Mitosis and Meiosis. *Biology (Basel).* **6:** 12

R?thnick D & Schiebel E (2016) Duplication of the Yeast Spindle Pole Body

Once per Cell Cycle. *Mol. Cell. Biol.* **36:** 1324–1331

Rankin KE & Wordeman L (2010) Long astral microtubules uncouple mitotic spindles from the cytokinetic furrow. *J. Cell Biol.* **190:** 35–43

Rieder CL, Cole RW, Khodjakov a & Sluder G (1995) The checkpoint delaying anaphase in response to chromosome monoorientation is mediated by an inhibitory signal produced by unattached kinetochores. *J. Cell Biol.* **130:** 941–8

Ritter A, Sanhaji M, Steinhäuser K, Roth S, Louwen F & Yuan J (2015) The activity regulation of the mitotic centromere-associated kinesin by Polo-like kinase 1. *Oncotarget* **6:** 6641–6655

Rizk RS, Discipio KA, Proudfoot KG, Gupta ML & Jr. (2014) The kinesin-8 Kip3 scales anaphase spindle length by suppression of midzone microtubule polymerization. *J. Cell Biol.* **204:** 965–75

Roeder GS (1997) Meiotic chromosomes: it takes two to tango. *Genes Dev.* **11:** 2600–21

Rogers GC, Rogers SL, Schwimmer TA, Ems-McClung SC, Walczak CE, Vale RD, Scholey JM & Sharp DJ (2004) Two mitotic kinesins cooperate to drive sister chromatid separation during anaphase. *Nature* **427:** 364–70

Roof DM, Meluh PB & Rose MD (1992) Kinesin-related proteins required for assembly of the mitotic spindle. *J. Cell Biol.* **118:** 95–108

Sanhaji M, Friel CT, Wordeman L, Louwen F & Yuan J (2011) Mitotic centromere-associated kinesin (MCAK): a potential cancer drug target. *Oncotarget* **2:** 935–947

Santamaria A, Wang B, Elowe S, Malik R, Zhang F, Bauer M, Schmidt A, Silljé HHW, Körner R & Nigg EA (2011) The Plk1-dependent phosphoproteome of the early mitotic spindle. *Mol. Cell. Proteomics* **10:** M110.004457

Saunders W, Hornack D, Lengyel V & Deng C (1997) The Saccharomyces cerevisiae kinesin-related motor Kar3p acts at preanaphase spindle poles to limit the number and length of cytoplasmic microtubules. *J. Cell Biol.* **137:** 417–31

Saunders WS (1993) Mitotic spindle pole separation. *Trends Cell Biol.* **3:** 432–7

Saunders WS & Hoyt MA (1992) Kinesin-related proteins required for structural integrity of the mitotic spindle. *Cell* **70:** 451–8

Sawin KE, LeGuellec K, Philippe M & Mitchison TJ (1992) Mitotic spindle organization by a plus-end-directed microtubule motor. *Nature* **359:** 540–543

Saxton WM, Stemple DL, Leslie RJ, Salmon ED, Zavortink M & McIntosh JR (1984) Tubulin dynamics in cultured mammalian cells. *J. Cell Biol.* **99:** 2175–86

Schindler K, Benjamin KR, Martin A, Boglioli A, Herskowitz I & Winter E (2003) The Cdk-activating kinase Cak1p promotes meiotic S phase through Ime2p. *Mol. Cell. Biol.* **23:** 8718–28

Schmidt M & Bastians H (2007) Mitotic drug targets and the development of novel anti-mitotic anticancer drugs. *Drug Resist. Updat.* **10:** 162–81

Shanks RM, Kamieniecki RJ & Dawson DS (2001) The Kar3-interacting protein Cik1p plays a critical role in passage through meiosis I in Saccharomyces cerevisiae. *Genetics* **159:** 939–51

Shanks RMQ, Bascom-Slack C & Dawson DS (2004) Analysis of the kar3 meiotic arrest in Saccharomyces cerevisiae. *Cell Cycle* **3:** 363–71

Shao H, Huang Y, Zhang L, Yuan K, Chu Y, Dou Z, Jin C, Garcia-Barrio M, Liu X & Yao X (2015) Spatiotemporal dynamics of Aurora B-PLK1-MCAK signaling axis orchestrates kinetochore bi-orientation and faithful chromosome segregation. **5:** 12204

She Z-Y & Yang W-X (2017) Molecular mechanisms of kinesin-14 motors in spindle assembly and chromosome segregation. *J. Cell Sci.* **130:** 2097–2110

Shrestha RLL & Draviam VMM (2013) Lateral to end-on conversion of chromosome-microtubule attachment requires kinesins CENP-E and MCAK. *Curr. Biol.* **23:** 1514–26

Sircar K, Huang H, Hu L, Liu Y, Dhillon J, Cogdell D, Aprikian A, Efstathiou E, Navone N, Troncoso P & Zhang W (2012) Mitosis Phase Enrichment with Identification of Mitotic Centromere-Associated Kinesin As a Therapeutic Target in Castration-Resistant Prostate Cancer. *PLoS One* **7:** e31259

Sproul LR, Anderson DJ, Mackey AT, Saunders WS & Gilbert SP (2005) Cik1 targets the minus-end kinesin depolymerase kar3 to microtubule plus ends. *Curr. Biol.* **15:** 1420–7

Stern BM (2003) FEARless in meiosis. *Mol. Cell* **11:** 1123–5

Stout A, D'Amico S, Enzenbacher T, Ebbert P & Lowery LA (2014) Using plusTipTracker Software to Measure Microtubule Dynamics in Xenopus

laevis Growth Cones. *J. Vis. Exp.***:** e52138

Straight AF, Sedat JW & Murray AW (1998) Time-lapse microscopy reveals unique roles for kinesins during anaphase in budding yeast. *J. Cell Biol.* **143:** 687–94

Stumpff J, von Dassow G, Wagenbach M, Asbury C & Wordeman L (2008) The kinesin-8 motor Kif18A suppresses kinetochore movements to control mitotic chromosome alignment. *Dev. Cell* **14:** 252–62

Stumpff J, Du Y, English CA, Maliga Z, Wagenbach M, Asbury CL, Wordeman L & Ohi R (2011) A tethering mechanism controls the processivity and kinetochore-microtubule plus-end enrichment of the kinesin-8 Kif18A. *Mol. Cell* **43:** 764–75

Stumpff J, Wagenbach M, Franck A, Asbury CL & Wordeman L (2012) Kif18A and chromokinesins confine centromere movements via microtubule growth suppression and spatial control of kinetochore tension. *Dev. Cell* **22:** 1017–29

Su X, Arellano-Santoyo H, Portran D, Gaillard J, Vantard M, Thery M & Pellman D (2013) Microtubule-sliding activity of a kinesin-8 promotes spindle assembly and spindle-length control. *Nat. Cell Biol.* **15:** 948–57

Sudakin V & Yen TJ (2007) Targeting mitosis for anti-cancer therapy. *BioDrugs* **21:** 225–33

Talapatra SKSKSK, Harker B & Welburn JPIJPI (2015) The C-terminal region of the motor protein MCAK controls its structure and activity through a conformational switch. *Elife* **4:** e06421

Tanenbaum ME, Macurek L, van der Vaart B, Galli M, Akhmanova A & Medema RH (2011a) A complex of Kif18b and MCAK promotes microtubule depolymerization and is negatively regulated by Aurora kinases. *Curr. Biol.* **21:** 1356–65

Tanenbaum ME & Medema RH (2011) Localized Aurora B activity spatially controls non-kinetochore microtubules during spindle assembly. *Chromosoma* **120:** 599–607

Tanenbaum ME, Medema RRH & Akhmanova A (2011b) Regulation of localization and activity of the microtubule depolymerase MCAK. *Bioarchitecture* **1:** 80–87

Tanenbaum ME, Vale RD & McKenney RJ (2013) Cytoplasmic dynein crosslinks and slides anti-parallel microtubules using its two motor domains. *Elife* **2:** e00943

Taxis C, Keller P, Kavagiou Z, Jensen LJ, Colombelli J, Bork P, Stelzer EHK

& Knop M (2005) Spore number control and breeding in Saccharomyces cerevisiae: a key role for a self-organizing system. *J. Cell Biol.* **171:** 627–40

Tytell JD & Sorger PK (2006) Analysis of kinesin motor function at budding yeast kinetochores. *J. Cell Biol.* **172:** 861–74

Vader G & Lens SM a (2008) The Aurora kinase family in cell division and cancer. *Biochim. Biophys. Acta* **1786:** 60–72

Vader G, Medema RH & Lens SM a (2006) The chromosomal passenger complex: guiding Aurora-B through mitosis. *J. Cell Biol.* **173:** 833–7

Vale RD & Fletterick RJ (2003) THE DESIGN PLAN OF KINESIN MOTORS. *Annu. Rev. Cell Dev. Biol.* **13:** 745–77

Varga V, Helenius J, Tanaka K, Hyman AA, Tanaka TU & Howard J (2006) Yeast kinesin-8 depolymerizes microtubules in a length-dependent manner. *Nat. Cell Biol.* **8:** 957–962

Walczak CE, Gan EC, Desai A, Mitchison TJ & Kline-Smith SL (2002) The microtubule-destabilizing kinesin XKCM1 is required for chromosome positioning during spindle assembly. *Curr. Biol.* **12:** 1885–9

Walczak CE, Mitchison TJ & Desai A (1996) XKCM1: a Xenopus kinesin-related protein that regulates microtubule dynamics during mitotic spindle assembly. *Cell* **84:** 37–47

Wang E, Ballister ER & Lampson MA (2011) Aurora B dynamics at centromeres create a diffusion-based phosphorylation gradient. *J. Cell Biol.* **194:** 539–49

Wang H-W & Nogales E (2005) Nucleotide-dependent bending flexibility of tubulin regulates microtubule assembly. *Nature* **435:** 911–5

Weaver LN, Ems-McClung SC, Stout JR, LeBlanc C, Shaw SL, Gardner MK & Walczak CE (2011) Kif18A uses a microtubule binding site in the tail for plus-end localization and spindle length regulation. *Curr. Biol.* **21:** 1500–6

Welburn JPI & Cheeseman IM (2012) The microtubule-binding protein Cep170 promotes the targeting of the kinesin-13 depolymerase Kif2b to the mitotic spindle. *Mol. Biol. Cell* **23:** 4786–95

Welburn JPI, Vleugel M, Liu D, Yates JR, Lampson MA, Fukagawa T & Cheeseman IM (2010) Aurora B phosphorylates spatially distinct targets to differentially regulate the kinetochore-microtubule interface. *Mol. Cell* **38:** 383–92

Whitfield ML, Sherlock G, Saldanha AJ, Murray JI, Ball CA, Alexander KE, Matese JC, Perou CM, Hurt MM, Brown PO & Botstein D (2002) Identification of genes periodically expressed in the human cell cycle and their expression in tumors. *Mol. Biol. Cell* **13:** 1977–2000

Wilde A & Zheng Y (1999) Stimulation of microtubule aster formation and spindle assembly by the small GTPase Ran. *Science* **284:** 1359–62

Wordeman L, Decarreau J, Vicente JJ & Wagenbach M (2016) Divergent microtubule assembly rates after short- versus long-term loss of end-modulating kinesins. *Mol. Biol. Cell* **27:** 1300–1309

Wordeman L & Mitchison TJ (1995) Identification and partial characterization of mitotic centromere-associated kinesin, a kinesin-related protein that associates with centromeres during mitosis.

Wordeman L, Wagenbach M & Maney T (1999) Mutations in the ATP-binding domain affect the subcellular distribution of mitotic centromere-associated kinesin (MCAK). *Cell Biol. Int.* **23:** 275–86

Wu X, Xiang X & Hammer JA (2006) Motor proteins at the microtubule plus-end. *Trends Cell Biol.* **16:** 135–43

Xu L, Ajimura M, Padmore R, Klein C & Kleckner N (1995) NDT80, a meiosis-specific gene required for exit from pachytene in Saccharomyces cerevisiae. *Mol. Cell. Biol.* **15:** 6572–81

Yamada M, Tanaka-Takiguchi Y, Hayashi M, Nishina M & Goshima G (2017) Multiple kinesin-14 family members drive microtubule minus end–directed transport in plant cells. *J. Cell Biol.* **216:** 1705–1714

Yount AL, Zong H & Walczak CE (2015) Regulatory Mechanisms that control mitotic kinesins. *Exp. Cell Res.*

Zhang L, Shao H, Huang Y, Yan F, Chu Y, Hou H, Zhu M, Fu C, Aikhionbare F, Fang G, Ding X & Yao X (2011) PLK1 Phosphorylates Mitotic Centromere-associated Kinesin and Promotes Its Depolymerase Activity. *J. Biol. Chem.* **286:** 3033–3046

Zhang X, Ems-McClung SSCS & Walczak CE (2008) Aurora A phosphorylates MCAK to control ran-dependent spindle bipolarity. *Mol. Biol.* **19:** 2752–2765

Zhang X, Lan W, Ems-McClung SCSSC, Stukenberg PT & Walczak CE (2007) Aurora B phosphorylates multiple sites on mitotic centromere-associated kinesin to spatially and temporally regulate its function. *Mol. Biol. Cell* **18:** 3264–3276

Zong H, Carnes SK, Moe C, Walczak CE & Ems-McClung SC (2016) The far

C-terminus of MCAK regulates its conformation and spindle pole focusing. *Mol. Biol. Cell* **27:** 1451–64